

Adjoint Monte Carlo Methods in Neutron Transport Calculations

J. E. Hoogenboom

Delft University Press

1187

1187 5331

Adjoint Monte Carlo Methods
in Neutron Transport Calculations



P1187
5331

C10030
33261

BIBLIOTHEEK TU Delft
P 1187 5331



C

303326

Adjoint Monte Carlo Methods in Neutron Transport Calculations

Proefschrift ter verkrijging
van de graad van doctor in de
technische wetenschappen
aan de Technische Hogeschool Delft,
op gezag van de rector magnificus
prof. ir. L. Huisman,
voor een commissie aangewezen
door het college van dekanen
te verdedigen op
woensdag 14 december 1977
te 16.00 uur door
Jan Eduard Hoogenboom
natuurkundig ingenieur
geboren te Rotterdam



Delft University Press/1977

1187 5331

1187 5331

Dit proefschrift is goedgekeurd door
de promotor Dr. ir. H. van Dam

CONTENTS

SUMMARY	9
CHAPTER I INTRODUCTION	13
CHAPTER II FORWARD AND ADJOINT TRANSPORT EQUATIONS IN INTEGRAL FORM	19
II.1. The integral forms of the neutron transport equation	19
II.2. Monte Carlo interpretation of integral equations	24
II.3. Adjoint kernels and equations	33
II.4. Monte Carlo interpretation of the adjoint equation	38
CHAPTER III TRANSFORMED ADJOINT EQUATIONS	43
III.1. A transformed adjoint equation and its Monte Carlo interpretation	43
III.2. Analysis of the adjoint cross section	51
III.3. Other transformations of the adjoint equation	58
III.4. Sampling the adjoint collision kernel	66
CHAPTER IV MULTIPLYING SYSTEMS	77
IV.1. Forward Monte Carlo methods for multiplying systems	77
IV.2. Adjoint methods for multiplying systems	87
IV.3. Monte Carlo interpretation of the adjoint equation for multiplying systems	98

CHAPTER V	NUMERICAL EXAMPLES AND DISCUSSION	111
V.1.	The computer code FOCUS and related programs	111
V.2.	A fixed-source shielding problem	115
V.3.	Calculations on a critical assembly	131
V.4.	Discussion and conclusions	138
APPENDIX A	MECHANICS OF INELASTIC NEUTRON SCATTERING	141
APPENDIX B	A PROPERTY OF THE DEFINITION I ADJOINT INELASTIC CROSS SECTION	147
REFERENCES		151
LIST OF IMPORTANT SYMBOLS		155
ACKNOWLEDGEMENTS		157

SUMMARY

This thesis describes the solution of the space, energy and direction dependent adjoint neutron transport equation by the Monte Carlo method, which enables the calculation of quantities that are not suited for a normal (forward) Monte Carlo calculation, because too few neutron histories would contribute to the desired quantity.

For a forward Monte Carlo simulation, the neutron transport equation in integral form is interpreted in terms of source probability density functions, transition probabilities and death probabilities. This has also been applied to the adjoint transport equation, resulting in the description of the transport of hypothetical "adjoint" particles with specific properties. It is shown that coordinate transformations of the neutron transport equation before deriving the adjoint equation lead to different adjoint equations, when interpreted in a Monte Carlo sense, and thus to different properties of the adjoint particles.

The adjoint equations describe a flux-like quantity. In a Monte Carlo simulation, density-like quantities are desired, which suggests a transformation of the adjoint equation. To facilitate the sampling of the transition probabilities resulting from the transformed adjoint equation, the concept of adjoint cross sections arises. Then the Monte Carlo simulation of a transformed adjoint equation shows close analogy with the simulation of the neutron transport equation. An important difference, however, is the fact that the partial adjoint cross sections, which replace the partial neutron cross sections, do not sum up to the total neutron cross section. Therefore, the ratio of the

total adjoint cross section to the total neutron cross section, which becomes the analogon of the neutron non-absorption probability, may be greater than unity and can no longer be interpreted as a probability. At every collision the adjoint particle weight is multiplied by this factor, which is called the adjoint weight factor. The behaviour of the adjoint cross sections and the adjoint weight factor is investigated for some typical cases. The selection of the energy and direction after a scattering event of an adjoint particle is discussed in detail.

It is shown that the transformed adjoint equation, obtained after an energy-coordinate transformation of the neutron transport equation is equivalent with an energy biasing of the transformed adjoint equation. Each energy biasing function corresponds to a different definition of the adjoint cross section and subsequently to a different behaviour of the adjoint weight factor. With an $1/E$ (E =energy) biasing function the adjoint cross sections exhibit some special properties, resulting in better statistics of the Monte Carlo calculation.

The theory for the Monte Carlo solution of an adjoint transport equation has been extended to include multiplying systems. A method has been developed to calculate quantities which are averages over the unknown fundamental mode neutron distribution of a multiplying system. This requires the simulation of successive generations of adjoint particles with the probability density function for the source parameters of the particles of the first generation depending on the quantity to be calculated. In contrast with forward calculations, the multiplication of all successive generations appears in the final estimation of the desired quantity, which increases its variance. The energy probability density function for particles of a next generation generally favours lower energies, while higher energies are needed to produce new progeny. Therefore, a source energy biasing function has been derived that improves the statistics of the calculation.

A versatile adjoint Monte Carlo computer code, called FOCUS, has been written to test the developed theories. Separate computer codes calculate the adjoint cross sections and prepare all necessary data for the adjoint Monte Carlo simulation. A numerical example has been

given with a neutron flux spectrum and detector response calculation for a shielding benchmark geometry. The results show good agreement with those obtained by a forward Monte Carlo code. To show the performance of the theory developed for multiplying systems, the neutron flux spectrum in a point of a fast critical assembly and the effective multiplication factor has been calculated, among other quantities.

From the numerical examples it is concluded that the developed adjoint Monte Carlo method is a significant expansion of the applicability range of the Monte Carlo method, especially for the calculation of those quantities that are defined only for a small or even zero space volume, energy range or solid angle.

CHAPTER I

INTRODUCTION

Although the Monte Carlo method, nowadays, is regarded as a branch of experimental mathematics, the method originates from reactor physics, in which it was first used to study neutron diffusion [1]. In its systematic development the application in reactor physics problems also played an important role. At present, the Monte Carlo method is used in many other fields of science and engineering and by the introduction of modern digital computers its applications are still growing.

In reactor physics the Monte Carlo method has been well established for calculating effective multiplication factors of reactor cores, reaction rates, dose rates in shielding problems, etc. Its potential power lies in the possibility to include with relative ease all desired variables, which may be three spatial coordinates, energy, two directional variables and time, and to represent accurately almost any physical model for particle scattering, cross sectional data and geometrical detail. This is often in contrast with calculational methods based on numerical analysis. The great detail generally allowed in Monte Carlo calculations makes the method suitable as a reference calculational method against which other approximating methods can be checked.

The Monte Carlo method is concerned with experiments on random numbers. With specified probability laws samples are drawn from some parent population and statistical data are collected from the samples to estimate a desired quantity. Because of this stochastic nature the outcome of a Monte Carlo calculation is always accompanied with an uncertainty. To diminish this uncertainty more samples may be drawn. Broadly speaking the uncertainty is inversely proportional to the square root of the number of samples. Thus a tenfold reduction of the uncertainty calls for a hundredfold increase in the number of samples and in computing time. Because of this slow decrease of the uncertainty the stochastic nature of the Monte Carlo method is also its most serious drawback, which limits the application of the method to those quantities that can be estimated with relatively small uncertainty, expressed in terms of variance or standard deviation, for a fixed number of samples.

In neutron transport calculations the samples drawn from the parent distribution are neutron histories. The probability laws, which govern the selection of the neutron histories are given by the physics of the neutron source and the interaction mechanisms of neutrons with matter. If the samples are drawn according to these physical laws the processes that occur during the Monte Carlo calculation are analog abstracts of the processes occurring in the real world. Therefore, this method is called "analog" Monte Carlo or "direct simulation". However, analog methods may be very inefficient, especially if we are interested in events that occur rarely in a given system. Then these events will also occur only rarely in an abstract analog of the system and we may expect large variances, because the estimation of the desired quantity is based only on the few neutron histories in which the events of interest occurred. In such cases we can modify the sampling laws in such a way that the variance in the desired quantity is reduced. At the same time the estimation procedure should also be altered as to remove any bias from the estimator. These variance reduction techniques as they are called, can have many different forms and their effective-

ness strongly depends on the system that is considered and the kind of quantity desired.

From the above considerations it will be clear that Monte Carlo is most suited for calculation of integral quantities to which estimate most of the selected neutron histories will give a contribution. Depending on geometrical and cross sectional complexity more differential quantities may also be economically calculated with Monte Carlo as illustrated in table I, taken from Schmidt [2]. In this table λ without arguments denotes an integral quantity; $\lambda(x_1)$ a quantity averaged over an interval of the variable x_1 for several intervals of x_1 ; $\lambda(x_1, x_2)$ a quantity averaged over intervals of the variables x_1 and x_2 for several intervals of both x_1 and x_2 .

Table I. Applicability range of the Monte Carlo method

geometry	one dimensional	two dimensional	three dimensional
use Monte Carlo if	very detailed cross section information is necessary	more than 10 groups greater P_{1*} greater S_8	anywhere, except where diffusion theory is sufficient
to calculate	λ e.g. k_{eff} , total dose, life time, etc.	λ $\lambda(x_1)$ e.g. group spectra, etc. $\lambda(x_1, x_2)$ e.g. group constants for various regions, time depen- dent spectra, etc.	λ $\lambda(x_1)$ $\lambda(x_1, x_2)$

* P_n denotes a Legendre expansion of the angular dependent scattering cross section of order n ; S_n denotes a discrete ordinates method of order n .

If one is interested in quantities averaged over small intervals of one or more variables, the Monte Carlo method becomes more and more inefficient and may become impracticable if a quantity in a single point is desired. Especially for these problems adjoint Monte Carlo methods

are of importance. In the adjoint formulation a completely different equation is simulated by Monte Carlo in which the source and estimation functions are interchanged. Therefore problems in which the estimation function is non-zero in a small volume of the phase space but the neutron source is distributed over a relatively large volume of the phase space, can much better be treated by adjoint Monte Carlo, at least in principle.

The explicit recognition of the importance of adjoint Monte Carlo to certain problems is due to Maynard [3]. However, his work, formulated in terms of the reciprocity theorem, is limited to one-energy problems which fundamentally simplifies the Monte Carlo interpretation of the adjoint equation. In this thesis the neutron energy is considered as a continuous variable and methods are derived to treat the adjoint transport equation for the general case, including critical reactor systems, by Monte Carlo methods.

Outline of the following chapters

In chapter II the integral forms of the neutron transport equation are given and their Monte Carlo interpretation as far as is needed for the discussion of adjoint methods. Next the adjoint equation is defined and some properties of this equation are discussed. Finally, the disadvantages of the adjoint equation for a direct Monte Carlo simulation are shown.

Chapter III gives a transformation of the adjoint equation for which the Monte Carlo interpretation becomes quite analogous to that of the neutron transport equation. Here the concept of adjoint cross sections is introduced, which facilitates the Monte Carlo interpretation. The properties of the adjoint cross sections are analysed and some disadvantages are established which negatively influence the statistics of the adjoint Monte Carlo simulation. Another transformation of the adjoint equation is discussed that meets most of these disadvantages. The sampling of the probability density functions appearing from this transformed adjoint equation is discussed in detail.

In chapter IV multiplying systems are treated. First Monte Carlo techniques used for neutron transport in multiplying systems are given. Next a formalism is developed to treat multiplying systems by adjoint Monte Carlo methods. The sampling of the probability density functions specific for multiplying systems is discussed in detail.

Chapter V describes the adjoint Monte Carlo code FOCUS which is based on the theory developed in chapter III and IV. Results are given for neutron flux spectrum and point-detector respons calculations on a shielding benchmark problem. For a critical assembly, the effective multiplication factor has been calculated and, among other quantities, the neutron flux spectrum at a point of the assembly. The results are compared with solutions obtained by forward Monte Carlo calculations or other numerical methods. Finally conclusions are given with respect to the applicability of the adjoint methods developed in this study.

CHAPTER II

FORWARD AND ADJOINT TRANSPORT EQUATIONS IN INTEGRAL FORM

II.1. The integral forms of the neutron transport equation

The most widely known form of the equation describing neutron transport is the Boltzmann equation in integro-differential form which reads in general time dependent form [4]

$$\frac{1}{v} \frac{\partial \phi(\underline{r}, E, \underline{\Omega}, t)}{\partial t} + \underline{\Omega} \cdot \nabla \phi(\underline{r}, E, \underline{\Omega}, t) + \Sigma_t(\underline{r}, E) \phi(\underline{r}, E, \underline{\Omega}, t) \\ = \iint \Sigma_t(\underline{r}, E') C(\underline{r}, E' \rightarrow E, \underline{\Omega}' \rightarrow \underline{\Omega}) \phi(\underline{r}, E', \underline{\Omega}', t) dE' d\Omega' + S(\underline{r}, E, \underline{\Omega}, t) \quad (2.1)$$

with \underline{r} the spatial coordinate,

E the neutron energy,

$\underline{\Omega}$ the flight direction,

t the time,

v the neutron speed,

$\phi(\underline{r}, E, \underline{\Omega}, t) dE d\Omega$ the neutron flux at \underline{r} at time t for neutrons with energy between E and $E+dE$ and direction in the solid angle $d\Omega$ about $\underline{\Omega}$,

$\Sigma_t(\underline{r}, E)$ the total cross section at \underline{r} for neutrons with energy E ,

$C(\underline{r}, E' \rightarrow E, \underline{\Omega}' \rightarrow \underline{\Omega}) dE d\Omega$ the expected number of neutrons leaving a collision with energy between E and $E+dE$ and direction in the solid angle $d\Omega$ about $\underline{\Omega}$ given a neutron with energy E' and direction $\underline{\Omega}'$ going into a collision,

$S(\underline{r}, E, \underline{\Omega}, t)$ an external neutron source, i.e. independent of the neutron flux.

The right hand side (RHS) of Eq.(2.1) is the density of neutrons emitted at \underline{r} with energy E and direction $\underline{\Omega}$ from any collision process or the source. We will call this density the emission density and denote it by $\chi(\underline{r}, E, \underline{\Omega}, t)$:

$$\chi(\underline{r}, E, \underline{\Omega}, t) = S(\underline{r}, E, \underline{\Omega}, t) + \iint \Sigma_t(\underline{r}, E') C(\underline{r}, E' \rightarrow E, \underline{\Omega}' \rightarrow \underline{\Omega}) \phi(\underline{r}, E', \underline{\Omega}', t) dE' d\Omega' \quad (2.2)$$

For Monte Carlo calculations Eq.(2.1) is not the most convenient form for describing the neutron transport. By integration we obtain [4]

$$\phi(\underline{r}, E, \underline{\Omega}, t) = \int_0^{\infty} \exp\left\{-\int_0^s \Sigma_t(\underline{r}-s'\underline{\Omega}, E) ds'\right\} \chi(\underline{r}-s\underline{\Omega}, E, \underline{\Omega}, t - \frac{s}{v}) ds \quad (2.3)$$

Now the flux ϕ is expressed as the contribution of all neutrons emitted along the line $\underline{r}-s\underline{\Omega}$ into the direction $\underline{\Omega}$. For the theoretical treatment it is desirable to write the integral in the RHS of Eq.(2.3) as a volume integral instead of a line integral. Doing so we have to include a δ -function to achieve that only neutrons emitted along the line $\underline{r}-s\underline{\Omega}$ contribute to the flux at \underline{r} . Introducing

$$\underline{r}' = \underline{r} - s\underline{\Omega}^* \quad (2.4)$$

and

$$dV' = s^2 ds d\Omega^* \quad (2.5)$$

we have

$$s = |\underline{r}-\underline{r}'| \quad \text{and} \quad \underline{\Omega}^* = \frac{\underline{r}-\underline{r}'}{|\underline{r}-\underline{r}'|} \quad (2.6)$$

and we can write Eq.(2.3) as

$$\phi(\underline{r}, E, \underline{\Omega}, t) = \int \exp\left\{-\int_0^{|\underline{r}-\underline{r}'|} \Sigma_t(\underline{r}-s'\underline{\Omega}^*, E) ds'\right\} \cdot \chi(\underline{r}', E, \underline{\Omega}, t - \frac{|\underline{r}-\underline{r}'|}{v}) \delta\left(\underline{\Omega} - \frac{\underline{r}-\underline{r}'}{|\underline{r}-\underline{r}'|}\right) \frac{dV'}{|\underline{r}-\underline{r}'|^2} \quad (2.7)$$

where the integration is over all space.

Because we are mainly concerned with stationary processes, we shall drop the time variable from now on. However, the treatment of the time variable in Monte Carlo calculations is extremely simple. If a neutron

moves from \underline{r}' to \underline{r} with speed v , time increases by $|\underline{r}-\underline{r}'|/v$ as can also be seen from Eq.(2.7). So it is easy to include time dependence in the calculation and there is no loss of generality by dropping the time variable. By introducing the time-independent collision density ψ

$$\psi(\underline{r}, E, \underline{\Omega}) = \Sigma_t(\underline{r}, E)\phi(\underline{r}, E, \underline{\Omega}) \quad (2.8)$$

and the transport kernel T

$$T(\underline{r}' \rightarrow \underline{r}, E, \underline{\Omega}) = \Sigma_t(\underline{r}, E) \exp\left\{-\int_0^{|\underline{r}-\underline{r}'|} \Sigma_t(\underline{r}-s\underline{\Omega}, E) ds\right\} \frac{\delta\left(\underline{\Omega} - \frac{\underline{r}-\underline{r}'}{|\underline{r}-\underline{r}'|}\right)}{|\underline{r}-\underline{r}'|^2} \quad (2.9)$$

we have the following time-independent relations between ψ and χ from Eqs.(2.2) and (2.7) respectively

$$\chi(\underline{r}, E, \underline{\Omega}) = S(\underline{r}, E, \underline{\Omega}) + \iint C(\underline{r}, E' \rightarrow E, \underline{\Omega}' \rightarrow \underline{\Omega}) \psi(\underline{r}, E', \underline{\Omega}') dE' d\Omega' \quad (2.10)$$

and

$$\psi(\underline{r}, E, \underline{\Omega}) = \int T(\underline{r}' \rightarrow \underline{r}, E, \underline{\Omega}) \chi(\underline{r}', E, \underline{\Omega}) dV' \quad (2.11)$$

$T(\underline{r}' \rightarrow \underline{r}, E, \underline{\Omega}) dV'$ represents the probability for a neutron at \underline{r}' with energy E and direction $\underline{\Omega}$ to have its next collision in the volume element dV' at \underline{r} . To obtain an integral equation for ψ only, we write \underline{r}' for \underline{r} in Eq.(2.10), multiply both sides by $T(\underline{r}' \rightarrow \underline{r}, E, \underline{\Omega})$ and integrate over \underline{r}' . With Eq.(2.11) we obtain

$$\begin{aligned} \psi(\underline{r}, E, \underline{\Omega}) &= \int T(\underline{r}' \rightarrow \underline{r}, E, \underline{\Omega}) S(\underline{r}', E, \underline{\Omega}) dV' \\ &+ \iiint C(\underline{r}', E' \rightarrow E, \underline{\Omega}' \rightarrow \underline{\Omega}) T(\underline{r}' \rightarrow \underline{r}, E, \underline{\Omega}) \psi(\underline{r}', E', \underline{\Omega}') dV' dE' d\Omega' \end{aligned} \quad (2.12)$$

By substitution of Eq.(2.11) into Eq.(2.10) we obtain the integral equation for χ only

$$\chi(\underline{r}, E, \underline{\Omega}) = S(\underline{r}, E, \underline{\Omega}) + \iiint T(\underline{r}' \rightarrow \underline{r}, E', \underline{\Omega}') C(\underline{r}, E' \rightarrow E, \underline{\Omega}' \rightarrow \underline{\Omega}) \chi(\underline{r}', E', \underline{\Omega}') dV' dE' d\Omega' \quad (2.13)$$

The aim of any Monte Carlo calculation concerning neutron transport may be formulated as estimating a quantity F , which is some average over the neutron flux ϕ or over the collision density ψ or over the emission density χ . So we can express F as

$$F = \iiint f(\underline{r}, E, \underline{\Omega}) \phi(\underline{r}, E, \underline{\Omega}) dV dE d\Omega \quad (2.14)$$

$$= \iiint g(\underline{r}, E, \underline{\Omega}) \psi(\underline{r}, E, \underline{\Omega}) dV dE d\Omega \quad (2.15)$$

$$= \iiint h(\underline{r}, E, \underline{\Omega}) \chi(\underline{r}, E, \underline{\Omega}) dV dE d\Omega \quad (2.16)$$

From Eq.(2.8) we have

$$g(\underline{r}, E, \underline{\Omega}) = f(\underline{r}, E, \underline{\Omega}) / \Sigma_t(\underline{r}, E) \quad (2.17)$$

and from Eq.(2.11)

$$h(\underline{r}, E, \underline{\Omega}) = \int g(\underline{r}', E, \underline{\Omega}) T(\underline{r} \rightarrow \underline{r}', E, \underline{\Omega}) dV' \quad (2.18)$$

In general the functions f or g follow easily from the physics of the problem and are mostly simple functions. For example, if F is the absorption rate in some volume of a reactor, then f equals the macroscopic absorption cross section and g equals the ratio of the absorption to the total cross section in that volume and both functions are zero outside that volume. However, h will not be a simple function as can be seen from Eq.(2.18). So, Monte Carlo simulation of χ from Eq.(2.13) and estimation of F from Eq.(2.16) does not seem to be feasible. However, we shall show in the next section that simulation of

ψ from Eq.(2.12) and χ from Eq.(2.13) can be done and is generally done in exactly the same way. Therefore, it is possible to use Eq.(2.15) for estimating F when we pretend to simulate χ from Eq.(2.13). For the derivation of adjoint equations, the integral equation for χ is preferred, because the source term in this equation is equal to the known external neutron source $S(\underline{r}, E, \underline{\Omega})$, in contrast with the density of first collisions, which acts as the (mathematical) source in Eq. (2.12) for ψ and which is generally not known in analytic form. However, the same results can be obtained if we start from the equation for ψ .

If we denote, for convenience, a point $(\underline{r}, E, \underline{\Omega})$ in the phase space by τ and $(\underline{r}', E', \underline{\Omega}')$ by τ' and introduce the kernel K by

$$K(\tau' \rightarrow \tau) = K(\underline{r}' \rightarrow \underline{r}, E' \rightarrow E, \underline{\Omega}' \rightarrow \underline{\Omega}) = T(\underline{r}' \rightarrow \underline{r}, E', \underline{\Omega}') C(\underline{r}, E' \rightarrow E, \underline{\Omega}' \rightarrow \underline{\Omega}) \quad (2.19)$$

we can write the equation for χ as

$$\chi(\tau) = S(\tau) + \int K(\tau' \rightarrow \tau) \chi(\tau') d\tau' \quad (2.20)$$

and F as

$$F = \int h(\tau) \chi(\tau) d\tau \quad (2.21)$$

$K(\tau' \rightarrow \tau) d\tau$ is the expected number of neutrons in $d\tau$ emitted from a collision at τ , given a neutron at τ' . The integral term in Eq.(2.20) is the number of neutrons emitted at τ due to all neutrons emitted from a previous collision or the source anywhere in the system. The first term in the RHS of Eq.(2.20) is the direct contribution of source neutrons to $\chi(\tau)$. Eqs.(2.20) and (2.21) will form the basis for the derivation of the adjoint equations.

If we denote the density of first collision by $S_1(\tau)$ we have

$$S_1(\tau) = \int T(\underline{r}' \rightarrow \underline{r}, E, \underline{\Omega}) S(\underline{r}', E, \underline{\Omega}) dV' \quad (2.22)$$

and Eq.(2.12) can be written as

$$\psi(\tau) = S_1(\tau) + \int H(\tau' \rightarrow \tau) \psi(\tau') d\tau' \quad (2.23)$$

with the kernel H defined by

$$H(\tau' \rightarrow \tau) = C(\underline{r}', E' \rightarrow E, \underline{\Omega}' \rightarrow \underline{\Omega}) T(\underline{r}' \rightarrow \underline{r}, E, \underline{\Omega}) \quad (2.24)$$

In this notation F is given by

$$F = \int g(\tau) \psi(\tau) d\tau \quad (2.25)$$

$H(\tau' \rightarrow \tau) d\tau$ is the expected number of neutrons having a collision in $d\tau$ at τ , given a neutron at τ' going into a collision.

II.2. Monte Carlo interpretation of integral equations

In this section we shall outline the simulation of integral equations as derived in the previous section and the estimation of integral quantities as given by Eqs.(2.21) and (2.25). Because our equations describe the physical process of neutron transport through matter, many of the methods used could be understood by physical intuition. Here we are interested in a more formal mathematical description in order to apply the results in the next chapters to other integral equations with the same mathematical structure, which do not describe an existing physical process. The Monte Carlo method is founded in probability theory and a rigorous description as far as neutron transport is concerned is given by Spanier and Gelbard [5].

From probability theory we know that if we construct random walks by selecting birth points from a probability density function (pdf) $p_b(\tau)$ with

$$p_b(\tau) \geq 0 \quad (2.26)$$

$$\int p_b(\tau) d\tau = 1 \quad (2.27)$$

and next event points τ with probability $p_t(\tau' \rightarrow \tau)$, if the previous event was at τ' , with

$$p_t(\tau' \rightarrow \tau) \geq 0 \quad (2.28)$$

and

$$\int p_t(\tau' \rightarrow \tau) d\tau = 1 - p_d(\tau') \leq 1 \quad (2.29)$$

where $p_d(\tau')$ is the probability for terminating a random walk at τ' , then the expected density of events $E(\tau)$ is given by the integral equation

$$E(\tau) = p_b(\tau) + \int p_t(\tau' \rightarrow \tau) E(\tau') d\tau' \quad (2.30)$$

Moreover, for a random walk $\alpha(\tau_0, \tau_1, \dots, \tau_k)$ starting at τ_0 and ending at τ_k , an estimator for the integral quantity λ

$$\lambda = \int b(\tau) E(\tau) d\tau \quad (2.31)$$

with $b(\tau)$ some given function, is

$$\eta(\alpha) = \eta(\tau_0, \tau_1, \dots, \tau_k) = \sum_i b(\tau_i) \quad (2.32)$$

For a non-multiplying medium we can directly connect this probability model with the neutron transport model, formulated in Eq.(2.23). A random walk is equivalent with a neutron history and an event is equivalent with a neutron going into a collision. The event

density corresponds to the collision density and the transition probability with the kernel $H(\tau' \rightarrow \tau)$. We shall mainly concern ourselves in this section with non-multiplying media and only a few remarks will be made about simulating multiplying media. This problem will be handled in chapter IV in more detail. For a non-multiplying medium we have indeed

$$\int H(\tau' \rightarrow \tau) d\tau = \frac{\Sigma_s(\tau')}{\Sigma_t(\tau')} = 1 - \frac{\Sigma_a(\tau')}{\Sigma_t(\tau')} \leq 1 \quad (2.23)$$

with Σ_s and Σ_a the macroscopic scattering and absorption cross sections. The density of birth points $p_b(\tau)$ should correspond to the first collision density $S_1(\tau)$. Although this density will not be normalized to unity, we can divide Eq.(2.23) by $\int S_1(\tau) d\tau$ to meet the condition of a normalized density of birth points and multiply the final results by this normalization factor. To estimate the quantity F from Eq.(2.25) we may use the estimator

$$\eta(\alpha) = \eta(\tau_0, \tau_1, \dots, \tau_k) = \sum_i g(\tau_i) \quad (2.34)$$

which means that we have to sum the value of the averaging or scoring function $g(\tau)$ at every collision point. Because the estimator η scores at every collision, this estimator is called a collision type estimator. There are, of course, many other estimators, but the collision estimator suffices here.

For a non-multiplying medium simulation of Eq.(2.23) is thus done by selecting birth points from the pdf $S_1(\tau)$, if properly normalized, and successive collision points τ by sampling the kernel $H(\tau' \rightarrow \tau)$, if the previous collision was at τ' . The first collision density $S_1(\tau)$ depends strongly on the neutron source $S(\tau)$, which may be different for each problem. Some remarks for sampling $S_1(\tau)$ will be made later.

The sampling of the kernel $H(\tau' \rightarrow \tau)$ is characteristic for Monte Carlo solutions of neutron transport problems and we shall discuss this first in more detail. The kernel H is the product of the transport kernel T and what we may call the collision kernel C , according to Eq.(2.24).

For a system with infinite dimensions, the transport kernel T is normalized

$$\int T(\underline{r}' \rightarrow \underline{r}, E, \underline{\Omega}) dV = 1 \quad (2.35)$$

because the integral represents the probability for a neutron at \underline{r}' to have its next collision anywhere in the system. For a finite system this is not true and the probability for escape from the system is

$$P_{\lambda}(\underline{r}', E, \underline{\Omega}) = 1 - \int_R T(\underline{r}' \rightarrow \underline{r}, E, \underline{\Omega}) dV \quad (2.36)$$

where the integration is over the total system R . However, we may continue to use the normalization of Eq.(2.35) if we consider the system surrounded by a purely absorbing medium and terminate a neutron history as soon as the neutron reaches this medium. Then all volume integrals may be taken over the total space. Thus $T(\underline{r}' \rightarrow \underline{r}, E, \underline{\Omega})$ can be understood as the conditional pdf for \underline{r} given \underline{r}' , E and $\underline{\Omega}$. From this pdf \underline{r} is selected by selection of the number of mean free paths z for the neutron to travel from the exponential distribution

$$p(z) = e^{-z} \quad 0 < z < \infty \quad (2.37)$$

and intersecting the geometry from \underline{r}' into the direction $\underline{\Omega}$ until the neutron has travelled the selected z mean free paths or it reaches the outer boundary of the system from which it can not reenter the system.

If the media in the system consist of one or more nuclides and if for each nuclide one or more collision types are possible, we can write the collision kernel C in general form as

$$C(\underline{r}, E' \rightarrow E, \underline{\Omega}' \rightarrow \underline{\Omega}) = \sum_A p_A(\underline{r}, E') \sum_j p_{j,A}(E') c_{j,A}(E') f_{j,A}(E' \rightarrow E, \underline{\Omega}' \rightarrow \underline{\Omega}) \quad (2.38)$$

where p_A is the probability for a collision with nuclide A

$$p_A(\underline{r}, E') = \frac{\Sigma_A(\underline{r}, E')}{\Sigma_t(\underline{r}, E')} \quad (2.39)$$

and $p_{j,A}(E')$ the probability for a collision of type j provided the neutron collides with nuclide A

$$p_{j,A}(E') = \frac{\sigma_{j,A}(E')}{\sigma_A(E')} \quad (2.40)$$

The summation over A in Eq.(2.38) is over all nuclides present at \underline{r} and the summation over j is over all possible collision types of nuclide A. Further $c_{j,A}(E')$ is the mean number of neutrons released in a collision of type j with nuclide A and $f_{j,A}(E' \rightarrow E, \underline{\Omega}' \rightarrow \underline{\Omega})$ is the probability for transferring the neutron energy from E' to E and its direction from $\underline{\Omega}'$ to $\underline{\Omega}$ in a collision of type j with nuclide A. For absorption $c=0$, for elastic and inelastic scattering $c=1$, for (n,2n) collisions $c=2$ and for fission c is equal to the mean number of neutrons per fission $\bar{\nu}(E')$.

Except for the case of absorption, $f_{j,A}$ is normalized to unity

$$\iint f_{j,A}(E' \rightarrow E, \underline{\Omega}' \rightarrow \underline{\Omega}) dE d\Omega = 1 \quad (2.41)$$

Thus $f_{j,A}$ is the joint pdf for E and $\underline{\Omega}$ given j and A. The collision kernel C can now be sampled by selecting first with probability $p_A(\underline{r}, E')$ the nuclide with which the neutron collides and then selecting the reaction type with probability $p_{j,A}(E')$. If this is absorption the history is terminated. Otherwise the energy and

direction after the collision can be selected from the joint pdf $f_{j,A}(E' \rightarrow E, \underline{\Omega}' \rightarrow \underline{\Omega})$. For scattering reactions the energy and direction after scattering are uniquely related due to the collision mechanics. Therefore it is easy to obtain the pdf for E only or the pdf for $\underline{\Omega}$ only, which must be sampled by elementary methods.

Thus the kernel $H(\tau' \rightarrow \tau)$ can be split in a pdf for $(E, \underline{\Omega})$ and a conditional pdf for \underline{r} , given E and $\underline{\Omega}$ and these two pdf's must be sampled in this order to select a new collision event.

For the simulation of Eq.(2.20) for the emission density $\chi(\tau)$ the events considered are now neutrons leaving a collision or the source. The pdf for birth points is the neutron source density $S(\tau)$, which is normally separable in the variables \underline{r} , E and $\underline{\Omega}$ and can thus be sampled easily. The kernel $K(\tau' \rightarrow \tau)$ which appears in the integral equation for χ is also a product of the transport kernel T and the collision kernel C , but with a different order of the variables. If the last event was at $\tau' = (\underline{r}', E', \underline{\Omega}')$, a next event is selected by sampling first the transport kernel $T(\underline{r}' \rightarrow \underline{r}, E', \underline{\Omega}')$, which is the pdf for \underline{r} and sampling the collision kernel $C(\underline{r}, E' \rightarrow E, \underline{\Omega}' \rightarrow \underline{\Omega})$ which is now the conditional pdf for $(E, \underline{\Omega})$ given \underline{r} , provided the neutron did not escape from the system. Now the quantity F is estimated from Eq.(2.21) by the estimator

$$\eta(\tau_0, \tau_1, \dots, \tau_k) = \sum_i h(\tau_i) \quad (2.42)$$

for a random walk starting at τ_0 , having next events at $\tau_1, \tau_2, \dots, \tau_k$ and terminating at τ_k .

The procedures for simulation of the integral equations for ψ and χ become identical if the density of first collision $S_1(\tau)$ in the simulation of ψ is sampled indirectly. From Eq.(2.22) it can be seen that $S_1(\tau)$ can be sampled by sampling first the neutron source density $S(\tau)$ and then sampling the kernel T . These are, however, just the first steps for the simulation of χ . Then for both equations

the kernels C and T are sampled successively, so the procedures become exactly identical. There is, however, a difference in scoring. In the simulation of ψ the scoring function is $g(\tau)$ and scoring takes place at the moment that a neutron goes into a collision. In the simulation of χ scoring takes place when a neutron comes out of a collision (or the source) and $h(\tau)$ is the scoring function. Which method is to be preferred depends on which of the functions $g(\tau)$ and $h(\tau)$ is the easier to compute. However, also statistical considerations may be important. If, for example, the absorption rate in some small volume W of the system has to be calculated, $g(\tau)$ is given by

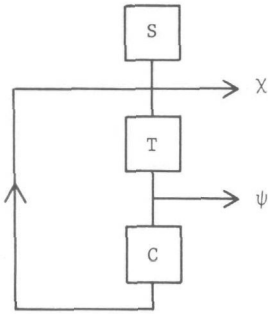
$$g(\tau) = \frac{\sum_a(\tau)}{\sum_t(\tau)} \quad \underline{r} \in W \quad (2.43)$$

Because the volume W is small, there will be only few collisions in W, so this procedure will not be very efficient. Then it may be more effective to use $h(\tau)$ which now reads

$$h(\tau) = \int \frac{\sum_a(\underline{r}', E)}{\sum_t(\underline{r}', E)} T(\underline{r} \rightarrow \underline{r}', E, \underline{\Omega}) dV' \quad (2.44)$$

Scoring takes place after a neutron leaves a collision (or the source). $h(\tau)$ will be non-zero if the line $\underline{r} + s\underline{\Omega}$ crosses the volume W for $s > 0$, so the collision point at \underline{r} need not to be in W. In fact the use of $h(\tau)$ here is a form of statistical estimation [5].

The equivalence of the equations for ψ and χ in a Monte Carlo simulation is shown graphically in the kind of flow scheme presented in Fig. 1. A box means sampling of the pdf inscribed. The arrows pointing to χ and ψ denote the moments in the selection of the random walk where one has drawn a sample of χ and ψ respectively. Not shown in the diagram are the possibilities for terminating the history when sampling T or C.

Fig. 1. Simulation of χ and ψ

Thus far we discussed the process of analog Monte Carlo to simulate ψ or χ and to estimate F , because we followed closely the pdf's originating from the physical model. From probability theory we know that χ can also be simulated by non-analog methods as follows [6]. We construct a random walk process based on an arbitrary pdf $p_b(\tau)$ for birth points, subject to the condition that if $S(\tau) \neq 0$ then $p_b(\tau) \neq 0$ and an arbitrary pdf $p_t(\tau' \rightarrow \tau)$ for transition from τ' to τ , subject to the condition that if $K(\tau' \rightarrow \tau) \neq 0$ then $p_t(\tau' \rightarrow \tau) \neq 0$. Suppose $\alpha(\tau_0, \tau_1, \dots, \tau_k)$ is an arbitrary random walk constructed this way, starting at τ_0 , with other event points at $\tau_1, \tau_2, \dots, \tau_k$ and terminating at τ_k . The (statistical) weight of the neutron at the n -th event point τ_n is defined by

$$W_n(\alpha) = \frac{S(\tau_0)}{p_b(\tau_0)} w(\tau_0, \tau_1) w(\tau_1, \tau_2) \dots w(\tau_{n-1}, \tau_n) \quad n \leq k \quad (2.45)$$

with

$$w(\tau', \tau) = \begin{cases} K(\tau' \rightarrow \tau) / p_t(\tau' \rightarrow \tau) & p_t(\tau' \rightarrow \tau) \neq 0 \\ 0 & p_t(\tau' \rightarrow \tau) = 0 \end{cases} \quad (2.46)$$

At every event point the weight of the neutron is an estimate for the event density at that point and an estimator for F is

$$\eta'(\alpha) = \eta'(\tau_0, \tau_1, \dots, \tau_k) = \sum_i W_i(\alpha) h(\tau_i) \quad (2.47)$$

The choices $p_b(\tau) = S(\tau)$ and $p_t(\tau' \rightarrow \tau) = K(\tau' \rightarrow \tau)$ result in the analog process with the neutron weight equal to unity at every event.

A very often used form of non-analog Monte Carlo corresponds to the choices $p_b(\tau) = S(\tau)$ and

$$p_t(\tau' \rightarrow \tau) = K(\tau' \rightarrow \tau) / \iint C(\underline{r}, E' \rightarrow E, \underline{\Omega}' \rightarrow \underline{\Omega}) dE d\Omega \quad (2.48)$$

Then the collision part of the kernel K is normalized to unity, so that no absorption can take place in the Monte Carlo process. The weight factor with which the weight of the neutron must be multiplied at every event is

$$w(\tau', \tau) = \iint C(\underline{r}, E' \rightarrow E, \underline{\Omega}' \rightarrow \underline{\Omega}) dE d\Omega = \frac{\Sigma_s(\underline{r}, E')}{\Sigma_t(\underline{r}, E')} \quad (2.49)$$

If the system has infinite dimensions the probability for terminating a history becomes

$$p_d(\tau') = 1 - \int p_t(\tau' \rightarrow \tau) d\tau = 0 \quad (2.50)$$

and some artificial means of terminating a history, such as Russian roulette [5], is necessary.

Playing a non-analog game is possible at every step in the simulation where a random variable is selected from a pdf. In fact, the above example affected only the sampling of the collision kernel C . Playing an altered game is a form of importance sampling. It does not change the expected value of the quantities to be calculated, provided the correct weight of the neutron is taken into account. But it does influence the variance of the estimators. It is therefore of interest to find sampling schemes which decrease variance.

For multiplying systems problems are only stationary if the system is subcritical. But $\int K(\tau' \rightarrow \tau) d\tau$ or $\int H(\tau' \rightarrow \tau) d\tau$ may still be greater than unity for certain regions of the system. One way to include multiplying reaction types for which $c_{j,A} > 1$ is to perform the sampling of $c_{j,A}(E') f_{j,A}(E' \rightarrow E, \underline{\Omega}' \rightarrow \underline{\Omega})$ of Eq.(2.38) after selection of A and j by non-analog Monte Carlo. The energy and direction after collision are selected from the normalized pdf $f_{j,A}(E' \rightarrow E, \underline{\Omega}' \rightarrow \underline{\Omega})$ and the factor $c_{j,A}(E')$ is included in the weight factor $w(\tau', \tau)$. Other methods for subcritical multiplying systems and eigenvalue problems are discussed in chapter IV.

II.3. Adjoint kernels and equations

In the previous section, we discussed briefly the sampling of the neutron transport equation and the estimation of an integral quantity F according to Eq.(2.25) or Eq.(2.21) with a collision estimator. It was also shown that in case of small "detection" volume i.e. the space volume for which the scoring function $g(\tau)$ is non-zero, it is more effective to use the scoring function $h(\tau)$ when a neutron leaves a collision (or the source). In fact part of the sampling process is then incorporated into the scoring function, namely the transport kernel T. This method may be continued to incorporate also the collision kernel C into the scoring function. This may be useful when the energy range or the solid angle for which $g(\tau)$ is non-zero is small or even zero. If the collision kernel is also incorporated into the scoring function, only scores from collided neutrons are taken into account and the contribution from uncollided source neutrons must be calculated or estimated as well. However, if more than one of the variables \underline{r} , E and $\underline{\Omega}$ are restricted to small intervals to let $g(\tau)$ be non-zero, this method of expected values become less and less effective when the intervals become smaller or even zero. A special problem is introduced if $g(\tau)$ is only non-zero in one

point \underline{r}_0 , due to the factor $|\underline{r}-\underline{r}_0|^{-2}$ in the transport kernel and hence in the expected value estimator. Although the averaged value remains finite, the variance becomes infinite [7]. For this type of problems, generally indicated by a small detection volume in the phase space, adjoint methods may be more practical. The remainder of this work will be devoted to these adjoint methods.

Adjoint methods may be defined in general terms for linear operators of any kind [8]. Here suffices the following definition for an adjoint kernel. If $v(\tau)$ and $w(\tau)$ are two arbitrary functions defined in the same phase space and $K(\tau' \rightarrow \tau)$ is a kernel then the adjoint kernel $K^\dagger(\tau' \rightarrow \tau)$ is defined by the relation

$$\int v(\tau) \int K(\tau' \rightarrow \tau) w(\tau') d\tau' d\tau = \int w(\tau) \int K^\dagger(\tau' \rightarrow \tau) v(\tau') d\tau' d\tau \quad (2.51)$$

for every set of functions $v(\tau)$ and $w(\tau)$. Interchanging the integration variables in the RHS of Eq.(2.51) we easily find that the adjoint kernel must be equal to

$$K^\dagger(\tau' \rightarrow \tau) = K(\tau \rightarrow \tau') \quad (2.52)$$

If K is the kernel defined by Eq.(2.19) and K^\dagger is its adjoint according to Eq.(2.52) and if $h(\tau)$ is a given function, then the following integral equation determines the function $\chi^\dagger(\tau)$

$$\chi^\dagger(\tau) = h(\tau) + \int K^\dagger(\tau' \rightarrow \tau) \chi^\dagger(\tau') d\tau' \quad (2.53)$$

If we multiply Eq.(2.20) by $\chi^\dagger(\tau)$ and Eq.(2.53) by $\chi(\tau)$, integrate over all phase space and subtract the results, we obtain the important relation

$$\int h(\tau) \chi(\tau) d\tau = \int S(\tau) \chi^\dagger(\tau) d\tau \quad (2.54)$$

The terms containing the kernels K and K^\dagger cancel, because of the definition of an adjoint kernel. If $h(\tau)$ is the averaging function for the emission density to obtain the desired quantity F according to Eq.(2.21) we can also calculate F from

$$F = \int S(\tau) \chi^\dagger(\tau) d\tau \quad (2.55)$$

It will be clear that $\chi^\dagger(\tau)$ may be interpreted as the importance of a neutron at τ to the quantity F . The pairs of equations Eqs.(2.20), (2.21) and Eqs.(2.53), (2.55) may be called adjoint equations. Generally, an equation that contains a kernel that is the adjoint of a kernel arising from a physical process, is called an adjoint equation and we shall adopt this usage.

Because Eq.(2.53) is mathematically of the same type as the transport equation Eq.(2.20) we can interpret Eq.(2.53) as describing the transport of hypothetical particles with properties defined by the kernel K^\dagger . Then $h(\tau)$ is the source density of these particles and $\chi^\dagger(\tau)$ the event density of the particles. So it should be possible to simulate Eq.(2.53) by Monte Carlo, selecting particles from the source $h(\tau)$ and selecting next event points in the phase space from the kernel K^\dagger . F can be estimated using the neutron source $S(\tau)$ as the scoring function at every point, according to Eq.(2.55). Techniques for sampling the kernel K^\dagger will be discussed in the next section.

Having defined the adjoint kernel K^\dagger by Eq.(2.52) there seems to be only one kernel adjoint to K . However, if we first apply a coordinate transformation $\rho = \rho(\tau)$, the adjoint equation does not describe the same process, or alternatively stated it describes the transport of other particles with different properties. This can be seen as follows. From the physical meaning of S , χ , K and h we have for the coordinate

transformation

$$S(\rho)d\rho = S(\tau)d\tau \quad (2.56)$$

$$\chi(\rho)d\rho = \chi(\tau)d\tau \quad (2.57)$$

$$K(\rho' \rightarrow \rho)d\rho = K(\tau' \rightarrow \tau)d\tau \quad (2.58)$$

$$h(\rho) = h(\tau) \quad (2.59)$$

Then Eqs.(2.20) and (2.21) transform into

$$\chi(\rho) = S(\rho) + \int K(\rho' \rightarrow \rho)\chi(\rho')d\rho' \quad (2.60)$$

and

$$F = \int h(\rho)\chi(\rho)d\rho \quad (2.61)$$

Eq.(2.60) still describes the same physical process as does Eq.(2.20) and the Monte Carlo simulation of these equations is in fact the same. Because of the definition of the adjoint kernel we have

$$K^\dagger(\rho' \rightarrow \rho) = K(\rho \rightarrow \rho') \quad (2.62)$$

so the adjoint equation in the variable ρ becomes

$$\chi^\dagger(\rho) = h(\rho) + \int K^\dagger(\rho' \rightarrow \rho)\chi^\dagger(\rho')d\rho' \quad (2.63)$$

and

$$F = \int S(\rho)\chi^\dagger(\rho)d\rho \quad (2.64)$$

If we interpret χ^\dagger as the importance of a neutron to the quantity F

we have

$$\chi^\dagger(\rho) = \chi^\dagger(\tau) \quad (2.65)$$

Further,

$$K^\dagger(\rho' \rightarrow \rho) = K(\rho \rightarrow \rho') = K(\tau \rightarrow \tau') \left| \frac{d\tau'}{d\rho'} \right| = K^\dagger(\tau' \rightarrow \tau) \left| \frac{d\tau'}{d\rho'} \right| \quad (2.66)$$

However, if we interpret Eq.(2.63) as describing the transport of hypothetical particles as is done in a Monte Carlo simulation then $K^\dagger(\rho' \rightarrow \rho)d\rho$ is the probability for an event in $d\rho$, given a particle suffering an event at ρ' . In a coordinate transformation the pdf $K^\dagger(\tau' \rightarrow \tau)$ transforms into the pdf

$$K^*(\rho' \rightarrow \rho) = K^\dagger(\tau' \rightarrow \tau) \left| \frac{d\tau}{d\rho} \right| \quad (2.67)$$

which differs from Eq.(2.66) for the former interpretation of χ^\dagger . Therefore, if we solve Eq.(2.63) by Monte Carlo, we solve an equation different from Eq.(2.53) when transformed to the variable ρ and sample a different kernel with different properties.

In practice, the only coordinate transformation to be considered is a transformation of the energy variable. In stead of the neutron energy one may use, for instance, the neutron speed v or the lethargy u defined by

$$u = \ln \frac{E_0}{E} \quad (2.68)$$

with E_0 some reference energy. The latter transformation will be discussed at length in the next chapters.

II.4. Monte Carlo interpretation of the adjoint equation

As stated in the previous section, the adjoint equation Eq.(2.53) has the same mathematical form as the neutron transport equation Eq.(2.20) and can therefore be considered as describing the transport of hypothetical particles, with properties defined by the adjoint kernel K^\dagger . We shall call these hypothetical particles adjoint particles to distinguish them from neutrons. The mathematical source $h(\tau)$ of the adjoint equation acts as the source density of the adjoint particles and χ^\dagger as the event density. The kernel $K^\dagger(\tau' \rightarrow \tau)$ gives the probability for an adjoint particle having an event at τ' to have its next event at τ . Because the procedure for constructing a random walk for the adjoint particles and estimating the quantity F from Eq.(2.55) by scoring at each event point with $S(\tau)$ as the scoring function is completely analogous with the neutron transport game, we have only to discuss here the sampling of the kernel K^\dagger , which is much less trivial than sampling the kernel K .

The adjoint kernel K^\dagger is given by

$$\begin{aligned} K^\dagger(\underline{r}' \rightarrow \underline{r}, E' \rightarrow E, \underline{\Omega}' \rightarrow \underline{\Omega}) &= K(\underline{r} \rightarrow \underline{r}', E \rightarrow E', \underline{\Omega} \rightarrow \underline{\Omega}') \\ &= T(\underline{r} \rightarrow \underline{r}', E, \underline{\Omega}) C(\underline{r}', E \rightarrow E', \underline{\Omega}' \rightarrow \underline{\Omega}') \end{aligned} \quad (2.69)$$

Because of the interchange of the variables the kernel K^\dagger is not normalized and $\int K^\dagger(\tau' \rightarrow \tau) d\tau$ may be greater than unity so that an analog simulation is not possible. The kernel can be simplified somewhat by the following reduction. The kernel $C(\underline{r}', E \rightarrow E', \underline{\Omega}' \rightarrow \underline{\Omega}')$ contains a factor $\Sigma_c(\underline{r}', E)$ in the denominator. Combined with the transport kernel we can write

$$\begin{aligned} \frac{T(\underline{r} \rightarrow \underline{r}', E, \underline{\Omega})}{\Sigma_t(\underline{r}', E)} &= \exp\left\{-\int_0^{|\underline{r}'-\underline{r}|} \Sigma_t(\underline{r}'-s\underline{\Omega}, E) ds\right\} \frac{\delta\left(\underline{\Omega}-\frac{\underline{r}'-\underline{r}}{|\underline{r}'-\underline{r}|}\right)}{|\underline{r}'-\underline{r}|^2} \\ &= \exp\left\{-\int_0^{|\underline{r}-\underline{r}'|} \Sigma_t(\underline{r}+s'\underline{\Omega}, E) ds'\right\} \frac{\delta\left(\underline{\Omega}+\frac{\underline{r}-\underline{r}'}{|\underline{r}-\underline{r}'|}\right)}{|\underline{r}-\underline{r}'|^2} = \frac{T(\underline{r}' \rightarrow \underline{r}, E, -\underline{\Omega})}{\Sigma_t(\underline{r}, E)} \end{aligned} \quad (2.70)$$

where the latter expression is obtained by the substitution

$$s' = |\underline{r}-\underline{r}'| - s \quad (2.71)$$

and by

$$\underline{r} = \underline{r}' - |\underline{r}-\underline{r}'| \underline{\Omega} \quad (2.72)$$

because of the δ -function. With the expression for the collision kernel from Eq.(2.38) we have for K^\dagger

$$\begin{aligned} K^\dagger(\underline{r}' \rightarrow \underline{r}, E' \rightarrow E, \underline{\Omega}' \rightarrow \underline{\Omega}) &= \frac{T(\underline{r}' \rightarrow \underline{r}, E, -\underline{\Omega})}{\Sigma_t(\underline{r}, E)} \\ &\cdot \sum_A N_A(\underline{r}') \sum_j \sigma_{j,A}(E) c_{j,A}(E) f_{j,A}(E \rightarrow E', \underline{\Omega} \rightarrow \underline{\Omega}') \end{aligned} \quad (2.73)$$

with N_A the atomic density of nuclide A. Given \underline{r}' , E' and $\underline{\Omega}'$ the last part of the right hand side of Eq.(2.73) only depends on E and $\underline{\Omega}$ and may form the basis for the pdf for $(E, \underline{\Omega})$. Once E and $\underline{\Omega}$ have been selected, \underline{r} should be selected from the first part of the right hand side of Eq.(2.73).

A normalized pdf for $(E, \underline{\Omega})$ is

$$\begin{aligned} p(E, \underline{\Omega}) &= \frac{1}{w_1(\underline{r}', E', \underline{\Omega}')} \sum_A N_A(\underline{r}') \\ &\cdot \sum_j \sigma_{j,A}(E) c_{j,A}(E) f_{j,A}(E \rightarrow E', \underline{\Omega} \rightarrow \underline{\Omega}') \end{aligned} \quad (2.74)$$

with

$$w_1(\underline{r}', E', \underline{\Omega}') = \iint \sum_A N_A(\underline{r}') \sum_j \sigma_{j,A}(E) c_{j,A}(E) f_{j,A}(E \rightarrow E', \underline{\Omega} \rightarrow \underline{\Omega}') dE d\Omega \quad (2.75)$$

Thus we can sample E and $\underline{\Omega}$ from the pdf of Eq.(2.74) and use w_1 as a weight factor at each event. It is possible, at least in theory, to compute a table of cumulative probabilities for E and $\underline{\Omega}$ and sample E and $\underline{\Omega}$ by interpolation. More practical procedures for dealing with pdf's like Eq.(2.74) will be discussed in the next chapter. A normalized pdf for selection of the next event point \underline{r} is

$$p(\underline{r}) = \frac{1}{w_2(\underline{r}', E, \underline{\Omega})} \exp\left\{-\int_0^{|\underline{r}-\underline{r}'|} \Sigma_t(\underline{r}'-s\underline{\Omega}, E) ds\right\} \frac{\delta\left(\underline{\Omega} + \frac{\underline{r}-\underline{r}'}{|\underline{r}-\underline{r}'|}\right)}{|\underline{r}-\underline{r}'|^2} \quad (2.76)$$

with

$$w_2(\underline{r}', E, \underline{\Omega}) = \int \exp\left\{-\int_0^{|\underline{r}-\underline{r}'|} \Sigma_t(\underline{r}'-s\underline{\Omega}, E) ds\right\} \delta\left(\underline{\Omega} + \frac{\underline{r}-\underline{r}'}{|\underline{r}-\underline{r}'|}\right) \frac{dV}{|\underline{r}-\underline{r}'|^2} \quad (2.77)$$

Thus we can sample \underline{r} from Eq.(2.76) and use w_2 also as a weight factor at each event. For systems with finite dimensions this leads to some ambiguity, because the normalization factor w_2 and hence the pdf depends on the total cross section of the material with which we thought the system to be surrounded to keep the neutron transport kernel normalized. With the cross section of the surrounding medium we can influence the probability for the adjoint particles to escape from the system. If we let this cross section increase to infinity, the adjoint particle will always have its next event in the system itself and no adjoint particle can escape.

Using this procedure to sample the adjoint kernel K^\dagger we have to multiply the weight of the adjoint particle at each event by a weight factor which is the product of w_1 and w_2 . This fact itself need not to be a disadvantage. As we have already seen in section

II.2, in forward Monte Carlo calculations it is usual to exclude absorption and use a weight factor Σ_s/Σ_t . However, now the weight factor depends not only on the parameters \underline{r}', E' and $\underline{\Omega}'$ of the adjoint particle before the event but also on E and $\underline{\Omega}$ after the event and is not separable in the parameters before and after a collision. An other disadvantage of sampling the kernel K^\dagger is that it is possible to sample an event in vacuum, because $p(\underline{r})$ does not contain the factor $\Sigma_t(\underline{r}, E)$. Therefore the adjoint equation Eq.(2.53) is said to be a flux-like equation. For Monte Carlo calculations it is more practical to solve an equation for a function that behaves like a collision density. So it may be obvious to multiply Eq.(2.53) on both sides by $\Sigma_t(\underline{r}, E)$ and solve this transformed adjoint equation. This kind of transformation will be discussed more fully in the next chapter.

From the kernel K^\dagger we can deduce some properties which are typical for adjoint equations. The pdf for selection of the energy E after a collision of an adjoint particle contains a term $f_{j,A}(E \rightarrow E', \underline{\Omega} \rightarrow \underline{\Omega}')$. This function is in the case of a scattering collision only non-zero for a certain energy range of E' given E with $E' < E$. This implies that $f_{j,A}(E \rightarrow E', \underline{\Omega} \rightarrow \underline{\Omega}')$ is only non-zero for a certain energy range of E by given E' with $E > E'$. So it is only possible in the adjoint game to select energies after a collision of the adjoint particle which are higher than the energy E' before collision. As far as the energy change in the neutron game is uniquely related to the scattering angle, as it is for elastic and inelastic level scattering, this will also be the case in the adjoint game. Concerning the transport of the adjoint particle, it can be seen from Eq.(2.72) or Eq.(2.70) that the adjoint particle moves into the direction $-\underline{\Omega}$, opposite to the neutron game. This leads to the conclusion that we are not allowed to speak about $\underline{\Omega}$ as the direction of the adjoint particle nor can we say that E is the energy of the adjoint particle, because the law of conservation of energy does not hold. Therefore,

we can call \underline{r} , E and $\underline{\Omega}$ only variables that characterize the state of the adjoint particle without any physical interpretation of these variables. Nevertheless, it is usual and convenient to call the variable E the energy of the adjoint particle and $\underline{\Omega}$ its direction and we will continue to do so. Thereby we accept that energy is not conserved in a collision and that the adjoint particle moves into the direction $-\underline{\Omega}$.

Chapter III

TRANSFORMED ADJOINT EQUATIONS¹

III.1. A transformed adjoint equation and its Monte Carlo interpretation

The adjoint integral equation Eq.(2.53) is not suitable for direct Monte Carlo simulation and in the previous chapter it was already suggested that the simulation of the quantity $\Sigma_{\mathbf{t}}(\tau)\chi^{\dagger}(\tau)$ should be more promising. We therefore define the transformation

$$\xi^{\dagger}(\tau) = \Sigma_{\mathbf{t}}(\tau)\chi^{\dagger}(\tau) \quad (3.1)$$

and

$$L^{\dagger}(\tau' \rightarrow \tau) = \frac{\Sigma_{\mathbf{t}}(\tau)}{\Sigma_{\mathbf{t}}(\tau')} K^{\dagger}(\tau' \rightarrow \tau) \quad (3.2)$$

Then Eq.(2.53) transforms into

$$\xi^{\dagger}(\tau) = \Sigma_{\mathbf{t}}(\tau)h(\tau) + \int L^{\dagger}(\tau' \rightarrow \tau)\xi^{\dagger}(\tau')d\tau' \quad (3.3)$$

From the expression for the kernel K^{\dagger} of Eq.(2.73) we have for the kernel L^{\dagger}

¹Parts of this chapter have already been published earlier [9]

$$L^\dagger(\tau' \rightarrow \tau) = T(\underline{r}' \rightarrow \underline{r}, E, -\underline{\Omega}) \cdot \sum_A N_A(\underline{r}') \sum_j \sigma_{j,A}(E) c_{j,A}(E) f_{j,A}(E \rightarrow E', \underline{\Omega} \rightarrow \underline{\Omega}') / \Sigma_t(\underline{r}', E') \quad (3.4)$$

The first part of the right hand side of Eq.(3.4) can be used as a normalized conditional pdf for the selection of \underline{r} , given E and $\underline{\Omega}$. The only difference with neutron transport is that tracking is done in the direction $-\underline{\Omega}$. The last part of Eq.(3.4) should serve as the pdf for E and $\underline{\Omega}$, but this pdf is unnormalized. The normalization factor is

$$P^\dagger(\tau') = \frac{\iint \sum_A N_A(\underline{r}') \sum_j \sigma_{j,A}(E) c_{j,A}(E) f_{j,A}(E \rightarrow E', \underline{\Omega} \rightarrow \underline{\Omega}') dE d\Omega}{\Sigma_t(\underline{r}', E')} \quad (3.5)$$

It is useful to abbreviate the numerator to $\Sigma^\dagger(\tau')$

$$\Sigma^\dagger(\tau') = \iint \sum_A N_A(\underline{r}') \sum_j \sigma_{j,A}(E) c_{j,A}(E) f_{j,A}(E \rightarrow E', \underline{\Omega} \rightarrow \underline{\Omega}') dE d\Omega \quad (3.6)$$

The normalized pdf for E and $\underline{\Omega}$ may be called the adjoint collision kernel and can be written as

$$C^\dagger(\underline{r}', E' \rightarrow E, \underline{\Omega}' \rightarrow \underline{\Omega}) = \sum_A N_A(\underline{r}') \sum_j \sigma_{j,A}(E) c_{j,A}(E) f_{j,A}(E \rightarrow E', \underline{\Omega} \rightarrow \underline{\Omega}') / \Sigma^\dagger(\underline{r}', E') \quad (3.7)$$

The kernel L^\dagger can now be sampled by selecting E and $\underline{\Omega}$ from the pdf C^\dagger , multiplying the weight of the adjoint particle by P^\dagger and selecting a new collision site from $T(\underline{r}' \rightarrow \underline{r}, E, -\underline{\Omega})$. We shall call P^\dagger the adjoint weight factor

$$P^\dagger(\tau) = \Sigma^\dagger(\tau) / \Sigma_t(\tau) \quad (3.8)$$

Further we introduce the adjoint transport kernel T^\dagger by

$$T^\dagger(\underline{r}' \rightarrow \underline{r}, E, \underline{\Omega}) = T(\underline{r}' \rightarrow \underline{r}, E, -\underline{\Omega}) \quad (3.9)$$

Then the kernel L^\dagger can be written as

$$L^\dagger(\tau' \rightarrow \tau) = P^\dagger(\tau') C^\dagger(\underline{r}', E' \rightarrow E, \underline{\Omega}' \rightarrow \underline{\Omega}) T^\dagger(\underline{r}' \rightarrow \underline{r}, E, \underline{\Omega}) \quad (3.10)$$

The sampling of the source term $\Sigma_t(\tau)h(\tau)$ of Eq.(3.3) is simplified by the use of Eq.(2.18) for $h(\tau)$

$$\begin{aligned} \Sigma_t(\tau)h(\tau) &= \Sigma_t(\tau) \int g(\underline{r}', E, \underline{\Omega}) T(\underline{r} \rightarrow \underline{r}', E, \underline{\Omega}) dV' \\ &= \int \Sigma_t(\underline{r}', E) g(\underline{r}', E, \underline{\Omega}) T(\underline{r}' \rightarrow \underline{r}, E, -\underline{\Omega}) dV' \\ &= \int f(\underline{r}', E, \underline{\Omega}) T^\dagger(\underline{r}' \rightarrow \underline{r}, E, \underline{\Omega}) dV' \end{aligned} \quad (3.11)$$

where the identities of Eqs.(2.70), (2.17) and (3.9) have been used. The source term $\Sigma_t(\tau)h(\tau)$ can thus be sampled by selecting \underline{r}', E and $\underline{\Omega}$ from $f(\underline{r}', E, \underline{\Omega})$ and sampling the adjoint transport kernel T^\dagger . If the pdf $f(\tau)$ is not normalized to unity we can sample the normalized pdf $f(\tau)/\int f(\tau)d\tau$ and multiply all final results by $\int f(\tau)d\tau$. The simulation of Eq.(3.3) is represented schematically in Fig. 2. From Eq.(2.55) it follows that F can be obtained from

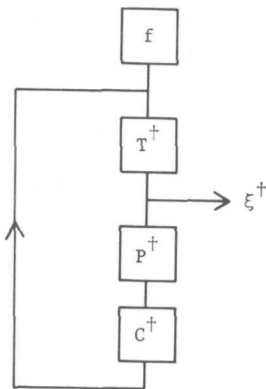


Fig. 2. Simulation of ξ^\dagger

$$F = \int \frac{S(\tau)}{\Sigma_t(\tau)} \xi^\dagger(\tau) d\tau \quad (3.12)$$

thus $S(\tau)/\Sigma_t(\tau)$ is the scoring function.

The simulation of $\xi^\dagger(\tau)$ is in fact the method used in the multigroup Monte Carlo code MORSE [10] which can be run in forward and adjoint mode. Because the relationship between energy degradation and scattering angle in a collision cannot be used in a multigroup treatment, pdf's for the scattering angle for all separate nuclides in a medium are no longer useful and only one pdf averaged over all nuclides in a medium is used to select the scattering angle when the neutron scatters from one energy group to another. In the adjoint mode such a pdf for the scattering angle can also be obtained by group averaging Eq.(3.7). The adjoint weight factor P^\dagger of Eq.(3.5) for an energy group replaces the non-absorption probability used as a weight factor in the neutron game. Therefore, it is relatively easy to solve the forward and adjoint equation in multigroup form in one computer code. Apart from the approximations introduced when using discrete energy groups instead of a continuous energy variable, multigroup adjoint transport codes will use for practical reasons the multigroup cross section sets derived on basis of a flux averaging instead of the solution ξ^\dagger of Eq.(3.3).

Because we are interested in adjoint methods with continuous energy handling the sampling of the adjoint collision kernel C^\dagger needs further attention. From Eq.(3.6) we see that the quantity Σ^\dagger , which appears in the adjoint weight factor P^\dagger has the dimension of a macroscopic cross section. We therefore call this quantity the macroscopic adjoint cross section. We also define the partial microscopic adjoint cross section of nuclide A for reaction type j

$$\sigma_{j,A}^\dagger(E', \underline{\Omega}') = \iint \sigma_{j,A}(E) c_{j,A}(E) f_{j,A}(E \rightarrow E', \underline{\Omega} \rightarrow \underline{\Omega}') dE d\Omega \quad (3.13)$$

For neutron reactions the directional dependence of the scattering function $f_{j,A}(E \rightarrow E', \underline{\Omega} \rightarrow \underline{\Omega}')$ is only through the inner product of $\underline{\Omega}$ and $\underline{\Omega}'$. The scattering function may even be independent of $\underline{\Omega}$ and $\underline{\Omega}'$, that is the scattering is isotropic and $f_{j,A}$ can be written as

$$f_{j,A}(E \rightarrow E', \underline{\Omega} \rightarrow \underline{\Omega}') = \frac{1}{4\pi} f_{j,A}(E \rightarrow E') \quad (3.14)$$

with $f_{j,A}(E \rightarrow E')$ the energy transfer function. In both cases the microscopic adjoint cross section becomes independent of $\underline{\Omega}'$ and can be written as

$$\sigma_{j,A}^\dagger(E') = \int \sigma_{j,A}(E) c_{j,A}(E) f_{j,A}(E \rightarrow E') dE \quad (3.15)$$

In analogy with normal cross sections we have

$$\sigma_A^\dagger(E) = \sum_j \sigma_{j,A}^\dagger(E) \quad (3.16)$$

$$\Sigma_A^\dagger(\underline{r}, E) = N_A(\underline{r}) \sigma_A^\dagger(E) \quad (3.17)$$

$$\Sigma^\dagger(\underline{r}, E) = \sum_A \Sigma_A^\dagger(\underline{r}, E) = \sum_A N_A(\underline{r}) \sum_j \sigma_{j,A}^\dagger(E) \quad (3.18)$$

σ_A^\dagger is the total microscopic adjoint cross section for nuclide A and Σ_A^\dagger the total macroscopic adjoint cross section for nuclide A. The adjoint cross section for absorption does not exist (or is identically zero) because $c=0$ for absorption. With the adjoint cross sections we can rewrite the adjoint collision kernel as

$$\begin{aligned} C^\dagger(\underline{r}', E' \rightarrow E, \underline{\Omega}' \rightarrow \underline{\Omega}) \\ = \sum_A P_A^\dagger(\underline{r}', E') \sum_j P_{j,A}^\dagger(E') \frac{\sigma_{j,A}(E) c_{j,A}(E) f_{j,A}(E \rightarrow E', \underline{\Omega} \rightarrow \underline{\Omega}')}{\sigma_{j,A}^\dagger(E')} \end{aligned} \quad (3.19)$$

with

$$P_A^\dagger(\underline{r}', E') = \frac{\Sigma_A^\dagger(\underline{r}', E')}{\Sigma^\dagger(\underline{r}', E')} \quad (3.20)$$

and

$$P_{j,A}^\dagger(E') = \frac{\sigma_{j,A}^\dagger(E')}{\sigma_A^\dagger(E')} \quad (3.21)$$

C^\dagger can now be sampled analogous to the neutron collision kernel by selecting a nuclide A with probability P_A^\dagger and selecting next a reaction type j with probability $P_{j,A}^\dagger$. Then E and $\underline{\Omega}$ should be selected from the normalized conditional pdf

$$p(E, \underline{\Omega} | j, A) = \frac{\sigma_{j,A}^\dagger(E) c_{j,A}^\dagger(E) f_{j,A}^\dagger(E \rightarrow E', \underline{\Omega} \rightarrow \underline{\Omega}')}{\sigma_{j,A}^\dagger(E')} \quad (3.22)$$

The computation of the adjoint cross section and the selection of E and $\underline{\Omega}$ from this pdf will be treated in detail in section 4 of this chapter.

The concept of the adjoint cross section was first introduced by Eriksson et al [11], but in a slightly different transformation of Eq.(2.53). They used the transformation

$$\mu^\dagger(\tau) = \Sigma^\dagger(\tau) \chi^\dagger(\tau) \quad (3.23)$$

and

$$G^\dagger(\tau' \rightarrow \tau) = \frac{\Sigma^\dagger(\tau)}{\Sigma^\dagger(\tau')} K^\dagger(\tau' \rightarrow \tau) \quad (3.24)$$

to obtain the integral equation

$$\mu^\dagger(\tau) = \Sigma^\dagger(\tau) h(\tau) + \int G^\dagger(\tau' \rightarrow \tau) \mu^\dagger(\tau') d\tau' \quad (3.25)$$

Then F is obtained from

$$F = \int \frac{S(\tau)}{\Sigma^{\dagger}(\tau)} \mu^{\dagger}(\tau) d\tau \quad (3.26)$$

With the expression for the kernel K^{\dagger} from Eq.(2.73) and the newly introduced kernels C^{\dagger} , T^{\dagger} and P^{\dagger} we can write for the kernel G^{\dagger}

$$G^{\dagger}(\tau' \rightarrow \tau) = C^{\dagger}(\underline{r}', E' \rightarrow E, \underline{\Omega}' \rightarrow \underline{\Omega}) T^{\dagger}(\underline{r}' \rightarrow \underline{r}, E, \underline{\Omega}) P^{\dagger}(\underline{r}, E) \quad (3.27)$$

The only difference with the kernel L^{\dagger} is that the weight of the adjoint particles is multiplied by P^{\dagger} after sampling the adjoint transport kernel instead of before sampling the adjoint collision kernel. For the source term of Eq.(3.25) we have

$$\Sigma^{\dagger}(\tau) h(\tau) = \int f(\underline{r}', E, \underline{\Omega}) T^{\dagger}(\underline{r}' \rightarrow \underline{r}, E, \underline{\Omega}) P^{\dagger}(\underline{r}, E) dV' \quad (3.28)$$

The simulation of μ^{\dagger} is schematized in Fig. 3. From a comparison

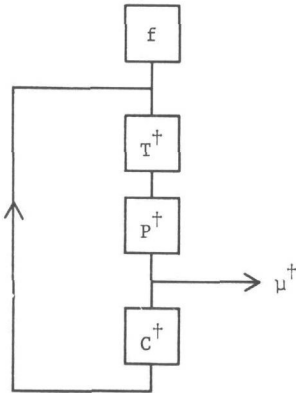


Fig. 3. Simulation of μ^{\dagger}

with Fig. 2 we see that the simulation of μ^{\dagger} is essentially the same as that for ξ^{\dagger} except that μ^{\dagger} is obtained at a different stage of the sampling process. μ^{\dagger} is simply related to ξ^{\dagger} by

$$\mu^{\dagger}(\tau) = P^{\dagger}(\tau) \xi^{\dagger}(\tau) \quad (3.29)$$

If the factor P^\dagger is taken into account by multiplying the weight of the adjoint particle by P^\dagger , both methods result in the same scores at corresponding event points and thus in equal variances for the quantity F . If we compare the simulation of ξ^\dagger from Fig. 2 with the simulation of the neutron game from Fig. 1 we can state that $\xi^\dagger(\tau)$ is the density of adjoint particles going into a collision. Then the source of adjoint particles is $f(\tau)$, the averaging function for the neutron flux to obtain F according to Eq.(2.14). The source term $\Sigma_t(\tau)h(\tau)$ which appears in Eq.(3.3) is the density of first collisions for the adjoint particles, equivalent with the density $S_1(\tau)$ of first neutron collisions, which acts as the (mathematical) source in Eq.(2.23) for the neutron collision density $\psi(\tau)$. As in the neutron game, it may be useful to consider also the density of particles leaving a collision or the source. If we denote this density for the adjoint particles by $\theta^\dagger(\tau)$ we have the following relations between $\theta^\dagger(\tau)$ and $\xi^\dagger(\tau)$

$$\theta^\dagger(\tau) = f(\tau) + \int P^\dagger(\underline{r}, E') C^\dagger(\underline{r}, E' \rightarrow E, \underline{\Omega}' \rightarrow \underline{\Omega}) \xi^\dagger(\underline{r}, E', \underline{\Omega}') dE' d\Omega' \quad (3.30)$$

$$\xi^\dagger(\tau) = \int T^\dagger(\underline{r}' \rightarrow \underline{r}, E, \underline{\Omega}) \theta^\dagger(\underline{r}', E, \underline{\Omega}) dV' \quad (3.31)$$

These equations show analogy with the relations between ψ and χ for the neutron game as given by Eqs.(2.10) and (2.11). For the neutron game the weight factor Σ_s/Σ_t for a non-analog Monte Carlo game is included in the unnormalized neutron collision kernel C . The simulation of ξ^\dagger , θ^\dagger and μ^\dagger is schematically given in Fig. 4.

Although the simulation of these equations shows a close analogy with the simulation of the neutron transport equations, an important difference is the fact that the adjoint weight factor P^\dagger needs not to be less than unity. We may therefore expect under certain circumstances that the weight of the adjoint particle increases much above unity during a random walk. This can influence the statistics in an unfavourable way. So it is necessary to gain more

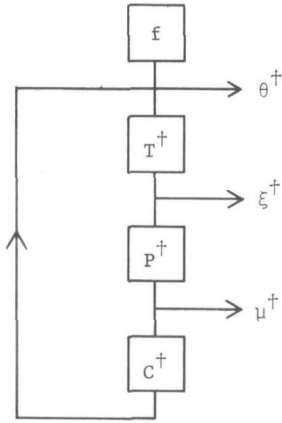


Fig. 4. Simulation of $\xi^\dagger, \theta^\dagger$ and μ^\dagger

insight in the behaviour of the adjoint weight factor P^\dagger and hence in the properties of the adjoint cross section.

III.2. Analysis of the adjoint cross section

The adjoint cross section for a certain reaction type as defined by Eq.(3.15) not only depends on the normal cross section for that reaction but also on the type of reaction and the anisotropy of the scattering. To gain more insight into the properties of the adjoint cross section we shall calculate it for a few typical cases. In each case the scattering is assumed to be isotropic in the centre of mass system.

As a first example we calculate the adjoint cross section for elastic scattering and a constant scattering cross section σ_{se} . For isotropic scattering, the scattering function is given by [4]

$$f_{se}(E \rightarrow E') = \begin{cases} \frac{1}{E(1-\alpha)} & \alpha E \leq E' \leq E \\ 0 & \text{else} \end{cases} \quad (3.32)$$

with

$$\alpha = \left(\frac{A-1}{A+1} \right)^2 \quad (3.33)$$

and A the ratio of the atomic mass of the nuclide to the neutron mass. Now we have

$$\sigma_{se}^{\dagger}(E') = \int_{E'}^{E'/\alpha} \sigma_{se} \frac{1}{E(1-\alpha)} dE = \sigma_{se} \frac{\ln 1/\alpha}{1-\alpha} \quad (3.34)$$

So, the adjoint cross section for this case is also constant in energy and differs from the scattering cross section by a factor

$$\gamma = \frac{\ln 1/\alpha}{1-\alpha} \quad (3.35)$$

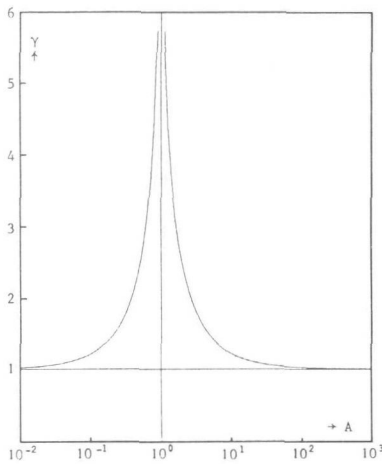


Fig. 5. γ as a function of A

Fig.5 shows the dependence of γ on A . For heavy nuclei γ approaches unity, but for light nuclei γ becomes large. In the case of hydrogen, γ becomes infinite if one neglects the mass difference between a proton and a neutron. If the proper atomic mass for hydrogen is taken into account γ becomes 15.57 for this case.

If we have a medium with only one elastic scatterer with constant scattering cross section and if there is no absorption, the adjoint weight factor P^{\dagger} is equal to

$$P^\dagger = \frac{\sigma_{se}^\dagger}{\sigma_t} = \frac{\sigma_{se}^\dagger}{\sigma_s} = \gamma \quad (3.36)$$

and is greater than unity for every nuclide. Thus the weight of the adjoint particle will increase at every collision and may become very large, especially if the adjoint particle collides with light nuclei. This mere fact needs not to result in large variances as long as all adjoint particles suffer about the same number of collisions in a history. However, if a system is composed of two or more nuclides with widely different masses, then the weight of an adjoint particle during its history strongly depends on the number of collisions made with the various nuclides present in the system and large variances are to be expected. If the absorption cross section is not negligible compared with the scattering cross section, as is generally the case at lower and thermal energies the adjoint weight factor P^\dagger may be well below unity and the effect on the weight of the adjoint particle is comparable with that of the non-absorption factor Σ_s/Σ_t in the neutron game.

A second case of interest is the behaviour of the adjoint elastic cross section and the adjoint weight factor when the cross section exhibits a scattering resonance. It will be sufficient here to study one isolated scattering resonance without Doppler broadening and phase shift factors but with interference between resonance and potential (background) cross section. The scattering cross section can then be written as [12]

$$\sigma_{se}(E) = \sigma_p + \frac{\sigma_{so}}{1 + \left(\frac{E-E_r}{\Gamma/2}\right)^2} + 2\sqrt{\sigma_{so}\sigma_p} \frac{(E-E_r)/(\Gamma/2)}{1 + \left(\frac{E-E_r}{\Gamma/2}\right)^2} \quad (3.37)$$

with σ_p the constant potential cross section

E_r the resonance energy

Γ the total width of the resonance

σ_{so} the resonance scattering cross section at the resonance

energy and the spin factor assumed to be unity in the interference term. The form of the adjoint cross section as a function of energy depends on the width of the resonance in comparison with the maximum energy loss of a neutron (or the maximum energy gain of the adjoint particle) in a collision. With the scattering function of Eq.(3.32) for elastic scattering, the adjoint cross section can be calculated analytically and is shown in Fig. 6 as a function of the dimensionless quantity $x=2(E-E_r)/\Gamma$ for various values of the parameter $q=2E_r(1-\alpha)/\Gamma$, the ratio of the maximum neutron energy loss at the resonance energy to the resonance half width. Yet the adjoint cross section depends

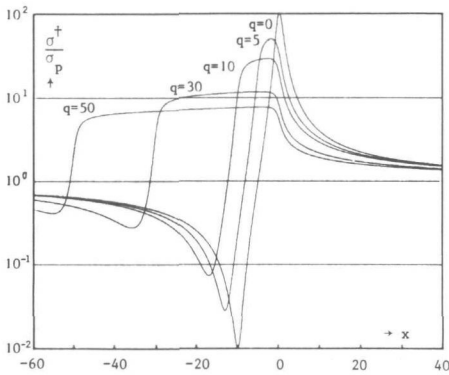


Fig. 6. Adjoint cross section at a scattering resonance

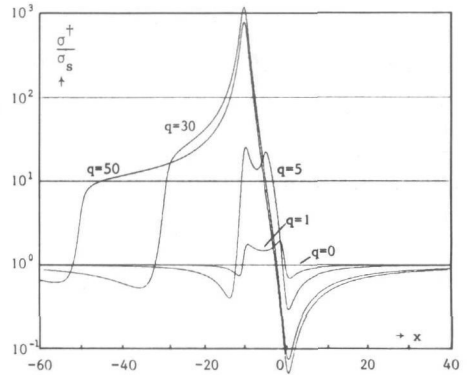


Fig. 7. Adjoint weight factor at a scattering resonance

on the atomic mass A only slightly and is therefore given for one value of A . In the limiting case $q=0$ the adjoint cross section becomes identical with the neutron scattering cross section which is also shown in Fig. 6. For small q the adjoint cross section resembles the scattering cross section but the figure is shifted to lower energies about half the integration interval. For large q the adjoint cross section will be about constant when the major part of the resonance lies within the integration interval. Then the resonance part of the adjoint cross section can be approximated by

$$\sigma_{\text{res}}^{\dagger}(E') \approx \int_{E'}^{E'/\alpha} \frac{\sigma_{\text{so}}}{1 + \left(\frac{E-E_r}{\Gamma/2}\right)^2} \frac{dE}{E(1-\alpha)} \approx \int_{-\infty}^{\infty} \frac{\sigma_{\text{so}}}{1+x^2} \frac{\Gamma/2}{E_r(1-\alpha)} dx = \frac{\pi\sigma_{\text{so}}}{q} \quad (3.38)$$

Because the interference term is an odd function in $E-E_r$, its contribution is neglected here. This approximation will roughly be valid for $\alpha E_r < E' < E_r$ and large q .

Again assuming a medium with only one nuclide and no absorption, we can calculate the adjoint weight factor $P^{\dagger}(E) = \sigma^{\dagger}(E) / \sigma_s(E)$, which is shown in Fig. 7. P^{\dagger} shows a minimum about the minimum of the adjoint cross section due to the interference of the resonance and potential cross section. About the interference minimum P^{\dagger} shows a maximum because of the small value of σ_s . About the resonance energy P^{\dagger} shows again a minimum due to the large scattering cross section and the decreasing adjoint cross section. The numerical value of P^{\dagger} at its maximum and minima strongly depends on the ratio $\sigma_{\text{so}} / \sigma_p$, which has been taken 100 in Fig. 6 and 7. For nuclides with much smaller ratio of $\sigma_{\text{so}} / \sigma_p$, for example ^{235}U and nuclides from construction materials as Cr, Fe and Ni, the variations in P^{\dagger} are much less pronounced. Fig. 6 and 7 are representative for several predominantly scattering resonances of ^{238}U at room temperature, with the resonances at low energies having a small value of q and the resonances at higher energies having larger values of q . For the predominantly absorption resonances σ_t near the resonance energy is much larger than σ_s . This results in a much lower maximum value of P^{\dagger} , possibly well below unity, because the total cross section at the interference minimum of the scattering cross section is now mainly determined by the absorption cross section and in a lower minimum about the resonance energy because of the much larger value of σ_t at the resonance energy.

As a third typical example for the calculation of the adjoint cross section we consider the case of inelastic level scattering. The scattering function for inelastic level scattering is derived in

section 4 of this chapter. For isotropic scattering it is given by

$$f_{si}(E \rightarrow E') = \frac{1}{E(1-\alpha)\sqrt{1-\epsilon/E}} \quad (3.39)$$

for the energy range

$$\left(\frac{A\sqrt{1-\epsilon/E}-1}{A+1} \right)^2 E \leq E' \leq \left(\frac{A\sqrt{1-\epsilon/E}+1}{A+1} \right)^2 E \quad (3.40)$$

and zero outside. We take for convenience the inelastic scattering cross section constant for energies above ϵ and equal to σ_{si} . In appendix B it is shown that then the adjoint inelastic cross section is constant for energies above $\epsilon/(A+1)^2$ and equal to

$$\sigma_{si}^{\dagger}(E') = \sigma_{si} \frac{\ln 1/\alpha}{1-\alpha} = \gamma \sigma_{si} \quad E' > \epsilon/(A+1)^2 \quad (3.41)$$

For energies below $\epsilon/(A+1)^2$ the adjoint cross section goes down to zero as shown in Fig. 8. To demonstrate the possible effect on the adjoint weight factor, we assume again a medium without absorption, with one nuclide that has the above mentioned inelastic cross section and a constant elastic cross section σ_{se} . The adjoint

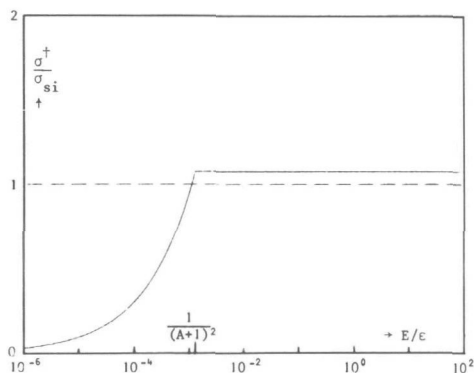


Fig. 8. Adjoint inelastic cross section

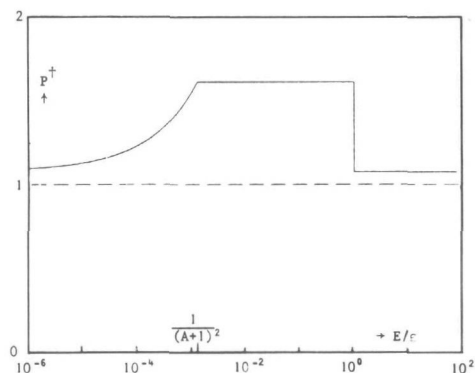


Fig. 9. Adjoint weight factor with inelastic scattering

elastic cross section is equal to $\sigma_{se}^{\dagger} = \gamma \sigma_{se}$ for all energies, with the factor γ given by Eq.(3.35). Then $P^{\dagger}(E) = (\sigma_{si}^{\dagger}(E) + \sigma_{se}^{\dagger}) / \sigma_t(E) = \gamma$ for $E > \epsilon$. For $\epsilon / (A+1)^2 < E < \epsilon$ we have

$$P^{\dagger} = \gamma \left(1 + \frac{\sigma_{si}}{\sigma_{se}} \right) \quad (3.42)$$

So, for heavy nuclides the adjoint weight factor may be much greater than unity for a very large energy range if the inelastic cross section above the threshold energy forms a substantial part of the total scattering cross section. The adjoint weight factor for this case is shown in Fig. 9.

The assumption of a constant inelastic scattering cross section from the threshold energy is physically rather unrealistic. In practice the inelastic scattering cross section increases only slowly from zero at the theoretical threshold or even from a higher energy. This results in a more rapid fall off of the adjoint inelastic cross section at lower energies than in Fig. 8 and the adjoint weight factor will be continuous at the threshold energy. However, the adjoint weight factor may still be greater than unity for a large energy range. As an example of a realistic case the adjoint weight factor for carbon with one inelastic level is shown in Fig. 10.

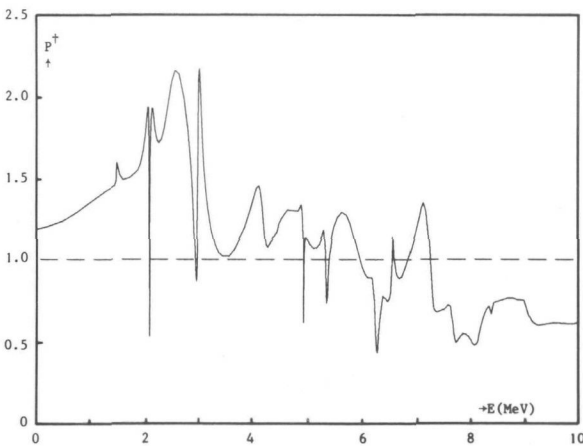


Fig. 10. Adjoint weight factor for ^{12}C

It will be clear from these examples that there are many cases in which the adjoint weight factor P^\dagger of a medium is greater than unity. Then the weight of the adjoint particle will show large differences from one history to another and large variances are to be expected. Therefore we shall study other transformations than that of Eq.(3.1) to diminish this disadvantage.

III.3. Other transformations of the adjoint equation

As pointed out in section II.3 the adjoint kernel interpreted in a Monte Carlo sense, depends upon the variables used in the neutron transport kernel, from which the adjoint kernel is obtained. If we had used from the beginning the lethargy u instead of the energy E , defined by

$$u = \ln \frac{E_0}{E} \quad (3.43)$$

with E_0 some reference energy and had carried out the same analysis as in section 1 of this chapter, we would have arrived at the adjoint equation in lethargy and the following definition for the adjoint cross section

$$\sigma_{j,A}^\dagger(u') = \int \sigma_{j,A}(u) c_{j,A}(u) f_{j,A}(u \rightarrow u') du \quad (3.44)$$

On physical grounds we have

$$f_{j,A}(u \rightarrow u') = f_{j,A}(E \rightarrow E') \left| \frac{dE'}{du'} \right| = E' f_{j,A}(E \rightarrow E') \quad (3.45)$$

If we use again the energy as the integration variable in the right hand side of Eq.(3.44) we arrive at a different definition for the adjoint cross section, which we shall call

$$\text{definition II: } \sigma_{j,A}^{\dagger}(E') = \int \sigma_{j,A}(E) c_{j,A}(E) f_{j,A}(E \rightarrow E') \frac{E'}{E} dE \quad (3.46)$$

as distinct from the definition of Eq.(3.15), which we shall call definition I henceforth.

The introduction of other variables instead of the energy, for instance the neutron speed, will lead to a new definition for the adjoint cross section and a new adjoint equation. Instead of transforming it back to energy, it is possible to obtain the new adjoint equation directly from Eq.(2.53). To arrive at definition II for the adjoint cross section we introduce the following transformation of Eq.(2.53)

$$\zeta^{\dagger}(\tau) = \Sigma_t(\tau) \chi^{\dagger}(\tau) / E \quad (3.47)$$

$$M^{\dagger}(\tau' \rightarrow \tau) = \frac{E'}{E} \frac{\Sigma_t(\tau)}{\Sigma_t(\tau')} K^{\dagger}(\tau' \rightarrow \tau) \quad (3.48)$$

to obtain the transformed adjoint equation

$$\zeta^{\dagger}(\tau) = \Sigma_t(\tau) h(\tau) / E + \int M^{\dagger}(\tau' \rightarrow \tau) \zeta^{\dagger}(\tau') d\tau' \quad (3.49)$$

F can now be obtained from

$$F = \int \frac{ES(\tau)}{\Sigma_t(\tau)} \zeta^{\dagger}(\tau) d\tau \quad (3.50)$$

For a Monte Carlo simulation of Eq.(3.49) we have to sample the kernel M^{\dagger} which can be factored into

$$M^{\dagger}(\tau' \rightarrow \tau) = P^{\dagger}(\underline{r}', E') D^{\dagger}(\underline{r}', E' \rightarrow E, \underline{\Omega}' \rightarrow \underline{\Omega}) T^{\dagger}(\underline{r}' \rightarrow \underline{r}, E, \underline{\Omega}) \quad (3.51)$$

with

$$\begin{aligned}
& D^\dagger(\underline{r}', E' \rightarrow E, \underline{\Omega}' \rightarrow \underline{\Omega}) \\
&= \sum_A N_A(\underline{r}') \sum_j \sigma_{j,A}^{(E)} c_{j,A}^{(E)} f_{j,A}^{(E \rightarrow E', \underline{\Omega}' \rightarrow \underline{\Omega}')} \frac{E'}{E} / \Sigma^\dagger(\underline{r}', E') \\
&= \sum_A P_A^\dagger(\underline{r}', E') \sum_j P_{j,A}^\dagger(E') \frac{\sigma_{j,A}^{(E)} c_{j,A}^{(E)} f_{j,A}^{(E \rightarrow E', \underline{\Omega}' \rightarrow \underline{\Omega}')}}{\sigma_{j,A}^\dagger(E')} \frac{E'}{E} \quad (3.52)
\end{aligned}$$

and T^\dagger and P^\dagger given by Eqs.(3.9) and (3.8) respectively. The probabilities p_A^\dagger and $p_{j,A}^\dagger$ are the same as those defined by Eqs.(3.20) and (3.21) with Eqs.(3.16) to (3.18) still holding, but $\sigma_{j,A}^\dagger$ not yet defined. The sampling procedure for M^\dagger is the same as for the kernel L^\dagger , discussed in section 1 of this chapter. Only the pdf for selection of E and $\underline{\Omega}$ for given A and j is different, namely

$$p(E, \underline{\Omega} | j, A) = \frac{\sigma_{j,A}^{(E)} c_{j,A}^{(E)} f_{j,A}^{(E \rightarrow E', \underline{\Omega}' \rightarrow \underline{\Omega}')}}{\sigma_{j,A}^\dagger(E')} \frac{E'}{E} \quad (3.53)$$

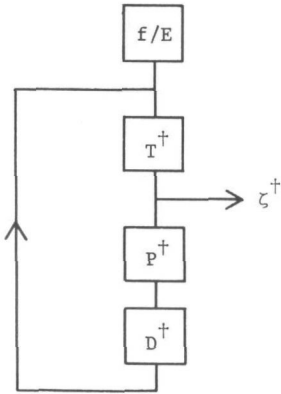
To let p be a normalized pdf the adjoint cross section $\sigma_{j,A}^\dagger$ must be defined according to Eq.(3.46). So, the transformation of Eq.(3.47) leads to definition II for the adjoint cross section.

The source term $\Sigma_t(\tau)h(\tau)/E$ in Eq.(3.49) can be written as

$$\frac{\Sigma_t(\tau)h(\tau)}{E} = \int \frac{f(\underline{r}', E, \underline{\Omega})}{E} T^\dagger(\underline{r}' \rightarrow \underline{r}, E, \underline{\Omega}) dV' \quad (3.54)$$

The source term is sampled by selecting \underline{r}' , E and $\underline{\Omega}$ from $f(\underline{r}', E, \underline{\Omega})/E$ and sampling the kernel T^\dagger . The sampling of ζ^\dagger is summarized in Fig. 11.

To judge the differences between the estimation of F via simulation of ζ^\dagger from Eq.(3.49) and via simulation of ξ^\dagger from Eq.(3.3) we have to look again at the behaviour of the adjoint cross section, now

Fig. 11. Simulation of ζ^\dagger

according to definition II. For the case of a constant elastic scattering cross section σ_{se} with isotropic scattering in the centre of mass system we have

$$\sigma_{se}^\dagger(E') = \int_{E'}^{E'/\alpha} \sigma_{se} \frac{1}{E(1-\alpha)} \frac{E'}{E} dE = \sigma_{se} \frac{E'}{1-\alpha} \left(\frac{1}{E'} - \frac{\alpha}{E'} \right) = \sigma_{se} \quad (3.55)$$

If the scattering is not isotropic, this result still holds for any degree of anisotropy, as can be seen as follows. If the probability for scattering through an angle of cosine μ_c in the centre of mass system is given by $p(\mu_c)$, the adjoint cross section becomes

$$\sigma_{se}^\dagger(E') = \int_{E'}^{E'/\alpha} \sigma_{se} \frac{2p[\mu_c(E, E')]}{E(1-\alpha)} \frac{E'}{E} dE \quad (3.56)$$

The relation between μ_c , E and E' [4] can be written as

$$E = \frac{2E'}{1+\alpha+(1-\alpha)\mu_c} \quad (3.57)$$

If we change the integration variable in Eq.(3.56) from E to μ_c we have

$$\left| \frac{dE}{d\mu_c} \right| = \frac{2E'(1-\alpha)}{\{1+\alpha+(1-\alpha)\mu_c\}^2} = \frac{(1-\alpha)E^2}{2E'} \quad (3.58)$$

and

$$\sigma_{se}^+(E') = \sigma_{se} \int_{-1}^{+1} p(\mu_c) d\mu_c = \sigma_{se} \quad (3.59)$$

For this case there is no difference between the adjoint weight factor P^\dagger and the scattering probability Σ_s/Σ_t in the neutron game, which is a substantial improvement with regard to definition I for the adjoint cross section, especially for light nuclides. If the scattering cross section $\sigma_s(E)$ increases with energy for a certain energy range, the adjoint cross section can still be greater than the scattering cross section. However, in general the elastic scattering cross section tends to decrease slowly with energy, except for resonances, and the adjoint elastic cross section will be somewhat smaller than the scattering cross section.

The case of resonance scattering does not show much difference because the factor E'/E in definition II is much less important than the rapid change of the scattering cross section $\sigma_s(E)$ with energy. So, large fluctuations in the adjoint weight factor in the resonance region are still to be expected.

In the case of inelastic scattering the factor E'/E is very important because E' and E can differ very much. For a constant inelastic cross section above the threshold energy the adjoint inelastic cross section is given in Fig. 12. For energies much higher than the threshold energy the adjoint cross section approaches the value of the constant inelastic scattering cross section. At the threshold energy the adjoint cross section is roughly half the scattering cross section. As a consequence the adjoint weight factor will be much less than for definition I at energies about the threshold. For a non-absorbing nuclide with

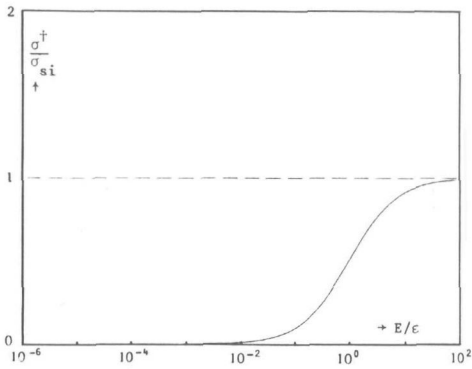


Fig. 12. Adjoint inelastic cross section according to definition II

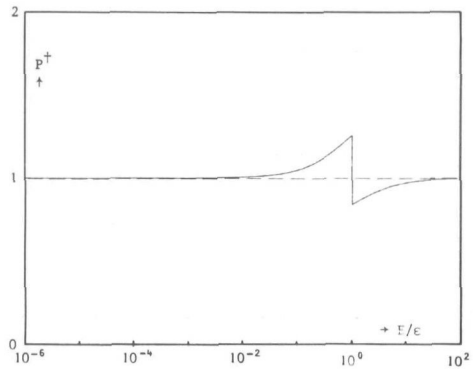


Fig. 13. Adjoint weight factor with inelastic scattering

such an inelastic scattering cross section and a constant elastic scattering cross section, the adjoint weight factor is shown in Fig. 13 with the maximum and minimum value of P^{\dagger} depending on the ratio of the inelastic to the elastic cross section. Because the adjoint inelastic cross section at the threshold energy is about half the inelastic scattering cross section above the threshold, the maximum value of P^{\dagger} is about

$$\max P^{\dagger} \approx 1 + 0.5 \frac{\sigma_{si}}{\sigma_{se}} \quad (3.60)$$

From a comparison with Fig. 9 and Eq.(3.42) it is clear that the maximum value of P^{\dagger} is much lower than for definition I and the energy range for which P^{\dagger} is noticeably greater than unity is very much smaller than for definition I.

In Fig. 14 the adjoint weight factor P^{\dagger} is shown for carbon with the adjoint cross sections according to definition II. This figure is to be compared with Fig. 10 for definition I.

To demonstrate the advantages of the use of definition II for the adjoint cross section over definition I, we calculated the flux at the centre of a sphere containing a fictitious non-absorbing

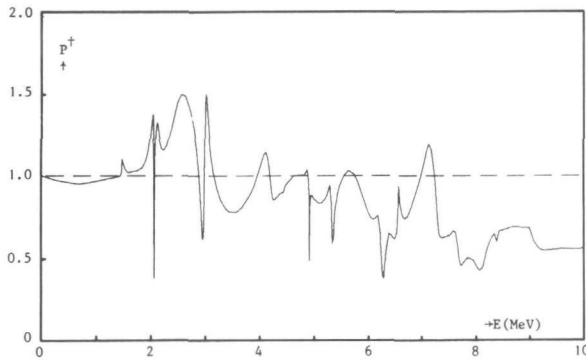


Fig. 14. Adjoint weight factor for ^{12}C according to definition II

nuclide with a constant elastic scattering cross section and a constant inelastic scattering cross section from the threshold energy. The level energy was chosen to be 1 MeV and the value of the inelastic cross section half that of the elastic cross section. The mass of the nuclide relative to the neutron mass was chosen to be 27. The system consisted of a homogeneous sphere with a radius of 5 mean free paths at energies below the inelastic threshold. An uniform and isotropic artificial neutron source with a fission spectrum was assumed in the sphere. In table II the flux per unit lethargy per source neutron at the centre of the sphere is given for the energy groups 0.1-0.2 MeV, 0.4-0.8 MeV and 1.4-2.5 MeV with their standard deviations after processing of 1000 particles in the adjoint game. The reduction of the variance in the flux calculation

Table II. Comparison of the use of definition I and II

energy range (MeV)	definition I		definition II	
	flux per unit lethargy	standard deviation	flux per unit lethargy	standard deviation
0.1 - 0.2	$5.55 \cdot 10^{-3}$	32 %	$6.89 \cdot 10^{-3}$	6.2 %
0.4 - 0.8	$9.15 \cdot 10^{-3}$	8.6 %	$9.26 \cdot 10^{-3}$	2.6 %
1.4 - 2.5	$2.79 \cdot 10^{-3}$	1.6 %	$2.79 \cdot 10^{-3}$	0.8 %

with definition II for the adjoint cross section is clear, especially at lower energies, as was to be expected from the above considerations.

The transformation of Eq.(3.47) leading to definition II for the adjoint cross section is, in fact, a form of energy importance sampling of Eq.(3.3) for ξ^\dagger . One may ask for the best energy importance function and the accompanying definition for the adjoint cross section. This question has been answered by Coveyou et al [13] for importance sampling of the neutron transport equation and their solution can be applied to our case. However, the solution for the best importance function in the sense of minimum variance in F is difficult to obtain in practice and depends on the system under consideration and the quantity to be calculated. Therefore it is more advantageous to choose on general grounds one of the possible transformed adjoint equations and use this equation for all problems to be solved by adjoint Monte Carlo. Then the definition for the adjoint cross section is fixed and problem independent. So the adjoint cross sections need to be calculated only once and can be kept in a nuclear data file together with the neutron cross sections.

Compared to other possible definitions for the adjoint cross section our definition II has the property that for a constant elastic cross section the adjoint cross section is equal to the scattering cross section, which is an important property because for a large energy range elastic scattering is the major or only scattering reaction. For other definitions the adjoint cross section will only approach the scattering cross section for heavy nuclides but may differ very well from it for light nuclides. Besides, definition II results in an inelastic adjoint cross section that resembles the inelastic scattering cross section to some extent. We therefore adopt the adjoint equation Eq.(3.49) and the accompanying definition II of Eq.(3.46) for the adjoint cross section as the one generally suitable for adjoint Monte Carlo calculations and the rest of this study will be based on this transformation.

III.4. Sampling the adjoint collision kernel

The adjoint collision kernel D^\dagger as given by Eq.(3.52) with adjoint cross sections evaluated according to definition II can be sampled by selection of a nuclide A with probability proportional to its total macroscopic adjoint cross section Σ_A^\dagger and for this nuclide selection of a reaction type j with probability proportional to its partial microscopic adjoint cross section $\sigma_{j,A}^\dagger$. Then energy and direction of the adjoint particle must be selected from the normalized pdf given by Eq.(3.53).

$$p(E, \underline{\Omega} | j, A) = \frac{\sigma_{j,A}(E) c_{j,A}(E) f_{j,A}(E \rightarrow E', \underline{\Omega} \rightarrow \underline{\Omega}')}{\sigma_{j,A}^\dagger(E')} \frac{E'}{E} \quad (3.61)$$

Now we shall discuss the selection of E and $\underline{\Omega}$ from this pdf in more detail. For convenience of notation we shall drop the indices j and A in this section.

If the neutron scattering process is described by a model in which there is no relation between energy degradation and scattering angle we can write for the scattering function

$$f(E \rightarrow E', \underline{\Omega} \rightarrow \underline{\Omega}') = f(E \rightarrow E') g(\underline{\Omega} \rightarrow \underline{\Omega}') \quad (3.62)$$

This will be the case for inelastic continuum scattering, (n,2n) reactions, etc. The function $g(\underline{\Omega} \rightarrow \underline{\Omega}')$ is normalized if integrated over $\underline{\Omega}'$. Often the scattering is assumed to be isotropic in the laboratory system and $g(\underline{\Omega} \rightarrow \underline{\Omega}')$ equals

$$g(\underline{\Omega} \rightarrow \underline{\Omega}') = \frac{1}{4\pi} \quad (3.63)$$

and is also normalized when considered as a pdf for $\underline{\Omega}$. Otherwise g will depend only on the scattering angle between $\underline{\Omega}$ and $\underline{\Omega}'$ and we

have

$$g(\underline{\Omega} \rightarrow \underline{\Omega}') = g(\underline{\Omega}, \underline{\Omega}') = g(\underline{\Omega}' \rightarrow \underline{\Omega}) \quad (3.64)$$

Then g is also a normalized pdf for $\underline{\Omega}$ and $\underline{\Omega}$ is selected exactly as in the neutron game. Now the pdf for E becomes

$$p(E) = \frac{\sigma(E)c(E)f(E \rightarrow E')}{\sigma^+(E')} \frac{E'}{E} \quad (3.65)$$

In case of the above mentioned reaction types an evaporation spectrum is often assumed for the energy transfer function

$$f(E \rightarrow E') = \frac{E' \exp\{-E'/\theta(E)\}}{\theta^2(E) \left(1 - \left\{1 + \frac{E-E_0}{\theta(E)}\right\} \exp\left\{-\frac{E-E_0}{\theta(E)}\right\}\right)} \quad 0 < E' < E - E_0 \quad (3.66)$$

where E_0 is the minimum energy needed for the reaction. $\theta(E)$ is the nuclear temperature, which depends on the energy of the neutron before collision. If $f(E \rightarrow E')$ is known, the adjoint cross section can be calculated according to Eq.(3.46). In case of the evaporation spectrum of Eq.(3.66) the range for E is $E' + E_0 \leq E < \infty$. Although the integral in the definition for the adjoint cross section generally will exist because the nuclear temperature $\theta(E)$ increases with energy, it is more practical to introduce an upper limit in the integration equal to or greater than the largest energy of interest in the problem at hand, that is the energy above which the scoring function and hence the physical neutron source S is assumed to be zero. In the neutron problem there can be no neutrons above this energy, so the cross section above this energy is irrelevant and we may assume the cross section to be zero, which justifies the introduction of this energy as the upper limit in the integral for the adjoint cross section. In order to keep the adjoint cross section problem independent the upper energy should be chosen such that it can be used for all practical reactor problems, which means

15 or 20 MeV.

Because $\sigma(E)$ and $\sigma^+(E')$ are mostly known in tabular form, a practical way for selecting E from Eq.(3.65) is the method of interpolation from probability tables. If the range for E is between E_{\min} and E_{\max} it is possible to calculate a set of $N+1$ energies E_n ($n=0,1,\dots,N$) for which

$$\int_{E_{\min}}^{E_n} p(E)dE = b_n \quad n=1,2,\dots,N-1 \quad (3.67)$$

with b_n some predetermined value, and $E_0=E_{\min}$ and $E_N=E_{\max}$. For convenience b_n may be taken as

$$b_n = \frac{n}{N} \quad (3.68)$$

The integrals in Eq.(3.67) are parts of the integral in the definition for the adjoint cross section. Hence the calculation of the energies E_n and the adjoint cross section should be combined and need to be done only once for each reaction type, because these quantities are problem independent.

If there exist a relation between energy degradation and scattering angle as in the case for neutron elastic and inelastic level scattering the computation of the adjoint cross section is more complicated. We shall consider here the case of inelastic level scattering. Then elastic scattering is automatically included by setting the level energy to zero. Because the relevant formulae are seldomly found in standard text books on reactor physics, a derivation of the relation between energy degradation and scattering angle is given in appendix A. If the inelastic level has an excitation energy Q , the neutron must have at least an energy

$$\epsilon = \frac{A+1}{A} Q \quad (3.69)$$

with A the mass of the target nucleus relative to the neutron mass. As derived in appendix A the energy E' after an inelastic neutron collision is given by

$$E' = \frac{A^2(1-\epsilon/E) + 2A\mu_c \sqrt{1-\epsilon/E} + 1}{(A+1)^2} E \quad (3.70)$$

with E the energy of the neutron before collision and μ_c the cosine of the scattering angle in the centre of mass system. The relation with the laboratory system is given by

$$\mu_o = \frac{A\mu_c \sqrt{1-\epsilon/E} + 1}{\sqrt{A^2(1-\epsilon/E) + 2A\mu_c \sqrt{1-\epsilon/E} + 1}} \quad (3.71)$$

with $\mu_o = \underline{\Omega} \cdot \underline{\Omega}'$ the cosine of the scattering angle in the laboratory system. The angular dependence of the scattering function is most often described in the centre of mass system by a function $f^c(E, \mu_c)$, denoting the probability for scattering of a neutron with energy E through an angle of cosine μ_c in the centre of mass system. Then

$$f^c(E \rightarrow E', \mu_c) = f^c(E, \mu_c) \delta\left(E' - \frac{A^2(1-\epsilon/E) + 2A\mu_c \sqrt{1-\epsilon/E} + 1}{(A+1)^2} E\right) \quad (3.72)$$

and for the energy transfer function $f(E \rightarrow E')$ we obtain

$$\begin{aligned} f(E \rightarrow E') &= \int f(E \rightarrow E', \underline{\Omega} \rightarrow \underline{\Omega}') d\Omega' = \int f(E \rightarrow E', \mu_o) d\mu_o = \int f^c(E \rightarrow E', \mu_c) d\mu_c \\ &= f^c(E, \mu_c [E, E']) \frac{(A+1)^2}{2AE\sqrt{1-\epsilon/E}} = \frac{2}{E(1-\alpha)\sqrt{1-\epsilon/E}} f^c(E, \mu_c [E, E']) \quad (3.73) \end{aligned}$$

In appendix A the range for E' is given for fixed E . However, for the computation of the adjoint cross section we must know the range for E for fixed E' . From Fig. A4 in appendix A we see that E is uniquely determined by E' and μ_c only for $E' > \epsilon/(A+1)^2$. But as a function of E' and μ_o E is uniquely determined for all values of E' . From Eqs.(3.70) and (3.71) E is obtained as a function of E' and μ_o

$$E = \left\{ (A+1)^2 (A^2 + 2\mu_0^2 - 1) E' + A^2 (A^2 - 1) \epsilon \right. \\ \left. - 2\mu_0 (A+1) \sqrt{(A+1)^2 (A^2 + \mu_0^2 - 1) E'^2 + A^2 (A^2 - 1) \epsilon E'} \right\} / (A^2 - 1)^2 \quad (3.74)$$

By setting $\mu_0 = +1$ and -1 respectively the minimum and maximum value E_{\min} and E_{\max} for E are obtained. The adjoint cross section for inelastic level scattering is then obtained as

$$\sigma_{si}^\dagger(E') = \int_{E_{\min}}^{E_{\max}} \sigma_{si}(E) \frac{E'}{E^2 (1-\alpha) \sqrt{1-\epsilon/E}} 2f^c(E, \mu_c [E, E']) dE \quad (3.75)$$

Often the function $f^c(E, \mu_c)$ is expanded into a series of Legendre polynomials

$$f^c(E, \mu_c) = \sum_{\ell} \frac{2\ell+1}{2} f_{\ell}^c(E) P_{\ell}(\mu_c) \quad (3.76)$$

with $f_{\ell}^c(E)$ the Legendre components in the centre of mass system. $P_{\ell}(\mu_c)$ denotes the ℓ -th order Legendre polynomial. If the scattering is described in the laboratory system by a function $f(E, \mu_0)$ we have

$$f^c(E, \mu_c) = f(E, \mu_0) \left| \frac{\partial \mu_0(E, \mu_c)}{\partial \mu_c} \right| \quad (3.77)$$

$f(E, \mu_0)$ may also be given as a series expansion

$$f(E, \mu_0) = \sum_{\ell} \frac{2\ell+1}{2} f_{\ell}(E) P_{\ell}(\mu_0) \quad (3.78)$$

with $f_{\ell}(E)$ the Legendre components in the laboratory system. If in this case the integrand of the integral in the right hand side of Eq.(3.75) has to be evaluated for a certain value of E , μ_c is calculated from Eq.(3.70) and μ_0 then follows from Eq.(3.71). From

Eqs.(3.78) and (3.77) $f^c(E, \mu_c)$ can be calculated. To sample E and $\underline{\Omega}$ from the pdf which is given in general form by Eq.(3.61) we first calculate the pdf for E only by integrating over $\underline{\Omega}$

$$p(E) = \frac{\sigma(E)f(E \rightarrow E')}{\sigma^\dagger(E')} \frac{E'}{E} = \frac{\sigma(E)}{\sigma^\dagger(E')} \frac{2E'}{E^2(1-\alpha)\sqrt{1-\epsilon/E}} f^c(E, \mu_c[E, E']) \quad (3.79)$$

As in the case of inelastic continuum scattering and $(n, 2n)$ reactions, it is most convenient to calculate a set of values E_n for which the cumulative probability distribution has prescribed values and to tabulate the values of E_n as a function of E' to select E from the pdf of Eq.(3.79). Once E is selected, μ_c and μ_o can be calculated and from this the direction $\underline{\Omega}$ of the adjoint particle after the collision can be determined.

An other possibility is to choose $\underline{\Omega}$ first from the proper pdf and then calculate the energy E . Because E is uniquely determined by E' and μ_o it is most easy to select first μ_o in stead of μ_c . Then E can be obtained from Eq.(3.74). The pdf for $\underline{\Omega}$ is obtained by integrating Eq.(3.61) over energy

$$\begin{aligned} p(\underline{\Omega}) &= \frac{1}{2\pi\sigma^\dagger(E')} \int \sigma(E)f(E \rightarrow E', \mu_o) \frac{E'}{E} dE \\ &= \frac{1}{2\pi\sigma^\dagger(E')} \int \sigma(E)f(E, \mu_o) \delta\left(E' - \frac{A^2(1-\epsilon/E) + 2A\mu_c\sqrt{1-\epsilon/E} + 1}{(A+1)^2} E\right) \frac{E'}{E} dE \quad (3.80) \end{aligned}$$

The factor $1/2\pi$ arises because the scattering is assumed to be azimuthally symmetric. Without this factor we have the pdf for μ_o . With the substitution for E

$$E''(E, \mu_o) = \frac{A^2(1-\epsilon/E) + 2A\mu_c(E, \mu_o)\sqrt{1-\epsilon/E} + 1}{(A+1)^2} E \quad (3.81)$$

with independent E'' and μ_0 , $p(\mu_0)$ becomes

$$p(\mu_0) = \frac{1}{\sigma^\dagger(E')} \int \sigma(E[E'', \mu_0]) f(E[E'', \mu_0], \mu_0) \delta(E' - E'') \\ \cdot \frac{E'}{E(E'', \mu_0)} \left| \frac{\partial E(E'', \mu_0)}{\partial E''} \right| dE'' = \frac{\sigma(E)}{\sigma^\dagger(E')} f(E, \mu_0) \frac{E'}{E} \left| \frac{\partial E(E', \mu_0)}{\partial E'} \right| \quad (3.82)$$

where E now is a function of E' and μ_0 according to Eq.(3.74). If the scattering is given in the centre of mass system $p(\mu_0)$ reads

$$p(\mu_0) = \frac{\sigma(E)}{\sigma^\dagger(E')} \frac{E'}{E} \left| \frac{\partial E(E', \mu_0)}{\partial E'} \right| \left| \frac{\partial \mu_c(E, \mu_0)}{\partial \mu_0} \right| f^c(E, \mu_c[E, \mu_0]) \quad (3.83)$$

μ_0 always ranges from -1 to $+1$ irrespective of the value of E' . For elastic scattering the factor $\frac{E'}{E} \left| \frac{\partial E}{\partial E'} \right|$ is equal to unity.

To select μ_0 from this pdf tables can be set up with a set of values $\mu_{0,n}$ for which the cumulative distribution has prescribed values for a certain value of E' . However, the calculation of the cumulative distribution for μ_0 is no longer part of the calculation of the adjoint cross section from Eq.(3.75), as it was for the cumulative distribution of E . The function $p(\mu_0)$ which must be integrated is even more complicated than $p(E)$, especially if the angular dependence is given in the centre of mass system. If there are reasons to select first μ_0 in stead of E , for example if one wants to do directional importance sampling or for statistical estimation, the pdf for $\underline{\Omega}$ still plays a role. Also if one wants to avoid the use of probability tables either for E or for μ_0 and selects $\underline{\Omega}$ isotropically for convenience, a weight factor should be used equal to

$$w = 4\pi p(\underline{\Omega}) = 2 \frac{\sigma(E)}{\sigma^\dagger(E')} \frac{E'}{E} \left| \frac{\partial E(E', \mu_0)}{\partial E'} \right| \left| \frac{\partial \mu_c(E, \mu_0)}{\partial \mu_0} \right| f^c(E, \mu_c) \quad (3.84)$$

Although this method has the advantage that no two-dimensional tables are needed for selection of E or $\underline{\Omega}$ it has the disadvantage that it is probably a form of non-importance sampling and is likely to increase the variance. Besides, partial scattering cross sections are needed and all data to describe $f^c(E, \mu_c)$ or $f(E, \mu_0)$, so that this method can not be recommended.

Thermal group

For the neutron scattering function $f(E \rightarrow E')$ used in the above analysis, it was assumed that the target nucleus has an energy that is negligibly small compared to the neutron energy. However, if the source of adjoint particles $f(\tau)/E$ extends down to thermal energies, this scattering function can no longer be used to calculate the adjoint cross section at thermal energies and a more complicated scattering function which accounts for the thermal motion of the target nucleus and possible binding effects [4] has to be used. Although this presents no principal difficulties, it complicates the calculation of the adjoint cross section and the distribution of energies of the adjoint particles after a collision.

In Monte Carlo neutron transport calculations the simple model of a one-velocity thermal energy group is often used. A neutron belongs to the thermal group if it is scattered down below some energy E_c . Then the neutron is assumed to have a fixed energy E_{th} , which remains unchanged in a collision. Thus the scattering function for all nuclides is assumed to be

$$f(E \rightarrow E') = \delta(E' - E_{th}) \quad E < E_c \quad (3.85)$$

The cross sections used for neutrons in the thermal group need not to be equal to the cross sections at energy E_{th} , but are usually averaged over the thermal neutron spectrum.

The same results can be obtained by a second model for thermal neutrons with continuous energy, but with all cross sections independent of energy and equal to the averaged thermal cross sections.

Except for the condition that no upscattering to energies above E_c is allowed, the scattering function for each nuclide can be chosen arbitrarily in this model. Therefore the first model can be seen as a special case of this second model.

In the adjoint calculation the scattering function of Eq.(3.85) can not be used for the calculation of the adjoint cross section, because the δ -function does not depend on E . We therefore have to adopt the second model for thermal energies and choose the following simple scattering function for all nuclides

$$f(E \rightarrow E') = \delta(E' - E) \quad E < E_c \quad (3.86)$$

We restrict the analysis for the moment to a medium with one nuclide with microscopic thermal scattering cross section $\sigma_{s,th}$ for $E < E_c$. The adjoint elastic scattering cross section for thermal energies becomes

$$\sigma^\dagger(E') = \begin{cases} \sigma_{s,th} & E' \leq \alpha E_c \\ \sigma_{s,th} + \int_{E_c}^{E'/\alpha} \sigma_s(E) f(E \rightarrow E') \frac{E'}{E} dE & \alpha E_c < E' < E_c \end{cases} \quad (3.87)$$

The pdf for the energy E after a collision, if the adjoint particle has an energy $E' \leq \alpha E_c$ before the collision, is

$$p(E) = \frac{\sigma(E) f(E \rightarrow E') E' / E}{\sigma^\dagger(E')} = \delta(E - E') \quad E' \leq \alpha E_c \quad (3.88)$$

Thus the energy of the adjoint particle remains unchanged. For $\alpha E_c < E' < E_c$ $p(E)$ becomes

$$p(E) = \frac{\sigma_{s,th} \delta(E - E') + \sigma_s(E) f(E \rightarrow E') E' / E}{\sigma^\dagger(E')} \quad \begin{matrix} E' \leq E \leq E' / \alpha \\ \alpha E_c \leq E' < E_c \end{matrix} \quad (3.89)$$

From this pdf the probability for an adjoint particle to stay in the thermal group after a collision is

$$p_{th}(E') = \int_{E'}^{E_c} p(E) dE = \sigma_{s,th} / \sigma^{\dagger}(E') \quad (3.90)$$

Then its energy remains unchanged. The adjoint particle will leave the thermal group and get an epithermal energy with probability $p_{ep}(E') = 1 - p_{th}(E')$ and its energy is then selected from the pdf

$$p(E) = \frac{\sigma_s(E) f(E \rightarrow E') E' / E}{p_{ep}(E') \sigma^{\dagger}(E')} \quad E_c \leq E \leq E' / \alpha \quad (3.91)$$

Because the scoring function $ES(\tau) / \Sigma_t(\tau)$ in the adjoint game will normally be zero for thermal energies because of the physical neutron source S , adjoint particles born with energies below αE_c will never give a contribution to the desired quantity F , because they can not be upscattered to epithermal energies. Therefore the adjoint source $f(\tau) / E$ should be restricted to the energy range $E > \alpha E_c$.

For hydrogen $\alpha = 0$ and the source of adjoint particles extends down to zero energy, which makes the source density function divergent. If the energy of the adjoint particles is selected from some convergent pdf, e.g. a flat pdf between 0 and E_c , particles with low energies will have a large weight because of the factor $1/E$ in the adjoint source. However, for $E' \rightarrow 0$ the adjoint cross section $\sigma^{\dagger}(E')$ for hydrogen becomes equal to $\sigma_{s,th}$ and the probability $p_{ep}(E')$ goes to zero, so that these particles have a vanishing probability to make a contribution to the desired quantity.

If there are more nuclides present in the system, the source of adjoint particles must extend to $\alpha_{\min} E_c$ with α_{\min} belonging to lightest nuclide present in the total system.

CHAPTER IV

MULTIPLYING SYSTEMS¹

IV.1. Forward Monte Carlo methods for multiplying systems

In the description of the Monte Carlo interpretation of the neutron transport equation in section II.2 we already included the possibility of multiplying reactions through the factor $c_{j,A}$ in the collision kernel C of Eq.(2.38) denoting the mean number of neutrons released in a collision of type j with nuclide A . But the discussion in the chapters II and III was mainly devoted to non-multiplying systems. In this chapter we shall include explicitly multiplying fission reactions and we shall first study some methods for the Monte Carlo solution of the neutron transport equation for multiplying systems before we direct our attention to adjoint methods. For multiplying systems we can distinguish two kinds of problems

- a) problems with a fixed (external) neutron source
- b) eigenvalue problems

Fixed-source problems

Multiplying systems with an external neutron source can only be stationary if the system is subcritical. Then this kind of problems may be handled like fixed-source problems for non-multiplying systems.

¹The main ideas developed in this chapter have already been published earlier [14]

For a neutron going into a collision we have to decide whether a capture collision or some scattering collision or a fission collision will occur. For a fission collision, $\bar{\nu}$ neutrons are emitted on the average, with the actual number of neutrons varying randomly from fission to fission. In a strictly analog Monte Carlo simulation the number of neutrons emitted in a certain fission collision is selected from the appropriate discrete distribution. However, there is no need to do so, because only the mean number of neutrons emitted in a collision entered our equation and analog Monte Carlo will only increase the variance. In a non-analog simulation one neutron is emitted with weight $\bar{\nu}$. The distribution of the directions of fission neutrons is normally assumed to be isotropic in the laboratory system. Then the energy of the fission neutron can be selected from the energy transfer function $f_{f,A}(E' \rightarrow E)$, which is now called the fission spectrum $\Pi_A(E, E')$ and, for example, described by the Watt spectrum [15]

$$\Pi_A(E, E') = \frac{e^{-E_f/T}}{\sqrt{\pi E_f T}} e^{-E/T} \sinh \frac{2}{T} \sqrt{EE_f} \quad (4.1)$$

where the parameters E_f and T may depend on the nuclide A and the energy E' of the neutron causing the fission. Then the problem can be handled as for non-multiplying systems, except for the fact that if capture is treated in a non-analog way, the weight factor by which the weight of the neutron is multiplied at a collision is no longer equal to Σ_s/Σ_t as in Eq.(2.49) but equals

$$w(\underline{r}, E') = \iint C(\underline{r}, E' \rightarrow E, \underline{\Omega}' \rightarrow \underline{\Omega}) dE d\Omega = \frac{\Sigma_{se} + \Sigma_{si} + 2\Sigma_{n,2n} + \bar{\nu}\Sigma_f + \dots}{\Sigma_t} \quad (4.2)$$

with Σ_{se} , Σ_{si} , $\Sigma_{n,2n}$ and Σ_f the macroscopic cross sections for elastic scattering, inelastic scattering, (n,2n) reactions and fission respectively and may be greater than unity.

Another way to treat multiplying reactions corresponds closely to the method used in eigenvalue problems. The collision kernel C is

split up in a scattering part C_s and a fission part C_f .

$C_f(\underline{r}, E' \rightarrow E, \underline{\Omega}' \rightarrow \underline{\Omega}) dE d\Omega$ is defined as the expected number of neutrons emitted in a fission with energy between E and $E+dE$ and direction in the solid angle $d\Omega$ about $\underline{\Omega}$, given a neutron with energy E' and direction $\underline{\Omega}'$ causing the fission. With the denotation of the fission spectrum we can express C_f as follows

$$C_f(\underline{r}, E' \rightarrow E, \underline{\Omega}' \rightarrow \underline{\Omega}) = \sum_A \frac{\bar{\nu}_A(E') \Sigma_{f,A}(\underline{r}, E')}{\Sigma_t(\underline{r}, E')} \frac{\Pi_A(E, E')}{4\pi} \quad (4.3)$$

C_s is the same kernel as the kernel C from chapter II, except that in the summation over different reaction types, fission reactions are excluded. As usual in reactor physics, multiplying reactions like $(n, 2n)$ reactions, etc. are included in the scattering kernel C_s and are treated by adjustment of the neutron weight in Monte Carlo calculations. From the kernels C_s and C_f we can derive the kernels $K_s(\tau' \rightarrow \tau)$ and $K_f(\tau' \rightarrow \tau)$ for transition of a neutron from τ' to τ via a scattering and a fission reaction respectively,

$$K_s(\tau' \rightarrow \tau) = T(\underline{r}' \rightarrow \underline{r}, E', \underline{\Omega}') C_s(\underline{r}, E' \rightarrow E, \underline{\Omega}' \rightarrow \underline{\Omega}) \quad (4.4)$$

and

$$K_f(\tau' \rightarrow \tau) = T(\underline{r}' \rightarrow \underline{r}, E', \underline{\Omega}') C_f(\underline{r}, E' \rightarrow E, \underline{\Omega}' \rightarrow \underline{\Omega}) \quad (4.5)$$

Then the transport equation reads

$$\chi(\tau) = S(\tau) + \int K_s(\tau' \rightarrow \tau) \chi(\tau') d\tau' + \int K_f(\tau' \rightarrow \tau) \chi(\tau') d\tau' \quad (4.6)$$

with $S(\tau)$ the external neutron source. If we define the functions $\chi^n(\tau)$ by

$$\chi^n(\tau) = S^n(\tau) + \int K_s(\tau' \rightarrow \tau) \chi^n(\tau') d\tau' \quad n=0, 1, 2, \dots \quad (4.7)$$

with

$$S^n(\tau) = \int K_f(\tau' \rightarrow \tau) \chi^{n-1}(\tau') d\tau' \quad n=1, 2, \dots \quad (4.8)$$

and

$$S^0(\tau) = S(\tau) \quad (4.9)$$

we have

$$\begin{aligned} \sum_{n=0}^{\infty} \chi^n(\tau) &= \sum_{n=0}^{\infty} S^n(\tau) + \int K_s(\tau' \rightarrow \tau) \sum_{n=0}^{\infty} \chi^n(\tau') d\tau' \\ &= S^0(\tau) + \int K_f(\tau' \rightarrow \tau) \sum_{n=1}^{\infty} \chi^{n-1}(\tau') d\tau' + \int K_s(\tau' \rightarrow \tau) \sum_{n=0}^{\infty} \chi^n(\tau') d\tau' \\ &= S(\tau) + \int K_f(\tau' \rightarrow \tau) \sum_{n=0}^{\infty} \chi^n(\tau') d\tau' + \int K_s(\tau' \rightarrow \tau) \sum_{n=0}^{\infty} \chi^n(\tau') d\tau' \end{aligned} \quad (4.10)$$

From a comparison with Eq.(4.6) we see that

$$\chi(\tau) = \sum_{n=0}^{\infty} \chi^n(\tau) \quad (4.11)$$

provided the series converges, which is ensured by the assumption of a subcritical system.

If we call the neutrons emitted by the external neutron source $S(\tau)$ to belong to the zero-th generation, then $\chi^0(\tau)$ is the emission density of the zero-th generation of neutrons. All neutrons emitted in a fission reaction caused by a neutron of the zero-th generation are said to belong to the first generation and so on. From Eq.(4.8) we see that $S^n(\tau)$ is the source of neutrons of the n-th generation and $\chi^n(\tau)$ is the emission density of neutrons of the n-th generation. Because the kernel K_s only contains scattering collisions, Eq.(4.7)

can be regarded as describing a non-multiplying system and could be solved by familiar methods if the source $S^n(\tau)$ is known. This is only true for $n=0$ for which $S^0(\tau)=S(\tau)$, the external neutron source. Thus $\chi^0(\tau)$ can be solved by Monte Carlo methods. From Eq.(4.8) we see that we get samples of the source $S^1(\tau)$ for the next generation of neutrons if we sample the kernel K_f every time we have a sample of $\chi^0(\tau)$. When $S^1(\tau)$ is known in the Monte Carlo sense we can solve Eq.(4.7) for $n=1$ by Monte Carlo and so on. We can estimate F from

$$F = \int h(\tau)\chi(\tau)d\tau = \sum_{n=0}^{\infty} \int h(\tau)\chi^n(\tau)d\tau \quad (4.12)$$

by scoring at every collision in every generation with $h(\tau)$ as the scoring function and summing the contribution from all generations.

Because both kernels K_s and K_f contain the kernel T we can simplify the sampling process by introducing again the collision density.

If $\psi^n(\tau)$ is the collision density for the n -th generation of neutrons we have

$$\psi^n(\tau) = \int T(\underline{r}' \rightarrow \underline{r}, E, \underline{\Omega}) \chi^n(\underline{r}', E, \underline{\Omega}) dV' \quad (4.13)$$

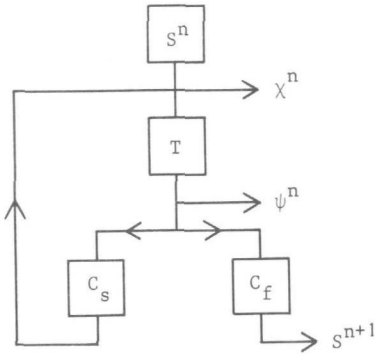
and

$$\chi^n(\tau) = S^n(\tau) + \iint C_s(\underline{r}, E' \rightarrow E, \underline{\Omega}' \rightarrow \underline{\Omega}) \psi^n(\underline{r}, E', \underline{\Omega}') dE' d\Omega' \quad (4.14)$$

and

$$S^{n+1}(\tau) = \iint C_f(\underline{r}, E' \rightarrow E, \underline{\Omega}' \rightarrow \underline{\Omega}) \psi^n(\underline{r}, E', \underline{\Omega}') dE' d\Omega' \quad (4.15)$$

The simulation of χ^n and ψ^n is schematically given in Fig. 15.

Fig. 15. Simulation of χ^n and ψ^n

The sampling of the kernel C_f needs further discussion. If a neutron with energy E' and direction $\underline{\Omega}'$ goes into a collision at \underline{r} , the expected number of fission neutrons is

$$P_f(\underline{r}, E') = \iint C_f(\underline{r}, E' \rightarrow E, \underline{\Omega}' \rightarrow \underline{\Omega}) dE' d\Omega' = \frac{\sum_A \bar{\nu}_A(E') \Sigma_{f,A}(\underline{r}, E')}{\Sigma_t(\underline{r}, E')} \quad (4.16)$$

Thus for a neutron of weight w the average weight of fission neutrons generated is equal to

$$w_f = w \cdot P_f(\underline{r}, E') \quad (4.17)$$

and fission weight is generated at every collision where $P_f \neq 0$. To avoid the problem of getting many fission neutrons with small weights, a Russian roulette technique must be used to decide whether the generated fission weight is accepted as a new fission neutron with a fixed weight or not. By choosing the weight of the fission neutron when surviving the Russian roulette we can influence the number of source neutrons for the next generation. Because the system was assumed to be subcritical the total fission weight generated in successive generations of neutrons will decrease and the number of fission neutrons surviving the Russian roulette can be made smaller

and smaller until it will become zero for some generation, which reduces the summation over an infinite number of generations in Eq.(4.12) to a finite number. This may influence, of course, the statistics but limits computer time, which may be more important after a number of generations.

Eigenvalue problems

The eigenvalue equation for the emission density reads in integral form

$$\chi_k(\tau) = \int K_s(\tau' \rightarrow \tau) \chi_k(\tau') d\tau' + \frac{1}{\lambda_k} \int K_f(\tau' \rightarrow \tau) \chi_k(\tau') d\tau' \quad (4.18)$$

with λ_k the k-th eigenvalue and χ_k the corresponding emission density eigenfunction. The method to obtain the largest eigenvalue and corresponding eigenfunction is analogous to the power method for matrix eigenvalue equations in numerical analysis [16]. We again define the functions $\chi^n(\tau)$ by

$$\chi^n(\tau) = S^n(\tau) + \int K_s(\tau' \rightarrow \tau) \chi^n(\tau') d\tau' \quad n=0,1,2,\dots \quad (4.19)$$

with

$$S^n(\tau) = \int K_f(\tau' \rightarrow \tau) \chi^{n-1}(\tau') d\tau' \quad n=1,2,\dots \quad (4.20)$$

For arbitrary $S^0(\tau)$ we can prove

$$\chi^n(\tau) \div \chi_0(\tau) \quad n \gg 1 \quad (4.21)$$

with $\chi_0(\tau)$ the eigenfunction corresponding to the largest eigenvalue λ_0 . To prove Eq.(4.21) we first introduce the adjoint eigenvalue equation

$$\chi_{\ell}^{\dagger}(\tau) = \int K_{\text{S}}^{\dagger}(\tau' \rightarrow \tau) \chi_{\ell}^{\dagger}(\tau') d\tau' + \frac{1}{\lambda_{\ell}} \int K_{\text{F}}^{\dagger}(\tau' \rightarrow \tau) \chi_{\ell}^{\dagger}(\tau') d\tau' \quad (4.22)$$

with the kernels K_{S}^{\dagger} and K_{F}^{\dagger} adjoint to K_{S} and K_{F} according to the definition of Eq.(2.52) for adjoint kernels:

$$K_{\text{S}}^{\dagger}(\tau' \rightarrow \tau) = K_{\text{S}}(\tau \rightarrow \tau') \quad (4.23)$$

and

$$K_{\text{F}}^{\dagger}(\tau' \rightarrow \tau) = K_{\text{F}}(\tau \rightarrow \tau') \quad (4.24)$$

Multiplication of Eq.(4.18) by χ_{ℓ}^{\dagger} and Eq.(4.22) by χ_{k} , integration over all phase space and subtraction gives

$$\left(\frac{1}{\lambda_{\text{k}}} - \frac{1}{\lambda_{\ell}} \right) \int \chi_{\ell}^{\dagger}(\tau) \int K_{\text{F}}^{\dagger}(\tau' \rightarrow \tau) \chi_{\text{k}}(\tau') d\tau' d\tau = 0 \quad (4.25)$$

where we have used the property for adjoint kernels of Eq.(2.51). Eq.(4.25) can be written equivalently

$$\int \chi_{\ell}^{\dagger}(\tau) \int K_{\text{F}}^{\dagger}(\tau' \rightarrow \tau) \chi_{\text{k}}(\tau') d\tau' d\tau = N_{\text{k}} \delta_{\text{k}\ell} \quad (4.26)$$

with

$$N_{\text{k}} = \int \chi_{\text{k}}^{\dagger}(\tau) \int K_{\text{F}}^{\dagger}(\tau' \rightarrow \tau) \chi_{\text{k}}(\tau') d\tau' d\tau \quad (4.27)$$

and $\delta_{\text{k}\ell}$ the Kronecker delta, which is zero for $\text{k} \neq \ell$ and unity for $\text{k} = \ell$. From Eq.(4.18) we can also deduce

$$\int \chi_{\ell}^{\dagger}(\tau) \chi_{\text{k}}(\tau) d\tau - \int \chi_{\ell}^{\dagger}(\tau) \int K_{\text{S}}^{\dagger}(\tau' \rightarrow \tau) \chi_{\text{k}}(\tau') d\tau' d\tau = \frac{1}{\lambda_{\text{k}}} N_{\text{k}} \delta_{\text{k}\ell} \quad (4.28)$$

Eqs.(4.26) and (4.28) show the orthogonality of the eigenfunctions.

Now we are able to express every function defined in the same phase space as a series of eigenfunctions

$$A(\tau) = \sum_k a_k \chi_k(\tau) \quad (4.29)$$

with the expansion coefficients given by

$$a_k = \frac{1}{N_k} \int \chi_k^\dagger(\tau) \int K_f(\tau' \rightarrow \tau) A(\tau') d\tau' d\tau \quad (4.30)$$

Thus the function $\chi^n(\tau)$ from Eq.(4.19) can be written as

$$\chi^n(\tau) = \sum_k x_k^n \chi_k(\tau) \quad (4.31)$$

Substitution into Eq.(4.19), multiplication by $\chi_\ell^\dagger(\tau)$ and integration leads to

$$\begin{aligned} \sum_k x_k^n \left\{ \int \chi_\ell^\dagger(\tau) \chi_k(\tau) d\tau - \int \chi_\ell^\dagger(\tau) \int K_s(\tau' \rightarrow \tau) \chi_k(\tau') d\tau' d\tau \right\} \\ = \int \chi_\ell^\dagger(\tau) S^n(\tau) d\tau \quad (4.32) \end{aligned}$$

or

$$x_\ell^n = \frac{\lambda_\ell}{N_\ell} \int \chi_\ell^\dagger(\tau) S^n(\tau) d\tau \quad (4.33)$$

With Eq.(4.20) we have

$$x_\ell^n = \frac{\lambda_\ell}{N_\ell} \sum_k x_k^{n-1} \int \chi_\ell^\dagger(\tau) \int K_f(\tau' \rightarrow \tau) \chi_k(\tau') d\tau' d\tau = \lambda_\ell x_\ell^{n-1} \quad (4.34)$$

Hence

$$x_\ell^n = (\lambda_\ell)^n x_\ell^0 \quad (4.35)$$

with x_k^0 the expansion coefficients of $\chi^0(\tau)$. In the limit for large n we have

$$\begin{aligned} \chi^n(\tau) &= \sum_k (\lambda_k)^n x_k^0 \chi_k(\tau) = (\lambda_0)^n \sum_k \left(\frac{\lambda_k}{\lambda_0}\right)^n x_k^0 \chi_k(\tau) \\ &= \lambda_0^n x_0^0 \chi_0(\tau) \div \chi_0(\tau) \end{aligned} \quad (4.36)$$

because

$$\lim_{n \rightarrow \infty} \left(\frac{\lambda_k}{\lambda_0}\right)^n = 0 \quad k=1,2,\dots \quad (4.37)$$

To estimate $\chi_0(\tau)$ or any average over the fundamental eigenfunction, we have to simulate Eq.(4.19) for $n=0$ with arbitrary $S^0(\tau)$. As for multiplying systems with a fixed source, the source $S^1(\tau)$ of neutrons of the first generation of fission neutrons can be estimated from Eq.(4.20) and so on. After a large number of generations $\chi^n(\tau)$ will closely approximate the fundamental eigenfunction $\chi_0(\tau)$ according to Eq.(4.36) and we can estimate a quantity F which is some average over the fundamental eigenfunction $\chi_0(\tau)$

$$F = \int h(\tau) \chi_0(\tau) d\tau \quad (4.38)$$

by scoring $h(\tau)$ at every collision of neutrons in the n -th generation, with n large enough.

Because the total fission source weight for successive generations of neutrons will decrease (on the average) if $\lambda_0 < 1$ and increase if $\lambda_0 > 1$, a renormalization is necessary before starting the neutron histories of a new generation. For a statistical fair game, the number of neutrons for successive generations should increase [17] and this number can be controlled by the survival probability of the Russian roulette used to decide whether generated fission weight in a collision is accepted as a new fission neutron or not.

The fundamental eigenvalue λ_0 may be estimated, for example, from

$\int S^{n+1}(\tau)d\tau$ for large n , if the source $S^n(\tau)$ for the n -th generation was normalized to unity, because from Eq.(4.20), the expansion of $\chi^n(\tau)$ and Eq.(4.35) it follows that

$$\lambda_0 = \frac{\int S^{n+1}(\tau)d\tau}{\int S^n(\tau)d\tau} \quad n \gg 1 \quad (4.39)$$

It will be clear that $\chi^n(\tau)$ converges faster to the fundamental eigenfunction if $\lambda_0 \gg \lambda_1$ and $S^0(\tau)$ resembles the fundamental source distribution.

IV.2. Adjoint methods for multiplying systems

Suppose we have to calculate a quantity F which is some average over the fundamental flux eigenfunction $\phi_0(\tau)$ or the fundamental collision density eigenfunction $\psi_0(\tau)$ or the fundamental emission density eigenfunction $\chi_0(\tau)$. Then F can be written as

$$F = \int f(\tau)\phi_0(\tau)d\tau = \int g(\tau)\psi_0(\tau)d\tau = \int h(\tau)\chi_0(\tau)d\tau \quad (4.40)$$

with f , g and h connected by Eqs.(2.17) and (2.18). The eigenvalue equation for $\chi_0(\tau)$, Eq.(4.18) with $k=0$, can be written as

$$\chi_0(\tau) = S_0(\tau) + \int K_S(\tau' \rightarrow \tau)\chi_0(\tau')d\tau' \quad (4.41)$$

with

$$S_0(\tau) = \frac{1}{\lambda_0} \int K_f(\tau' \rightarrow \tau)\chi_0(\tau')d\tau' \quad (4.42)$$

$S_0(\tau)$ is the source distribution corresponding to the fundamental eigenfunction. The equation adjoint to Eqs.(4.41) and (4.40) reads

$$\chi^\dagger(\tau) = h(\tau) + \int K_S^\dagger(\tau' \rightarrow \tau)\chi^\dagger(\tau')d\tau' \quad (4.43)$$

According to section II.3 we have

$$F = \int h(\tau) \chi_0(\tau) d\tau = \int S_0(\tau) \chi^\dagger(\tau) d\tau \quad (4.44)$$

So we could obtain F by Monte Carlo by solving the adjoint equation Eq.(4.43) and estimating F with $S_0(\tau)$ as the scoring function. However, the fundamental source eigenfunction $S_0(\tau)$ is not known. Following a suggestion of Kalos [18] we introduce the following set of equations

$$\theta_n^\dagger(\tau) = Q_n^\dagger(\tau) + \int K_s^\dagger(\tau' \rightarrow \tau) \theta_{n-1}^\dagger(\tau') d\tau' \quad n=1,2,\dots \quad (4.45)$$

with

$$Q_n^\dagger(\tau) = \int K_f^\dagger(\tau' \rightarrow \tau) \theta_{n-1}^\dagger(\tau') d\tau' \quad n=2,3,\dots \quad (4.46)$$

and

$$Q_1^\dagger(\tau) = \delta(\tau - \tau_0) \quad (4.47)$$

with τ_0 some given point in the phase space. We shall first prove that

$$\int \theta_n^\dagger(\tau) d\tau \div \chi_0(\tau_0) \quad n \gg 1 \quad (4.48)$$

$\theta_n^\dagger(\tau)$ can be expanded into a series of adjoint eigenfunctions as follows

$$\theta_n^\dagger(\tau) = \sum_{\lambda} t_{\lambda}^n \chi_{\lambda}^\dagger(\tau) \quad (4.49)$$

To determine the expansion coefficients of an arbitrary function, we need the orthogonality properties of Eqs.(4.26) and (4.28) in adjoint form:

$$\begin{aligned} & \int \chi_k(\tau) \int K_f^\dagger(\tau' \rightarrow \tau) \chi_\ell^\dagger(\tau') d\tau' d\tau \\ &= \lambda_k \left\{ \int \chi_k(\tau) \chi_\ell^\dagger(\tau) d\tau - \int \chi_k(\tau) \int K_s^\dagger(\tau' \rightarrow \tau) \chi_\ell^\dagger(\tau') d\tau' d\tau \right\} = N_k \delta_{k\ell} \end{aligned} \quad (4.50)$$

With these orthogonality relations we can see that in general t_ℓ^n is given by

$$t_\ell^n = \frac{1}{N_\ell} \int \chi_\ell(\tau) \int K_f^\dagger(\tau' \rightarrow \tau) \theta_n^\dagger(\tau') d\tau' d\tau \quad (4.51)$$

Substitution of the expansion of $\theta_n^\dagger(\tau)$ into Eq.(4.45) gives after multiplication by $\chi_k(\tau)$ and integration

$$t_k^n = \frac{\lambda_k}{N_k} \int \chi_k(\tau) Q_n^\dagger(\tau) d\tau \quad n=1,2,\dots \quad (4.52)$$

From Eq.(4.46) we have

$$\int \chi_k(\tau) Q_n^\dagger(\tau) d\tau = t_k^{n-1} N_k \quad n=2,3,\dots \quad (4.53)$$

Thus

$$t_k^n = \lambda_k t_k^{n-1} = (\lambda_k)^{n-1} t_k^1 \quad (4.54)$$

From Eqs.(4.52) and (4.47) we also have

$$t_k^1 = \frac{\lambda_k}{N_k} \int \chi_k(\tau) Q_1^\dagger(\tau) d\tau = \frac{\lambda_k}{N_k} \chi_k(\tau_0) \quad (4.55)$$

So

$$t_k^n = \frac{(\lambda_k)^n}{N_k} \chi_k(\tau_0) \quad (4.56)$$

Because $\lambda_0 > \lambda_1 > \dots$ we have for $n \gg 1$

$$\theta_n^\dagger(\tau) = \frac{(\lambda_0)^n}{N_0} \chi_0(\tau_0) \chi_0^\dagger(\tau) \quad (4.57)$$

and

$$\int \theta_n^\dagger(\tau) d\tau = \frac{(\lambda_0)^n}{N_0} \int \chi_0^\dagger(\tau) d\tau \cdot \chi_0(\tau_0) = C_n \chi_0(\tau_0) \quad (4.58)$$

which proves Eq.(4.48). From this proof it will be clear that if we had multiplied $\theta_n^\dagger(\tau)$ by some arbitrary function before integration, the integral still would have been proportional to $\chi_0(\tau_0)$. Thus by solving the equations for θ_n^\dagger we are able to determine the fundamental eigenfunction in some given point τ_0 in the phase space. To obtain F from the last part of Eq.(4.44) we have to express $S_0(\tau)$ in terms of $\chi_0(\tau)$ by means of Eq.(4.42)

$$\begin{aligned} F &= \int \chi^\dagger(\tau) S_0(\tau) d\tau = \frac{1}{\lambda_0} \int \chi^\dagger(\tau) \int K_f^\dagger(\tau' \rightarrow \tau) \chi_0(\tau') d\tau' d\tau \\ &= \frac{1}{\lambda_0} \int \chi_0(\tau) \int K_f^\dagger(\tau' \rightarrow \tau) \chi^\dagger(\tau') d\tau' d\tau \quad (4.59) \end{aligned}$$

Because we are able to estimate $\chi_0(\tau_0)$, we can estimate F from the last part of Eq.(4.59) by superposition. If we take

$$Q_1^\dagger(\tau) = \int \delta(\tau - \tau_0) \int K_f^\dagger(\tau' \rightarrow \tau_0) \chi^\dagger(\tau') d\tau' d\tau_0 = \int K_f^\dagger(\tau' \rightarrow \tau) \chi^\dagger(\tau') d\tau' \quad (4.60)$$

instead of $Q_1^\dagger(\tau) = \delta(\tau - \tau_0)$ we arrive at

$$\int \theta_n^\dagger(\tau) d\tau = \int C_n \chi_0(\tau_0) \int K_f^\dagger(\tau' \rightarrow \tau_0) \chi^\dagger(\tau') d\tau' d\tau_0 = \lambda_0 C_n F \quad (4.61)$$

Thus a possible procedure to estimate F by adjoint Monte Carlo is as follows. We first simulate $\chi^\dagger(\tau)$ from Eq.(4.43). Then we can estimate

$Q_1^\dagger(\tau)$ from Eq.(4.60) by sampling the kernel K_f^\dagger . Next we can simulate θ_n^\dagger from Eq.(4.45) for $n=1,2,\dots$ with the source Q_n^\dagger estimated from Eq.(4.46) for $n=2,3,\dots$. If n is large enough so that the influence of other eigenfunctions than the fundamental can be neglected, we can estimate $\int \theta_n^\dagger(\tau) d\tau$ by simply summing all weights of adjoint particles of generation n having had an event anywhere in the system and this estimate is proportional to F , according to Eq.(4.61). Because Eq.(4.43) for χ^\dagger is the same as Eq.(4.45) for θ_n^\dagger except for the source term, we can simplify the description by defining $\theta_0^\dagger(\tau) = \chi^\dagger(\tau)$ and

$$\theta_n^\dagger(\tau) = Q_n^\dagger(\tau) + \int K_s^\dagger(\tau' \rightarrow \tau) \theta_{n-1}^\dagger(\tau') d\tau' \quad n=0,1,2,\dots \quad (4.62)$$

with

$$Q_n^\dagger(\tau) = \int K_f^\dagger(\tau' \rightarrow \tau) \theta_{n-1}^\dagger(\tau') d\tau' \quad n=1,2,\dots \quad (4.63)$$

and

$$Q_0^\dagger(\tau) = h(\tau) \quad (4.64)$$

Then we have

$$\int \theta_n^\dagger(\tau) d\tau = \frac{(\lambda_0)_{n+1}}{N_0} \int \chi_0^\dagger(\tau) d\tau \cdot \int h(\tau') \chi_0(\tau') d\tau' \div F \quad n \gg 1 \quad (4.65)$$

The eigenfunction χ_0 can only be determined up to a multiplicative constant. So there will always be some ambiguity in the definition of F . However, the proportionality constant in Eq.(4.65) only depends on n and not on the particular quantity to be calculated. So, we can estimate the true ratio of two quantities if they are estimated after the same number of generations of adjoint particles.

If the quantity F must be normalized, for example by

$$\int S_o(\tau) d\tau = 1 \quad (4.66)$$

as is normally done in forward calculations, the problem is to calculate

$$\begin{aligned} \tilde{F} &= \frac{\int h(\tau) \chi_o(\tau) d\tau}{\int S_o(\tau) d\tau} = \lambda_o \frac{\int h(\tau) \chi_o(\tau) d\tau}{\iint K_f(\tau' \rightarrow \tau) \chi_o(\tau') d\tau' d\tau} \\ &= \lambda_o \frac{\int h(\tau) \chi_o(\tau) d\tau}{\int \chi_o(\tau) \int K_f^\dagger(\tau' \rightarrow \tau) d\tau' d\tau} \end{aligned} \quad (4.67)$$

The denominator can be estimated in the same way as the numerator with the only change that we have to take

$$Q_o^\dagger(\tau) = \int K_f^\dagger(\tau' \rightarrow \tau) d\tau' \quad (4.68)$$

instead of Eq.(4.64). If we call the solution of Eqs.(4.62) and (4.63) with this initial source $\theta_n^\dagger(\tau)$ we have for $n \gg 1$

$$\int \theta_n^\dagger(\tau) d\tau = \frac{(\lambda_o)^{n+1}}{N_o} \int \chi_o^\dagger(\tau) d\tau \cdot \int \chi_o(\tau_o) \int K_f^\dagger(\tau' \rightarrow \tau_o) d\tau' d\tau_o \quad (4.69)$$

and

$$\tilde{F} = \frac{\int \theta_n^\dagger(\tau) d\tau}{\int \theta_{n-1}^\dagger(\tau) d\tau} \quad n \gg 1 \quad (4.70)$$

with the index $n-1$ of θ^\dagger in the denominator because of the factor λ_o in Eq.(4.67) and the fact that the proportionality constant in Eq.(4.65) contains a factor $(\lambda_o)^{n+1}$.

Thus far we used the kernels K_s^\dagger and K_f^\dagger in the adjoint equation. In chapter III we saw that a transformed kernel may have better statistical properties. We therefore define the adjoint kernels M_s^\dagger and M_f^\dagger by

$$M_s^\dagger(\tau' \rightarrow \tau) = \frac{E' \Sigma_t(\tau)}{E \Sigma_t(\tau')} K_s^\dagger(\tau' \rightarrow \tau) \quad (4.71)$$

and

$$M_f^\dagger(\tau' \rightarrow \tau) = \frac{E' \Sigma_t(\tau)}{E \Sigma_t(\tau')} K_f^\dagger(\tau' \rightarrow \tau) \quad (4.72)$$

and solve the equations

$$\rho_n^\dagger(\tau) = R_n^\dagger(\tau) + \int M_s^\dagger(\tau' \rightarrow \tau) \rho_n^\dagger(\tau') d\tau' \quad n=0, 1, 2, \dots, \quad (4.73)$$

with

$$R_n^\dagger(\tau) = \int M_f^\dagger(\tau' \rightarrow \tau) \rho_{n-1}^\dagger(\tau') d\tau' \quad n=1, 2, \dots \quad (4.74)$$

and

$$R_0^\dagger(\tau) = \Sigma_t(\tau) h(\tau) / E \quad (4.75)$$

We shall prove that

$$\int \eta(\tau) \rho_n^\dagger(\tau) d\tau \div F \quad n \gg 1 \quad (4.76)$$

with $\eta(\tau)$ an arbitrary function. $\rho_n^\dagger(\tau)$ may be expanded into a series of adjoint eigenfunctions as follows

$$\rho_n^\dagger(\tau) = \sum_k r_k^n \frac{\Sigma_t(\tau)}{E} \chi_k^\dagger(\tau) \quad (4.77)$$

Substitution into Eq.(4.73) gives after multiplication by $E\chi_\ell(\tau)/\Sigma_t(\tau)$ and integration

$$\begin{aligned} \sum_k r_k^n \int \chi_k^\dagger(\tau) \chi_\ell(\tau) d\tau &= \int \frac{ER_n^\dagger(\tau)}{\Sigma_t(\tau)} \chi_\ell(\tau) d\tau \\ &+ \sum_k r_k^n \int \frac{E\chi_\ell(\tau)}{\Sigma_t(\tau)} \int M_s^\dagger(\tau' \rightarrow \tau) \frac{\Sigma_t(\tau')}{E'} \chi_k^\dagger(\tau') d\tau' d\tau \end{aligned} \quad (4.78)$$

Using the definition for M_s^\dagger from Eq.(4.71) and the orthogonality relation Eq.(4.50) we have

$$r_\ell^n = \frac{\lambda_\ell}{N_\ell} \int \frac{ER_n^\dagger(\tau)}{\Sigma_t(\tau)} \chi_\ell(\tau) d\tau \quad (4.79)$$

From Eq.(4.74) we obtain after multiplication by $E\chi_\ell(\tau)/\Sigma_t(E)$ and integration

$$\begin{aligned} \int \frac{ER_n^\dagger(\tau)}{\Sigma_t(\tau)} \chi_\ell(\tau) d\tau &= \sum_k r_k^{n-1} \int \frac{E\chi_\ell(\tau)}{\Sigma_t(\tau)} \int M_f^\dagger(\tau' \rightarrow \tau) \frac{\Sigma_t(\tau')}{E'} \chi_k^\dagger(\tau') d\tau' d\tau \\ &= \sum_k r_k^{n-1} \int \chi_\ell(\tau) \int K_f^\dagger(\tau' \rightarrow \tau) \chi_k^\dagger(\tau') d\tau' d\tau = r_\ell^{n-1} N_\ell \end{aligned} \quad (4.80)$$

So

$$r_\ell^n = \lambda r_\ell^{n-1} = (\lambda_\ell)^n r_\ell^0 \quad (4.81)$$

From Eq.(4.79) we have for $n=0$

$$r_\ell^0 = \frac{\lambda_\ell}{N_\ell} \int \frac{ER_o^\dagger(\tau)}{\Sigma_t(\tau)} \chi_\ell(\tau) d\tau = \frac{\lambda_\ell}{N_\ell} \int h(\tau) \chi_\ell(\tau) d\tau \quad (4.82)$$

For $n \gg 1$ we get for $\rho_n^\dagger(\tau)$

$$\rho_n^\dagger(\tau) = \frac{(\lambda_o)^{n+1}}{N_o} \int h(\tau_o) \chi_o(\tau_o) d\tau_o \cdot \frac{\Sigma_t(\tau)}{E} \chi_o^\dagger(\tau) \quad (4.83)$$

and

$$\int \eta(\tau) \rho_n^\dagger(\tau) d\tau = \frac{(\lambda_o)^{n+1}}{N_o} \int h(\tau_o) \chi_o(\tau_o) d\tau_o \cdot \int \eta(\tau) \frac{\Sigma_t(\tau)}{E} \chi_o^\dagger(\tau) d\tau = D_n F \quad (4.84)$$

with the proportionality constant D_n given by

$$D_n = \frac{(\lambda_o)^{n+1}}{N_o} \int \eta(\tau) \frac{\Sigma_t(\tau)}{E} \chi_o^\dagger(\tau) d\tau \quad (4.85)$$

which proves Eq.(4.76). The Monte Carlo estimation of F can be done as follows. Source events of the zero-th generation of adjoint particles are selected from $R_o^\dagger(\tau) = \Sigma_t(\tau)h(\tau)/E$. Next-event points are found by repeatedly sampling the kernel M_s^\dagger . Particles of the next generation are generated by sampling the kernel M_f^\dagger at each event point. With these particles the histories of the next generation are started and so on for each generation. After a sufficient number of generations, a quantity proportional to F is estimated using $\eta(\tau)$ as the scoring function according to Eq.(4.84). The choice for the arbitrary function $\eta(\tau)$ is discussed in the next section.

If F must be normalized by $\int S_o(\tau) d\tau = 1$ we set

$$R_o^\dagger(\tau) = \int M_f^\dagger(\tau' \rightarrow \tau) \frac{\Sigma_t(\tau')}{E} d\tau' \quad (4.86)$$

and solve again Eq.(4.73). If we call the solution of this equation with the initial source $R_0^\dagger(\tau)$ from Eq.(4.86) $\rho_n^\dagger(\tau)$, we have for the normalized quantity \tilde{F}

$$\tilde{F} = \frac{\int h(\tau)\chi_0(\tau)d\tau}{\int S_0(\tau)d\tau} = \frac{\int \eta(\tau)\rho_n^\dagger(\tau)d\tau}{\int \eta(\tau)\rho_{n-1}^\dagger(\tau)d\tau} \quad n \gg 1 \quad (4.87)$$

It should be emphasized that the total source weight of the successive generations of adjoint particles from which F is finally estimated can not be arbitrarily normalized. If they are normalized, which will be desirable from a statistical point of view, the normalization factor of each generation should be taken into account at the final estimation of F to keep the proportionality constant D_n in Eq.(4.84) the same for every quantity F .

The fundamental eigenvalue λ_0 can also be estimated from the adjoint calculation. From Eqs.(4.84) and (4.74) it follows that

$$\lambda_0 = \frac{\int \eta(\tau)\rho_n^\dagger(\tau)d\tau}{\int \eta(\tau)\rho_{n-1}^\dagger(\tau)d\tau} = \frac{\int R_n^\dagger(\tau)d\tau}{\int R_{n-1}^\dagger(\tau)d\tau} \quad n \gg 1 \quad (4.88)$$

For fixed source problems in a subcritical system the adjoint equation reads

$$\chi^\dagger(\tau) = h(\tau) + \int K_S^\dagger(\tau' \rightarrow \tau)\chi^\dagger(\tau')d\tau' + \int K_F^\dagger(\tau' \rightarrow \tau)\chi^\dagger(\tau')d\tau' \quad (4.89)$$

With the transformation

$$\zeta^\dagger(\tau) = \frac{\Sigma_t(\tau)}{E} \chi^\dagger(\tau) \quad (4.90)$$

this becomes

$$\zeta^\dagger(\tau) = \frac{\sum_{\mathbf{t}}(\tau)h(\tau)}{E} + \int M_S^\dagger(\tau' \rightarrow \tau) \zeta^\dagger(\tau') d\tau' + \int M_F^\dagger(\tau' \rightarrow \tau) \zeta^\dagger(\tau') d\tau' \quad (4.91)$$

and F is given by

$$F = \int \frac{ES(\tau)}{\sum_{\mathbf{t}}(\tau)} \zeta^\dagger(\tau) d\tau \quad (4.92)$$

as for non-multiplying systems. It is possible to solve Eq.(4.91) by combining the kernels M_S^\dagger and M_F^\dagger into one kernel M^\dagger and sampling this combined kernel. Then we have to include also fission reactions into the definition of the total macroscopic adjoint cross section.

However, we prefer the method analogous to that for eigenvalue problems. Then F is written as a sum over contributions of successive generations of adjoint particles. For that purpose we have to solve again Eqs. (4.73) to (4.75). Then

$$\begin{aligned} \sum_{n=0}^{\infty} \rho_n^\dagger(\tau) &= \sum_{n=0}^{\infty} R_n^\dagger(\tau) + \int M_S^\dagger(\tau' \rightarrow \tau) \sum_{n=0}^{\infty} \rho_n^\dagger(\tau') d\tau' \\ &= R_0^\dagger(\tau) + \int M_F^\dagger(\tau' \rightarrow \tau) \sum_{n=1}^{\infty} \rho_{n-1}^\dagger(\tau') d\tau' + \int M_S^\dagger(\tau' \rightarrow \tau) \sum_{n=0}^{\infty} \rho_n^\dagger(\tau') d\tau' \\ &= \frac{\sum_{\mathbf{t}}(\tau)h(\tau)}{E} + \int M_F^\dagger(\tau' \rightarrow \tau) \sum_{n=0}^{\infty} \rho_n^\dagger(\tau') d\tau' + \int M_S^\dagger(\tau' \rightarrow \tau) \sum_{n=0}^{\infty} \rho_n^\dagger(\tau') d\tau' \end{aligned} \quad (4.93)$$

From a comparison with Eq.(4.91) we see that

$$\zeta^\dagger(\tau) = \sum_{n=0}^{\infty} \rho_n^\dagger(\tau) \quad (4.94)$$

and thus

$$F = \sum_{n=0}^{\infty} \int \frac{ES(\tau)}{\sum_{\mathbf{t}}(\tau)} \rho_n^\dagger(\tau) d\tau \quad (4.95)$$

The convergence of the series is ensured if the system is subcritical. Except for the scoring, this method is the same as for eigenvalue problems. However, the total source weight of new generations should not be renormalized and the number of adjoint particles for successive generation should decrease to zero.

Both for fixed source problems and eigenvalue problems the same set of equations Eqs.(4.73) to (4.75) has to be solved. Eq.(4.73) is essentially the same as Eq.(3.49) for non-multiplying systems except for the source term and its Monte Carlo solution needs no further discussion here. We only note that because of the kernel M_S^\dagger no fission reactions are considered when solving this equation, which means fission is considered as absorption. Therefore, in the definition of the adjoint cross section $\Sigma^\dagger(\tau)$ from Eq.(3.18) fission reactions are excluded. Typical for multiplying systems is the sampling of the kernel M_F^\dagger of Eq.(4.72) to estimate the source of next generation adjoint particles and we shall discuss this further in the next section.

IV.3. Monte Carlo interpretation of the adjoint equation for multiplying systems

Solving a problem for a multiplying system by adjoint Monte Carlo means simulation of the Eqs.(4.73) to (4.75) and estimating the desired quantity F either from Eq.(4.76) for an eigenvalue problem or from Eq.(4.95) for a fixed source problem. To solve Eq.(4.73) we can decompose the kernel M_S^\dagger as in Eq.(3.51).

$$M_S^\dagger(\tau' \rightarrow \tau) = P^\dagger(\underline{r}', E') D_S^\dagger(\underline{r}', E' \rightarrow E, \underline{\Omega}' \rightarrow \underline{\Omega}) T^\dagger(\underline{r}' \rightarrow \underline{r}, E, \underline{\Omega}) \quad (4.96)$$

with D_S given by

$$D_S^\dagger(\underline{r}', E' \rightarrow E, \underline{\Omega}' \rightarrow \underline{\Omega}) = \sum_A p_A^\dagger(\underline{r}', E') \sum_j p_{j,A}^\dagger(E') p(E, \underline{\Omega} | j, A) \quad (4.97)$$

p_A^\dagger and $p_{j,A}^\dagger$ are still defined by Eqs.(3.20) and (3.21) respectively, with the adjoint cross sections evaluated according to definition II of Eq.(3.46). The summation over j is over all scattering reactions (including $(n,2n)$ reactions, etc.) but fission excluded. The pdf $p(E, \underline{\Omega} | j, A)$ is still given by Eq.(3.53). The kernel D_S^\dagger is thus exactly the same as the kernel D^\dagger used in chapter III.

From Eq.(4.72) it follows that

$$\begin{aligned} M_f^\dagger(\tau' \rightarrow \tau) &= \frac{\Sigma_t(\tau)}{\Sigma_t(\tau')} \frac{E'}{E} K_f(\tau \rightarrow \tau') \\ &= \frac{\Sigma_t(\underline{r}, E)}{\Sigma_t(\underline{r}', E')} T(\underline{r} \rightarrow \underline{r}', E, \underline{\Omega}) C_f(\underline{r}', E \rightarrow E', \underline{\Omega} \rightarrow \underline{\Omega}') \frac{E'}{E} \\ &= \frac{\Sigma_t(\underline{r}', E)}{\Sigma_t(\underline{r}', E')} T^\dagger(\underline{r}' \rightarrow \underline{r}, E, \underline{\Omega}) \sum_A \frac{\bar{v}_A(E) \Sigma_{f,A}(\underline{r}', E) \Pi_A(E', E)}{\Sigma_t(\underline{r}', E)} \frac{\Pi_A(E', E)}{4\pi} \frac{E'}{E} \\ &= T^\dagger(\underline{r}' \rightarrow \underline{r}, E, \underline{\Omega}) \sum_A \frac{\bar{v}_A(E) \Sigma_{f,A}(\underline{r}', E) \Pi_A(E', E) E' / E}{4\pi \Sigma_t(\underline{r}', E')} \end{aligned} \quad (4.98)$$

with $\Pi_A(E', E)$ the fission spectrum as a function of E' for a fission of nuclide A caused by a neutron with energy E . M_f^\dagger can thus be factored into

$$M_f^\dagger(\tau' \rightarrow \tau) = D_f^\dagger(\underline{r}', E' \rightarrow E, \underline{\Omega}' \rightarrow \underline{\Omega}) T^\dagger(\underline{r}' \rightarrow \underline{r}, E, \underline{\Omega}) \quad (4.99)$$

with

$$D_f^\dagger(\underline{r}', E' \rightarrow E, \underline{\Omega}' \rightarrow \underline{\Omega}) = \frac{1}{4\pi} \sum_A \bar{v}_A(E) \Sigma_{f,A}(\underline{r}', E) \Pi_A(E', E) \frac{E'}{E} / \Sigma_t(\underline{r}', E') \quad (4.100)$$

In the decomposition of M_s^\dagger the adjoint weight factor P^\dagger is included because then the remaining factors are normalized kernels. However, inclusion of a factor P^\dagger in the decomposition of M_f^\dagger does not lead to a normalized kernel D_f^\dagger and is therefore omitted.

To arrive at a sampling scheme analogous to that of Fig. 11 in section III.3 we define

$$\Gamma_o^\dagger(\tau) = \frac{f(\tau)}{E} \quad (4.101)$$

$$\Gamma_n^\dagger(\tau) = \iint D_f^\dagger(\underline{r}, E' \rightarrow E, \underline{\Omega}' \rightarrow \underline{\Omega}) \rho_{n-1}^\dagger(\underline{r}, E', \underline{\Omega}') dE' d\Omega' \quad n=1, 2, \dots \quad (4.102)$$

and

$$\Lambda_n^\dagger(\tau) = \Gamma_n^\dagger(\tau) + \iint P(\underline{r}, E') D_s^\dagger(\underline{r}, E' \rightarrow E, \underline{\Omega}' \rightarrow \underline{\Omega}) \rho_n^\dagger(\underline{r}, E', \underline{\Omega}') dE' d\Omega' \quad (4.103)$$

n=0, 1, 2, ...

Then we have

$$R_o^\dagger(\tau) = \frac{\sum_t(\tau)h(\tau)}{E} = \int T^\dagger(\underline{r}' \rightarrow \underline{r}, E, \underline{\Omega}) \Gamma_o^\dagger(\underline{r}', E, \underline{\Omega}) dV' \quad (4.104)$$

$$R_n^\dagger(\tau) = \int T^\dagger(\underline{r}' \rightarrow \underline{r}, E, \underline{\Omega}) \Gamma_n^\dagger(\underline{r}', E, \underline{\Omega}) dV' \quad n=0, 1, 2, \dots \quad (4.105)$$

and

$$\rho_n^\dagger(\tau) = \int T^\dagger(\underline{r}' \rightarrow \underline{r}, E, \underline{\Omega}) \Lambda_n^\dagger(\underline{r}', E, \underline{\Omega}) dV' \quad n=0, 1, 2, \dots \quad (4.106)$$

The relations between ρ_n^\dagger , Λ_n^\dagger and Γ_n^\dagger may be clarified by the diagram of Fig. 16. If we call Γ_n^\dagger the source of adjoint particles for the n-th generation then Λ_n^\dagger is the density of particles leaving a collision or the source and ρ_n^\dagger the density of particles going into a collision. A sample of the source Γ_{n+1}^\dagger of the next generation of adjoint particles is obtained from a sample of ρ_n^\dagger by sampling the kernel D_f^\dagger .

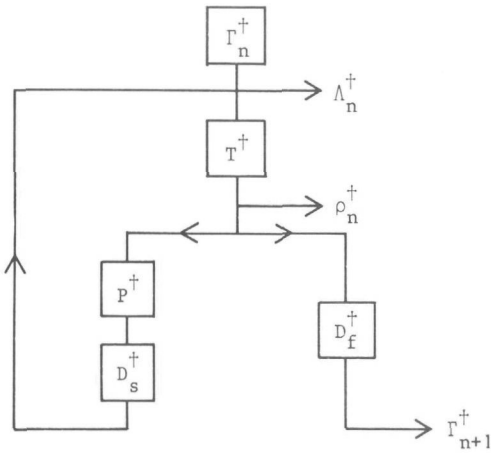


Fig. 16. Simulation of ρ_n^{\dagger} and Λ_n^{\dagger}

To facilitate the sampling of the kernel D_f^{\dagger} we introduce the adjoint fission cross section

$$\sigma_{f,A}^{\dagger}(E') = \int \bar{v}_A(E) \sigma_{f,A}(E) \Pi_A(E', E) \frac{E'}{E} dE \quad (4.107)$$

and

$$\Sigma_{f,A}^{\dagger}(\underline{r}, E') = N_A(\underline{r}) \sigma_{f,A}^{\dagger}(E') \quad (4.108)$$

$$\Sigma_f^{\dagger}(\underline{r}, E') = \sum_A N_A(\underline{r}) \sigma_{f,A}^{\dagger}(E') \quad (4.109)$$

in accordance with the adjoint cross sections for other reaction types. The kernel D_f^{\dagger} is normalized to

$$P_f^{\dagger}(\underline{r}, E') = \iint D_f^{\dagger}(\underline{r}, E' \rightarrow E, \underline{\Omega}' \rightarrow \underline{\Omega}) dE d\Omega = \frac{\Sigma_f^{\dagger}(\underline{r}, E')}{\Sigma_t(\underline{r}, E')} \quad (4.110)$$

So, if an adjoint particle of weight w goes into a collision, it will generate an adjoint particle of the next generation with weight

$$w_f = w \cdot P_f^\dagger(\underline{r}, E') \quad (4.111)$$

The energy and direction of the new particle have to be selected from the pdf

$$\begin{aligned} p(E, \underline{\Omega}) &= \frac{1}{4\pi} \frac{\sum_A \bar{v}_A(E) \Sigma_{f,A}(\underline{r}, E) \Pi_A(E', E) \frac{E'}{E}}{\Sigma_f^\dagger(\underline{r}, E')} \\ &= \frac{1}{4\pi} \sum_A P_{f,A}^\dagger(\underline{r}, E') \frac{\bar{v}_A(E) \sigma_{f,A}(E) \Pi_A(E', E) \frac{E'}{E}}{\sigma_{f,A}^\dagger(E')} \quad (4.112) \end{aligned}$$

with

$$P_{f,A}^\dagger(\underline{r}, E') = \frac{\Sigma_{f,A}^\dagger(\underline{r}, E')}{\Sigma_f^\dagger(\underline{r}, E')} \quad (4.113)$$

Thus its direction is selected isotropically and if more than one fissionable nuclide is present in the medium at \underline{r} the nuclide A is selected with probability $P_{f,A}^\dagger$. Then the energy is selected from

$$p(E|A) = \frac{\bar{v}_A(E) \sigma_{f,A}(E) \Pi_A(E', E) \frac{E'}{E}}{\sigma_{f,A}^\dagger(E')} \quad (4.114)$$

In general this pdf can best be handled by computing tables giving the energy E for which the cumulative distribution has prescribed values for a set of values of E'.

Some simplifications are possible if the fission spectrum is assumed to be independent of the energy of the neutron causing the fission and of the nuclide fissioned. Then

$$\sigma_{f,A}^\dagger(E') = E' \Pi(E') \int \bar{v}_A(E) \sigma_{f,A}(E) \frac{dE}{E} = E' \Pi(E') I_{f,A} \quad (4.115)$$

with

$$I_{f,A} = \int \bar{v}_A(E) \sigma_{f,A}(E) \frac{dE}{E} \quad (4.116)$$

$$P_{f,A}^\dagger(\underline{r}, E') = \frac{N_A(\underline{r}) I_{f,A}}{\sum_A N_A(\underline{r}) I_{f,A}} \quad (4.117)$$

$$p(E|A) = \frac{\bar{v}_A(E) \sigma_{f,A}(E) / E}{I_{f,A}} \quad (4.118)$$

and the pdf for selection of E does no longer depend on E'.

If F has to be normalized by $\int S_0(\tau) d\tau = 1$ with $S_0(\tau)$ the fission source distribution corresponding to the fundamental eigenfunction, R_0^\dagger is given by Eq.(4.86) to obtain the normalization factor. From Eq.(4.105) it follows for $n=0$ that in this case

$$\begin{aligned} \Gamma_0^\dagger(\tau) &= \iint D_f^\dagger(\underline{r}, E' \rightarrow E, \underline{\Omega}' \rightarrow \underline{\Omega}) \frac{\Sigma_t(\underline{r}, E')}{E'} dE' d\Omega' \\ &= \int \frac{\sum_A \bar{v}_A(E) \Sigma_{f,A}(\underline{r}, E) \Pi_A(E', E) \frac{E'}{E}}{\Sigma_t(\underline{r}, E')} \frac{\Sigma_t(\underline{r}, E')}{E'} dE' \\ &= \sum_A \bar{v}_A(E) \Sigma_{f,A}(\underline{r}, E) / E \end{aligned} \quad (4.119)$$

Γ_0^\dagger is unnormalized and

$$\int \Gamma_0^\dagger(\tau) d\tau = 4\pi \int \sum_A N_A(\underline{r}) I_{f,A} dV \quad (4.120)$$

We can select a starting point from the normalized pdf $\Gamma_0^\dagger(\tau) / \int \Gamma_0^\dagger(\tau) d\tau$ and assign each adjoint particle of the zero-th generation a weight $\int \Gamma_0^\dagger(\tau) d\tau$ or multiply all final results by this factor. If V_A is the volume of the system in which the fissionable nuclide A is present

with atomic density N_A and if we call nuclides present at different regions in the system with different atomic densities different nuclides for the moment, we can select A from the discrete pdf

$$p(A) = \frac{N_A I_{f,A} V_A}{\sum_A N_A I_{f,A} V_A} \quad (4.121)$$

Then we select \underline{r} homogeneous in all regions with the fissionable nuclide A present and finally select $\underline{\Omega}$ isotropically and E from the pdf

$$p(E|A) = \frac{\bar{V}_A(E) \sigma_{f,A}(E)/E}{I_{f,A}} \quad (4.122)$$

If the system is strongly heterogeneous as the core of a nuclear reactor generally is, the selection of \underline{r} can probably most simply be done by selection of \underline{r} homogeneous from the total system and rejecting the sample if the fissionable nuclide is not present in the medium at the selected point.

While the pdf for the selection of the energy of source particles of new generations as given by Eq.(4.118) only holds for the assumptions mentioned above, the same pdf of Eq.(4.122) for the energy selection of source particles of the zero-th generation for the normalization factor always holds.

The integrals in the normalization factors of the pdf $p(E|A)$ from Eq.(4.118) and Eq.(4.122) and in $\sigma_{f,A}^+$ from Eq.(4.107) have to be taken over all energies and may diverge because for low energies the fission cross section $\sigma_f(E)$ generally behaves as $1/\sqrt{E}$. However, in the neutron game there will be almost no neutrons with very low energy, so that the fission cross section at very low energies is irrelevant and may be assumed to be zero below some energy when evaluating the integrals to obtain $\sigma_{f,A}^+$ or $I_{f,A}$. The use of a thermal group as discussed in section

III.4 also leads to a lower bound for the energy of adjoint particles. Inspection of $p(E|A)$ under the condition of a lower bound E_{\min} for E shows that the adjoint particles of a new generation will have preferentially low energies. But adjoint particles can only generate progeny at energies for which the factor P_f^\dagger from Eq.(4.110) is relatively large. Because the energy dependence of P_f^\dagger is dominated by the fission spectrum $\Pi_A(E',E)$, this will only be the case at higher energies. Thus adjoint particles starting at low energies must be scattered up to high energies before they can contribute significantly to the next generation of adjoint particles. Especially in fast systems absorption at low energies will be large and adjoint particles will have only a small probability to be scattered up to higher energies without a drastic reduction of their weights. We may therefore expect that selection of the energy from the pdf of Eq.(4.118) or Eq.(4.114) for the general case will lead to large statistical errors.

To reduce variance, source biasing may be used. Coveyou et al [13] showed that the solution of the equation adjoint to the one to be solved is likely to be a good biasing function. The equation to be solved for the n -th generation of adjoint particles is Eq.(4.73) and if this generation is not yet used to estimate F by Eq.(4.76) the aim of introducing a source biasing function is to reduce the variance of the total weight of adjoint particles of the next generation $\int \Gamma_{n+1}^\dagger(\tau) d\tau$ which can be written as

$$\begin{aligned} \int \Gamma_{n+1}^\dagger(\tau) d\tau &= \iiint D_f^\dagger(\underline{r}, E' \rightarrow E, \underline{\Omega}' \rightarrow \underline{\Omega}) \rho_n^\dagger(\underline{r}, E', \underline{\Omega}') dE' d\Omega' d\tau \\ &= \int \rho_n^\dagger(\tau) \iiint D_f^\dagger(\underline{r}, E \rightarrow E', \underline{\Omega} \rightarrow \underline{\Omega}') dE' d\Omega' d\tau \quad (4.123) \end{aligned}$$

The equation adjoint to Eqs.(4.73) and (4.123) is

$$\rho(\tau) = \iiint D_f^\dagger(\underline{r}, E \rightarrow E', \underline{\Omega} \rightarrow \underline{\Omega}') dE' d\Omega' + \int M_s^\dagger(\tau \rightarrow \tau') \rho(\tau') d\tau' \quad (4.124)$$

independent of n . If we set

$$\theta(\tau) = \Sigma_t(\tau)\rho(\tau)/E \quad (4.125)$$

we have for $\theta(\tau)$

$$\theta(\tau) = \iiint \frac{\Sigma_t(\underline{r}, E)}{E} D_f^\dagger(\underline{r}, E \rightarrow E', \underline{\Omega} \rightarrow \underline{\Omega}') dE' d\Omega' + \int K_s(\tau' \rightarrow \tau) \theta(\tau') d\tau' \quad (4.126)$$

This is the forward neutron transport equation for a seemingly non-multiplying system with an external source $S(\tau)$ equal to

$$S(\tau) = \iiint \frac{\Sigma_t(\underline{r}, E)}{E} D_f^\dagger(\underline{r}, E \rightarrow E', \underline{\Omega} \rightarrow \underline{\Omega}') dE' d\Omega' = \Pi(E) \sum_A N_A(\underline{r}) I_{f,A} \quad (4.127)$$

again assuming the fission spectrum to be independent of E' and A . As compared to the forward eigenfunction equation Eq.(4.41) the energy and direction distribution of the source term is the same as for the fission source corresponding to the fundamental eigenfunction and only the spatial distributions differ. Because we seek for a reasonable energy dependent biasing function for $p(E|A)$ of Eq.(4.114), we may disregard for the moment all space and direction dependence and obtain $\theta(E)$ with some approximation from the equation

$$\theta(E) = \Pi(E) + \int C_s(E' \rightarrow E) \theta(E') dE' \quad (4.128)$$

This equation is the same as the energy dependent eigenvalue equation, so its solution $\theta(E)$ is equal to the fundamental collision density or emission density

$$\theta(E) = \psi_0(E) = \Sigma_t(E)\phi_0(E) \quad (4.129)$$

Then the energy dependent biasing function is approximated by

$$\rho(E) = E\phi_0(E) \quad (4.130)$$

Although this biasing function will not be optimal, it will help to reduce the statistical error. The biased conditional pdf for the selection of the energy E of a new born particle, given the nuclide type A , will be

$$p^*(E|A) = \bar{v}_A(E)\sigma_{f,A}(E)\phi_0(E)/z_A \quad (4.131)$$

with

$$z_A = \int \bar{v}_A(E)\sigma_{f,A}(E)\phi_0(E)dE \quad (4.132)$$

The nuclide type A is selected with probability

$$p_{f,A}^\dagger(\underline{r}) = N_A(\underline{r})z_A/Z \quad (4.133)$$

with

$$Z = \sum_A N_A(\underline{r})z_A \quad (4.134)$$

Then the weight factor to be used instead of P_f^\dagger as in Eq.(4.111) becomes

$$w^* = \frac{E'\Pi_A(E',E)}{\Sigma_t(\underline{r},E')} \frac{Z}{E\phi_0(E)} \quad (4.135)$$

The constants $I_{f,A}$ need no longer to be evaluated, which also removes any difficulties with divergent integrals. For the selection of the energy E of a new born particle, only one pdf per fissionable nuclide is needed because $p^*(E|A)$ does not depend on E' . If the fission spectrum $\Pi_A(E',E)$ is independent of the nuclide A fissioned and the energy E of the neutron causing the fission, we may use the weight factor $E'\Pi(E')/\Sigma_t(\underline{r},E')$, in analogy with the scoring function $E.S(\underline{r},E,\Omega)/\Sigma_t(\underline{r},E)$ for non-multiplying systems, to determine the total

weight of generated particles in a collision and from this the number of generated particles, without already selecting the energy and direction of the new particles. When all particles of the current generation have been processed, the energy and direction of all particles of the next generation can be selected and the second term of w^* from Eq.(4.135) is then used as the initial particle weight.

The sampling of Γ_0^+ from Eq.(4.119) in a normalization calculation is analogous to the biased sampling of the fission kernel as shown above, except for the fact that first a medium m has to be selected, in which the particle will start. This may be done with probability

$$p_m^* = V_m Z_m / \sum_m V_m Z_m, \quad (4.136)$$

with V_m the volume of medium m . Because a medium determines the number and types of nuclides, Z depends on m , as indicated explicitly in Eq.(4.136). The starting point for a particle is then selected uniform within the volume of the selected medium. The initial weight may be chosen as

$$w_i^* = \sum_m V_m Z_m / E \phi_0(E) V \quad (4.137)$$

with V the total volume of the system. Then a constant factor $4\pi V$ remains with which the final result must be multiplied.

The source biasing function $E\phi_0(E)$ for the source of adjoint particles of the i -th generation is used to reduce the variance in the total weight of source particles $\int \Gamma_{i+1}(\tau) d\tau$ of the $(i+1)$ -th generation. However, if the quantity $\int \eta(\tau) \rho_n^+(\tau) d\tau$, which is proportional to F according to Eq.(4.84), is estimated from the n -th generation of adjoint particles, a different source biasing for the n -th generation will be needed in general. Because the scoring function $\eta(\tau)$ was arbitrary, we can determine $\eta(\tau)$ in such a way that the source biasing used for previous generations will also be useful for the last

generation from which F is estimated. If we take

$$\eta(\tau) = \iint D_f^\dagger(\underline{r}, E \rightarrow E', \underline{\Omega} \rightarrow \underline{\Omega}') dE' d\Omega' \quad (4.138)$$

we have with Eq.(4.123)

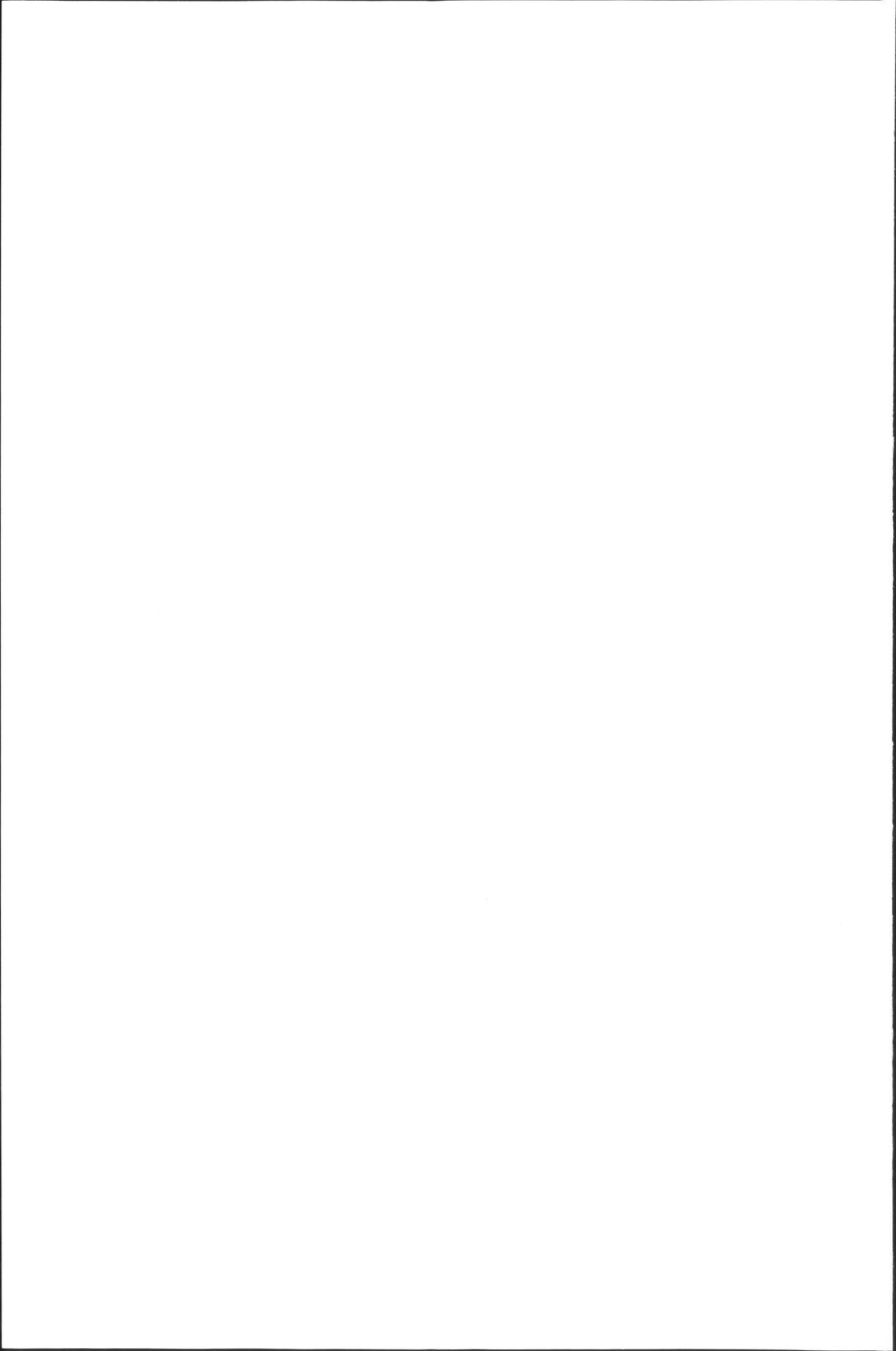
$$F \doteq \int \eta(\tau) \rho_n^\dagger(\tau) d\tau = \int \Gamma_{n+1}^\dagger(\tau) d\tau \quad (4.139)$$

and we use in fact the same scoring function as for the generation of new adjoint particles, so that the source biasing will also be reasonably good for the estimation of F .

If we assume the fission spectrum again independent of the energy of the neutron causing the fission and the type of nuclide fissioned, we can equivalently use for η in those regions of the system where fissionable nuclides are present

$$\eta(\tau) = \frac{E \Pi(E)}{\Sigma_t(\underline{r}, E)} \quad (4.140)$$

because this only differs a constant factor with Eq.(4.138). Again all problems with divergent integrals have been removed. For the general case an averaged fission spectrum should be used. However, the use of the fission spectrum of the most dominating fissionable nuclide in the system may also be used, because the only purpose was to determine a scoring function $\eta(\tau)$ for which the source biasing is adequate.



CHAPTER V

NUMERICAL EXAMPLES AND DISCUSSION

V.1. The computer code FOCUS and related programs

The theory developed in the preceding chapters has been used to write a versatile adjoint Monte Carlo computer code, which was called FOCUS [19]. It solves the adjoint equation Eq.(3.49) for non-multiplying systems and Eq.(4.73) for multiplying systems.

The code consists of four modules: the random walk module, the geometry module, the random number generation module and the analysis module. The random walk module reads in the general input data, calls the geometry module to input the geometry description and reads in the cross section data. Further, it controls the selection of source parameters of the adjoint particle, the selection of next collision points and the selection of energy and direction after a collision of an adjoint particle. It calls the analysis module at different moments during a particle history to allow all types of estimators and the calculation of averages and variances.

The geometry module traces the path of an adjoint particle from its last emission point into the direction opposite to its parameter Ω , until the particle has travelled the selected number of mean free paths, or it reaches a medium boundary. The geometry package of the Monte Carlo codes MORSE [10] and O6R [20] was adopted for the geometry handling. This package consists of special modules for slab, sphere

and cylinder geometry and a general module, which allows the description of material media bounded by any combination of linear and quadratic surfaces. These modules need not any modification for use in FOCUS.

The random number generation module has also been taken from the above-mentioned codes. Its basic random number generator for generating pseudo random numbers equally distributed between 0 and 1 is based on the congruential method [21]. A next random number ρ_{n+1} is obtained from the previous random number ρ_n by

$$\rho_{n+1} = M \cdot \rho_n \quad \text{mod } 2^{48} \quad (5.1)$$

with M a constant multiplier. The initial random number ρ_0 with which the generator starts, can be set by the user. To allow for correlated sampling, the random numbers used to generate a particle history must be controlled. Therefore, the random number is also kept as a particle parameter. If a particle history is temporarily interrupted to process first other particle histories for some reason, the current random number for the interrupted history is also stored with the other particle parameters and this random number is restored in the random number generator if the history is continued. An independent random number generation device is needed to provide the initial random number for each history. Because no severe demands are made on this generator, the midsquare principle [22] can be used for this generator.

The analysis module is used to estimate the desired quantity F either from Eq.(3.50) for non-multiplying systems or from Eq.(4.95) for multiplying systems with a fixed source or from Eq.(4.76) for eigenvalue problems. To allow for several possible scoring techniques the analysis routines are called at the start of each history, before and after a collision, at boundary crossings and when a particle escapes from the system. The analysis module also performs the necessary bookkeeping to calculate the average estimate of F and its standard deviation. For multiplying systems it accumulates the contributions to F from all particles of successive generations (or from the final generation only, in case of eigenvalue problems) that are descendants of the same parent

particle from the zero-th generation. From these sums and its squares the standard deviation in F is calculated. To accomplish this, the identification of the parent particle of each adjoint particle must also be recorded.

To calculate the adjoint cross sections according to definition II of Eq.(3.46), a separate computer code ADX [23] was written. This code calculates the microscopic adjoint cross sections and the energy distributions for the selection of the energy after a collision of an adjoint particle for all scattering reaction types of a nuclide from cross section data given in ENDF/B format [24] and stores its results also in this format. It also calculates the total adjoint cross section as the sum of all partial adjoint cross sections. With the existing program RIGEL [25] the results can be combined with the original ENDF/B tape. In the program ADX extensive use has been made of the standard subroutines developed for processing and manipulating data in ENDF/B format [26]. The adjoint cross section $\sigma_{j,A}^{\dagger}(E')$ for a certain nuclide and reaction type is calculated in tabular form with interpolation rules by the subroutine GENT1 from the ENDF/B processing routines, which was intended for the tabulation of an analytic function. The function subprogram that should supply the value of the analytic function for a given argument was designed to evaluate the integral in Eq.(3.46) by the use of the ENDF/B processing routines to integrate a tabulated function in ENDF/B format. A tabulation of the integrand in Eq.(3.46) as a function of E was again calculated by the subroutine GENT1, which was now given a different name to avoid recursive subroutine calls. From a tabulation of the integrand, partial integrals can easily be computed and from these, the energies can be calculated at which the cumulative distribution of the energy after a collision has a certain value according to Eq.(3.67). For a certain release of the ENDF/B library the adjoint cross sections need to be calculated only once.

For those nuclides in the ENDF/B library for which the cross sections must be calculated in a certain energy range from the supplied resonance parameters, the NPTXS module from the AMPX code system [27] can be used

to tabulate the cross sections for the entire energy range.

From an ENDF/B library supplemented with adjoint cross sections and energy distributions calculated by ADX, a system cross section tape for a problem to be treated by FOCUS can be composed by the program ETOF [28]. This code calculates for all material media in the system the total macroscopic cross section Σ_t , the adjoint weight factor $P^\dagger = \Sigma^\dagger / \Sigma_t$ and the probabilities p_A^\dagger for scattering with the distinct nuclides in a medium. For all nuclides in the system it also calculates the probabilities $p_{j,A}^\dagger$ for all distinct reaction types of nuclide A. Together with the energy distributions these data are grouped per energy range to permit FOCUS to read in only part of the cross section data at a time and to process only those particles of which the energy lies in that energy range, before the data for the next energy range is read in. The energy points at which a quantity is given are chosen such that linear interpolation in energy

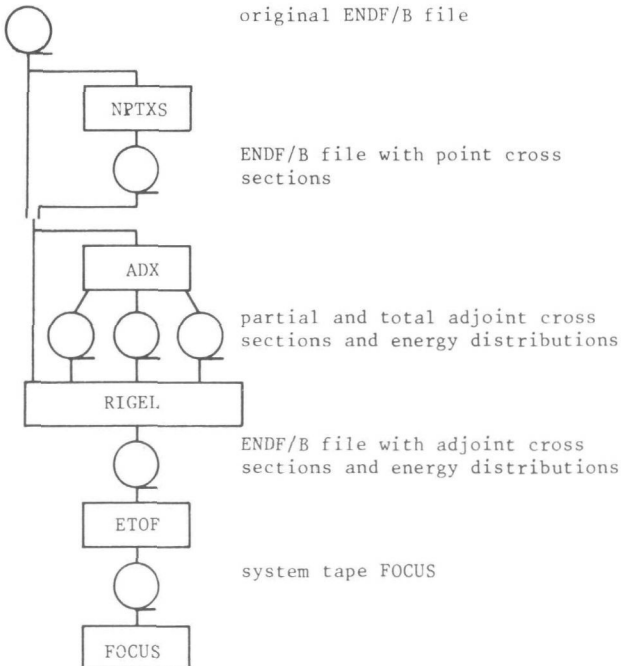


Fig. 17. Relation between FOCUS and data processing codes

results in values accurate to an accuracy, specified by the user. The energy ranges are chosen such that each energy range needs about an equal number of data words to describe all necessary quantities for that energy range. For multiplying systems ETOF also calculates the pdf for the selection of energies of generated adjoint particles from the function $\bar{v}(E)\sigma_f(E)\phi_0(E)$ according to Eq.(4.131). The guessed energy spectrum $\phi_0(E)$ must be supplied by the user.

The connection between the various programs is shown in Fig. 17.

V.2. A fixed-source shielding problem

To test the computer code FOCUS and to demonstrate the performance of the developed adjoint Monte Carlo technique, calculations have been made for some benchmark problems. Benchmark problems in reactor physics are designed to provide well-documented computational standards for several configurations of interest with reliable solutions obtained by several methods. They may be used to test computational methods and to judge the precision and efficiency of different computer codes.

As an example of an adjoint Monte Carlo calculation for a non-multiplying system we chose number 6 of the shielding benchmark problems accepted by the Benchmark Problem Group of the American Nuclear Society Shielding Standards Subcommittee [29]. In this problem the transmission of neutrons and secondary gamma-rays through a slab of borated polyethylene is studied. Fig. 18 shows the geometry of interest. A mono-

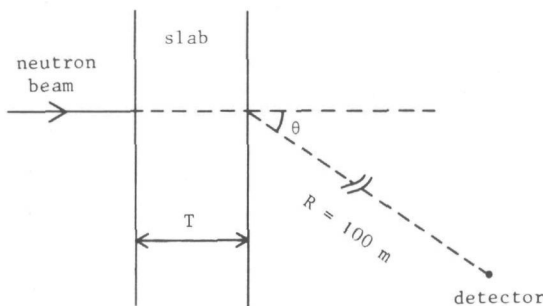


Fig. 18. Geometry of shielding benchmark problem

directional narrow neutron beam with a fission source energy spectrum impinges perpendicularly on a polyethylene slab containing about 2% weight of the nuclide ^{10}B . Table III gives the constituent nuclides and their atomic densities. Two slab thicknesses are considered: 2.54 cm and 15.24 cm. Four hypothetical point detectors registering the neutron flux are located at 100 m from the slab at different angles. To be able to treat this benchmark problem by one-dimensional discrete ordinates codes, the assumption was made, that all neutrons reaching a detector, view this detector under the same angle and the same distance. The angles at which the detectors have been placed are given in table IV.

Table III. Slab composition

nuclide	atomic density $\frac{24}{3}$ in 10^3 /cm ³
^1H	0.037873
^{10}B	0.075746
^{12}C	0.0010019

Table IV. Detector angles

detector	cos θ	θ
1	0.98561	9.7 ^o
2	0.89632	26.3 ^o
3	0.73218	42.9 ^o
4	0.14447	81.7 ^o

These angles correspond to four of the discrete directions used in the S_{32} discrete ordinates calculation reported in the benchmark problem documentation. The energy group division and the source energy spectrum is shown in table V. The aim of the calculation is the response of the detectors for both slab thicknesses. Besides, the volume integrated flux in the slab is calculated per energy group specified in table V. In the benchmark problem documentation, calculational results are given from two multigroup discrete ordinates codes, the multigroup Monte Carlo code MORSE [10] and the pseudo point cross section code O6R [20]. Because the use of multigroup cross sections introduces a source of errors in the calculational results compared with codes using basic point cross sections directly, the O6R code is most suited to check the results of the adjoint Monte Carlo code FOCUS. All calculations discussed in the benchmark problem documentation were carried out using

Table V. Energy group division and source spectrum

energy group	upper energy	fraction of source neutrons	fission spectrum (MeV ⁻¹)
1	15.0 MeV	1.566 10 ⁻⁴	5.593 10 ⁻⁵
2	12.2 MeV	8.979 10 ⁻⁴	4.081 10 ⁻⁴
3	10.0 MeV	3.496 10 ⁻³	1.921 10 ⁻³
4	8.18 MeV	1.397 10 ⁻²	7.676 10 ⁻³
5	6.36 MeV	3.473 10 ⁻²	2.481 10 ⁻²
6	4.96 MeV	3.522 10 ⁻²	3.913 10 ⁻²
7	4.06 MeV	1.078 10 ⁻¹	1.027 10 ⁻¹
8	3.01 MeV	8.941 10 ⁻²	1.626 10 ⁻¹
9	2.46 MeV	2.330 10 ⁻²	2.118 10 ⁻¹
10	2.35 MeV	1.209 10 ⁻¹	2.325 10 ⁻¹
11	1.83 MeV	2.191 10 ⁻¹	3.043 10 ⁻¹
12	1.11 MeV	1.994 10 ⁻¹	3.561 10 ⁻¹
13	550. keV	1.360 10 ⁻¹	3.098 10 ⁻¹
14	111. keV	1.557 10 ⁻²	1.446 10 ⁻¹
15	3.35 keV	0	0
16	583. eV	0	0
17	101. eV	0	0
18	29.0 eV	0	0
19	10.7 eV	0	0
20	3.06 eV	0	0
21	1.12 eV	0	0
22	.414 eV	0	0

the ENDF/B-II library as the basic source of cross section data. We therefore used this version of ENDF/B also for our calculations. Because the treatment of inelastic level and continuum scattering in O6R shows some deviations from the inelastic collision mechanics and the procedures specified by ENDF/B [24], we carried out again the O6R calculations with the correct treatment of inelastic scattering, to be sure that exactly the same data and scattering models were used in the FOCUS and O6R calculations. For thermal energies a one-velocity treatment was adopted with 2200 m/s cross sections for convenience, because comparisons are only made between calculational results.

First the volume integrated scalar neutron flux per unit energy was calculated for each energy group. For an energy group with limits E_1 and E_2 we have

$$F = \iiint \eta(E) \phi(\underline{r}, E, \underline{\Omega}) dV dE d\Omega \quad (5.2)$$

with

$$\eta(E) = \begin{cases} \frac{1}{E_2 - E_1} & E_1 \leq E \leq E_2 \\ 0 & \text{else} \end{cases} \quad (5.3)$$

if the neutron source is normalized to one neutron per unit time. Thus the averaging function $f(\underline{r}, E, \underline{\Omega})$ as defined by Eq. (2.14) equals

$$f(\underline{r}, E, \underline{\Omega}) = \eta(E) \quad (5.4)$$

Because neutrons that escape from the slab without having had a collision do not give a contribution to the flux if a collision estimator is used, this type of estimator is rather inefficient, especially for the smaller slab thickness of 2.54 cm. We therefore used a track length estimator [5] in the forward 06R calculations. Then every neutron contributes to the estimated flux. To calculate the neutron flux for the energy groups above 4.96 MeV with reasonable statistics, a separate calculation has been done using source energy importance sampling.

For the adjoint calculation we have to look first at the scoring function for F , which was given by $ES(\tau)/\Sigma_t(\tau)$ according to Eq. (3.50). The neutron source is given by

$$S(\underline{r}, E, \underline{\Omega}) = \delta(\underline{r} - \underline{r}_s) \Pi(E) \delta(\underline{\Omega} - \underline{\Omega}_s) \quad (5.5)$$

with \underline{r}_s the point on the slab face at which the neutrons impinge and $\underline{\Omega}_s$ the direction of the neutron beam. $\Pi(E)$ is the fission spectrum

given in the last column of table V. Because both Monte Carlo codes need the neutron source strength per unit energy instead of a fraction per energy group, it was assumed that the source energy distribution is constant per unit energy within each energy group. The neutron source of Eq.(5.5) is not suited for an adjoint Monte Carlo calculation because both \underline{r} and $\underline{\Omega}$ must have a unique value to let the scoring function in the adjoint calculation differ from zero. We therefore redefine the problem as follows. Instead of a narrow neutron beam we suppose a plane source emitting Q neutrons per unit area and per unit time perpendicularly to the slab face. We shall show that the volume integrated slab flux in the original problem is proportional to the flux due to the plane source, integrated over the slab width. If we introduce a Cartesian coordinate system with the X-direction coinciding with the direction of the source neutrons, the neutron source per unit area of the slab face can be written as

$$S'(\underline{r}, E, \underline{\Omega}) = Q\delta(x-x_s)\Pi(E)\delta(\underline{\Omega}-\underline{\Omega}_s) \quad (5.6)$$

with x_s the x-coordinate of the slab face on which the neutrons impinge. If the flux in the original problem with the narrow beam impinging at (x_s, y_s, z_s) to the slab is denoted by $\phi_b(x, y, z, E, \underline{\Omega} | y_s, z_s) = \phi_b(x, y-y_s, z-z_s, E, \underline{\Omega})$, the flux in the modified problem is given by

$$\begin{aligned} \phi_{p1}(x, y, z, E, \underline{\Omega}) &= \iint \phi_b(x, y, z, E, \underline{\Omega} | y_s, z_s) Q dy_s dz_s \\ &= Q \iint \phi_b(x, y', z', E, \underline{\Omega}) dy' dz' \end{aligned} \quad (5.7)$$

independent of y and z . The volume integrated flux is for the original problem

$$\begin{aligned} \Phi_b(E, \underline{\Omega}) &= \iiint \phi_b(x, y, z, E, \underline{\Omega} | y_s, z_s) dx dy dz \\ &= \iiint \phi_b(x, y', z', E, \underline{\Omega}) dx dy' dz' \end{aligned} \quad (5.8)$$

In the modified problem the flux integrated over all x values is

$$\Phi_{p1}(y, z, E, \underline{\Omega}) = \int \Phi_{p1}(x, y, z, E, \underline{\Omega}) dx = Q \iiint \Phi_b(x, y', z', E, \underline{\Omega}) dx dy' dz' \quad (5.9)$$

from which we have

$$\Phi_b(E, \underline{\Omega}) = \Phi_{p1}(y_o, z_o, E, \underline{\Omega}) / Q \quad (5.10)$$

with arbitrary y_o and z_o . Thus the volume integrated group flux in the original problem can also be obtained as

$$\begin{aligned} F &= \iint \eta(E) \Phi_b(E, \underline{\Omega}) dE d\Omega = \frac{1}{Q} \iint \eta(E) \Phi_{p1}(y_o, z_o, E, \underline{\Omega}) dE d\Omega \\ &= \frac{1}{Q} \iiint \eta(E) \delta(y - y_o) \delta(z - z_o) \Phi_{p1}(\underline{r}, E, \underline{\Omega}) dV dE d\Omega \end{aligned} \quad (5.11)$$

The averaging function for the flux in the modified problem is

$$f'(\underline{r}, E, \underline{\Omega}) = \frac{1}{Q} \eta(E) \delta(y - y_o) \delta(z - z_o) \quad (5.12)$$

The source of Eq.(5.6) has still zero volume in the phase space, but now an expected value estimator can be used for the scoring in the adjoint calculation. This can be derived as follows. From Eqs.(3.50) and (3.49) we have

$$F = \int \frac{ES'(\tau)}{\Sigma_t(\tau)} \left\{ \frac{\Sigma_t(\tau) h'(\tau)}{E} + \int M^\dagger(\tau' \rightarrow \tau) \zeta^\dagger(\tau') d\tau' \right\} d\tau \quad (5.13)$$

With Eqs.(3.54) and (3.51) we obtain

$$\begin{aligned} F &= \int ES'(\tau) \int \frac{T^\dagger(\underline{r}' \rightarrow \underline{r}, E, \underline{\Omega})}{\Sigma_t(\underline{r}, E)} \left\{ \frac{f'(\underline{r}', E, \underline{\Omega})}{E} \right. \\ &\quad \left. + \iint P^\dagger(\underline{r}', E') D^\dagger(\underline{r}', E' \rightarrow E, \underline{\Omega}' \rightarrow \underline{\Omega}) \zeta^\dagger(\underline{r}', E', \underline{\Omega}') dE' d\Omega' \right\} dV' d\tau \end{aligned} \quad (5.14)$$

For abbreviation we set

$$\Theta(\underline{r}, E, \underline{\Omega}) = f'(\underline{r}, E, \underline{\Omega})/E + \iint P^\dagger(\underline{r}, E') D^\dagger(\underline{r}, E' \rightarrow E, \underline{\Omega}' \rightarrow \underline{\Omega}) \zeta^\dagger(\underline{r}, E', \underline{\Omega}') dE' d\Omega' \quad (5.15)$$

Θ is the density of adjoint particles coming out of a collision or the source of adjoint particles f'/E . With the expression for the neutron source $S'(\tau)$ of Eq.(5.6) and that for T^\dagger/Σ_t from Eqs.(2.70) and (3.9) we can carry out the integration over $\underline{\Omega}$. With the abbreviation

$$\beta(\underline{r}, E, \underline{\Omega}, d) = \exp \left\{ - \int_0^d \Sigma_t(\underline{r}-s\underline{\Omega}, E) ds \right\} \quad d \geq 0 \quad (5.16)$$

we obtain

$$F = Q \iint E \Pi(E) \delta(x-x_s) \cdot \int \beta(\underline{r}', E, \underline{\Omega}_s, |\underline{r}-\underline{r}'|) \frac{\delta \left(\underline{\Omega}_s + \frac{\underline{r}-\underline{r}'}{|\underline{r}-\underline{r}'|} \right)}{|\underline{r}-\underline{r}'|^2} \Theta(\underline{r}', E, \underline{\Omega}_s) dV' dV dE \quad (5.17)$$

With the new coordinates l and $\underline{\Omega}^*$ instead of \underline{r}

$$\underline{r} = \underline{r}' + l \underline{\Omega}^* \quad (5.18)$$

and

$$dV = l^2 dl d\Omega^* \quad (5.19)$$

we can also carry out the integration over \underline{r} and obtain

$$F = Q \iiint E \Pi(E) \delta(x' + l \underline{\Omega}_x^* - x_s) .$$

$$\begin{aligned}
 & \cdot \int \beta(\underline{r}', E, \underline{\Omega}_s, 1) \delta(\underline{\Omega}_s + \underline{\Omega}^*) \Theta(\underline{r}', E, \underline{\Omega}_s) dV' d\Omega^* dE \\
 & = Q \int E \Pi(E) \frac{1}{|\underline{\Omega}_{sx}|} \int \beta(\underline{r}', E, \underline{\Omega}_s, |x' - x_s| / \Omega_{sx}) \Theta(\underline{r}', E, \underline{\Omega}_s) dV' dE \quad (5.20)
 \end{aligned}$$

Here $\underline{\Omega}_x^*$ and $\underline{\Omega}_{sx}$ are the length of the components of $\underline{\Omega}^*$ and $\underline{\Omega}_s$ in the X-direction respectively. Because $\underline{\Omega}_s$ coincides with the X-direction we have $\Omega_{sx} = 1$. Because Θ is composed of adjoint particles leaving directly the source f'/E and of adjoint particles coming out of a collision, F is also composed of a direct source contribution and a collided contribution. The uncollided contribution is evaluated as follows. A sample of the uncollided part of $\Theta(\underline{r}', E, \underline{\Omega}_s)$ is obtained by selecting \underline{r}' and E from the conditional pdf

$$p(\underline{r}', E | \underline{\Omega}_s) = \frac{f'(\underline{r}', E, \underline{\Omega}_s) / E}{\iint f'(\underline{r}'', E'', \underline{\Omega}_s) / E'' dV'' dE''} \quad (5.21)$$

and taking the normalization factor in the denominator as a weight factor. Then the score for the uncollided contribution to F for the homogeneous slab is

$$w_s = \iint f(\underline{r}'', E'', \underline{\Omega}_s) / E'' dV'' dE'' \cdot Q E \Pi(E) \exp\{-\Sigma_t(E) |x' - x_s|\} \quad (5.22)$$

The collided part can be estimated by selecting a nuclide A and reaction type j as usual for an adjoint particle at τ' with weight w going into a collision. Then calculate the probability $p_{j,A}(\underline{\Omega}' \rightarrow \underline{\Omega}_s)$ for scattering into the direction $\underline{\Omega}_s$. If there exist a unique relationship between scattering angle and energy change for reaction type j , E is also determined. Otherwise E is selected from the appropriate pdf. Then the score for the adjoint particle going into a collision is

$$w_s = w P^\dagger(\underline{r}', E') p_{j,A}(\underline{\Omega}' \rightarrow \underline{\Omega}_s) Q E \Pi(E) \exp\{-\Sigma_t(E) |x' - x_s|\} \quad (5.23)$$

The source of adjoint particles is f'/E with f' given by Eq.(5.12).

A normalized pdf for the source is

$$p(\underline{r}, E, \underline{\Omega}) = \frac{1}{4\pi T} \frac{1}{E \ln E_2/E_1} \delta(y-y_0) \delta(z-z_0) \quad E_1 \leq E \leq E_2 \quad (5.24)$$

with T the slab thickness and arbitrary y_0 and z_0 . This pdf is easy to sample. The weight factor to be used for sampling the unnormalized adjoint particle source is

$$w_n = \frac{f(\underline{r}, E, \underline{\Omega})/E}{p(\underline{r}, E, \underline{\Omega})} = \frac{4\pi T \ln E_2/E_1}{Q E_2 - E_1} \quad (5.25)$$

With the expression of Eq.(5.23) for each score, the neutron source strength Q cancels.

In table VI the results are given from the FOCUS and O6R calculations for the volume integrated scalar neutron flux in the slab. For the O6R calculations 16000 neutrons were processed, which took about 13.5 minutes computer time on the IBM 370/158 computer of the Delft University of Technology Computer Centre for a slab thickness of 2.54 cm and about 30 minutes for the 15.24 cm slab. Because the source of adjoint particles is different for each energy group for which the neutron flux has to be calculated, a separate adjoint Monte Carlo calculation is needed for each energy group. The FOCUS calculations were done using 2000 adjoint particle histories for each energy group. The computer time raises from about 25 sec for the highest energy groups to 70 sec for the lowest energy groups for a slab thickness of 2.54 cm. For the 15.24 cm slab the computer times run from 0.6 to 2.7 minutes. The energy spectra calculated by FOCUS are also shown in Fig. 19.

It will be clear that if fluxes are required for smaller energy groups, the forward calculations become worse, while the adjoint calculations do not. Also point fluxes at several depths in the slab can easily be calculated by FOCUS by modifying the adjoint particle source f'/E from

Table VI. Volume integrated slab flux

energy group	energy range	15.24 cm slab				2.54 cm slab			
		FOCUS		O6R		FOCUS		O6R	
		ϕ n.cm/s/eV	σ %	ϕ n.cm/s/eV	σ %	ϕ n.cm/s/eV	σ %	ϕ n.cm/s/eV	σ %
1	12.2-15.0 MeV	$4.81 \cdot 10^{-10}$	1.5	$5.02 \cdot 10^{-10}$	5.8	$1.28 \cdot 10^{-10}$	0.6	$1.29 \cdot 10^{-10}$	5.1
2	10.0-12.2 MeV	$3.36 \cdot 10^{-9}$	1.2	$3.50 \cdot 10^{-9}$	6.0	$9.35 \cdot 10^{-10}$	0.8	$9.52 \cdot 10^{-10}$	5.2
3	8.18-10.0 MeV	$1.60 \cdot 10^{-8}$	1.1	$1.58 \cdot 10^{-8}$	5.8	$4.36 \cdot 10^{-9}$	0.5	$4.45 \cdot 10^{-9}$	5.3
4	6.36-8.18 MeV	$5.93 \cdot 10^{-8}$	2.9	$5.95 \cdot 10^{-8}$	5.9	$1.75 \cdot 10^{-8}$	1.3	$1.74 \cdot 10^{-8}$	5.2
5	4.96-6.36 MeV	$1.78 \cdot 10^{-7}$	2.2	$1.82 \cdot 10^{-7}$	5.2	$5.62 \cdot 10^{-8}$	1.0	$5.46 \cdot 10^{-8}$	4.6
6	4.06-4.96 MeV	$2.86 \cdot 10^{-7}$	1.9	$3.19 \cdot 10^{-7}$	4.6	$9.09 \cdot 10^{-8}$	0.9	$9.35 \cdot 10^{-8}$	4.6
7	3.01-4.06 MeV	$6.74 \cdot 10^{-7}$	2.2	$6.48 \cdot 10^{-7}$	2.8	$2.32 \cdot 10^{-7}$	0.9	$2.23 \cdot 10^{-7}$	2.4
8	2.46-3.01 MeV	$1.08 \cdot 10^{-6}$	2.9	$1.09 \cdot 10^{-6}$	2.8	$3.61 \cdot 10^{-7}$	1.4	$3.59 \cdot 10^{-7}$	2.7
9	2.35-2.46 MeV	$1.39 \cdot 10^{-6}$	2.7	$1.44 \cdot 10^{-6}$	5.2	$4.81 \cdot 10^{-7}$	0.9	$4.78 \cdot 10^{-7}$	5.2
10	1.83-2.35 MeV	$1.56 \cdot 10^{-6}$	2.5	$1.56 \cdot 10^{-6}$	2.3	$5.30 \cdot 10^{-7}$	1.6	$5.48 \cdot 10^{-7}$	2.2
11	1.11-1.83 MeV	$2.03 \cdot 10^{-6}$	3.4	$2.13 \cdot 10^{-6}$	1.6	$7.51 \cdot 10^{-7}$	1.5	$7.34 \cdot 10^{-7}$	1.6
12	0.55-1.11 MeV	$2.89 \cdot 10^{-6}$	4.8	$2.95 \cdot 10^{-6}$	1.3	$9.90 \cdot 10^{-7}$	1.4	$1.02 \cdot 10^{-6}$	1.5
13	111 - 550 keV	$4.30 \cdot 10^{-6}$	4.4	$4.70 \cdot 10^{-6}$	1.0	$1.43 \cdot 10^{-6}$	2.8	$1.39 \cdot 10^{-6}$	1.6
14	3.35- 111 keV	$1.82 \cdot 10^{-5}$	3.4	$1.96 \cdot 10^{-5}$	0.7	$4.38 \cdot 10^{-6}$	3.2	$4.44 \cdot 10^{-6}$	1.8
15	.583-3.35 keV	$3.20 \cdot 10^{-4}$	3.6	$3.13 \cdot 10^{-4}$	1.0	$5.30 \cdot 10^{-5}$	3.8	$4.96 \cdot 10^{-5}$	2.7
16	101 - 583 eV	$1.53 \cdot 10^{-3}$	4.9	$1.61 \cdot 10^{-3}$	1.0	$2.13 \cdot 10^{-4}$	6.6	$2.29 \cdot 10^{-4}$	3.0
17	29.0- 101 eV	$7.33 \cdot 10^{-3}$	5.3	$6.87 \cdot 10^{-3}$	1.2	$8.34 \cdot 10^{-4}$	6.5	$8.11 \cdot 10^{-4}$	3.9
18	10.7-29.0 eV	$2.02 \cdot 10^{-2}$	7.4	$1.91 \cdot 10^{-2}$	1.4	$2.13 \cdot 10^{-3}$	7.5	$1.94 \cdot 10^{-3}$	4.5
19	3.06-10.7 eV	$4.68 \cdot 10^{-2}$	5.1	$4.67 \cdot 10^{-2}$	1.2	$4.18 \cdot 10^{-3}$	6.2	$4.16 \cdot 10^{-3}$	4.5
20	1.12-3.06 eV	$1.01 \cdot 10^{-1}$	5.2	$1.10 \cdot 10^{-1}$	1.4	$8.5 \cdot 10^{-3}$	12	$9.86 \cdot 10^{-3}$	4.9
21	.414-1.12 eV	$2.04 \cdot 10^{-1}$	11	$1.92 \cdot 10^{-1}$	1.5	$1.46 \cdot 10^{-2}$	7.8	$1.65 \cdot 10^{-2}$	5.3
22	thermal	$1.86 \cdot 10^{-1}$	11	$1.65 \cdot 10^{-1}$	1.0	$1.27 \cdot 10^{-2}$	15	$1.35 \cdot 10^{-2}$	4.7

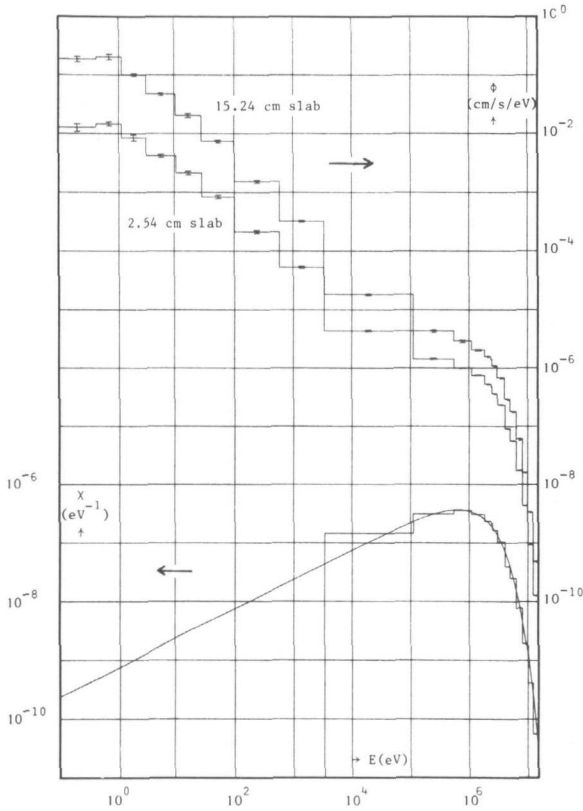


Fig. 19. Volume integrated slab flux and source spectrum

a constant value with respect to x into a delta function. The same can be done with the energy range. As an illustration the flux distribution through the 15.24 cm slab at an energy of 3.0 MeV was calculated and is shown in Fig. 20. Such a calculation cannot be made by a forward Monte Carlo code, nor by any discrete ordinates or diffusion code.

Because the neutron source S only appears in the scoring function in an adjoint calculation, it is very easy to calculate accurately the flux difference due to different neutron sources by a correlated adjoint calculation. For the 3.35-111 keV energy group and the 2.54 cm thick slab the flux difference was calculated for the groupwise constant source energy spectrum and the continuous fission spectrum of ^{235}U as specified by ENDF/B. Both source spectra are shown in Fig. 19. The results are shown in table VII. The estimation of the flux difference

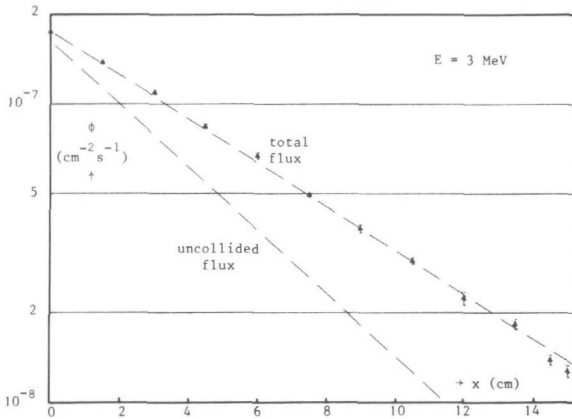


Fig. 20. Flux distribution through the 15.24 cm slab at 3 MeV

with the same accuracy from two independent calculations would have cost about 300 times as much computer time.

Table VII. Correlated flux difference calculation

neutron source spectrum	ϕ n.cm/s/eV	σ n.cm/s/eV
group wise constant	$4.38 \cdot 10^{-6}$	$0.14 \cdot 10^{-6}$
continuous	$4.42 \cdot 10^{-6}$	$0.15 \cdot 10^{-6}$
difference	$4.1 \cdot 10^{-8}$	$1.2 \cdot 10^{-8}$

The primary aim of the benchmark problem was to calculate the response to the neutron flux of a hypothetical point detector at \underline{r}_d outside the slab. If we denote the detector response function by $\eta(E)$, the desired quantity is given by

$$F = \iint \eta(E) \phi_b(\underline{r}_d, E, \underline{\Omega} | y_s, z_s) dE d\Omega \quad (5.26)$$

To be able to treat this problem by an one-dimensional discrete ordinates code, a slightly different quantity was in fact calculated, using the leakage flux from the slab. The integration over $\underline{\Omega}$ in Eq.(5.26) can be transformed into an integration over the slab face. If \underline{r}_f is the

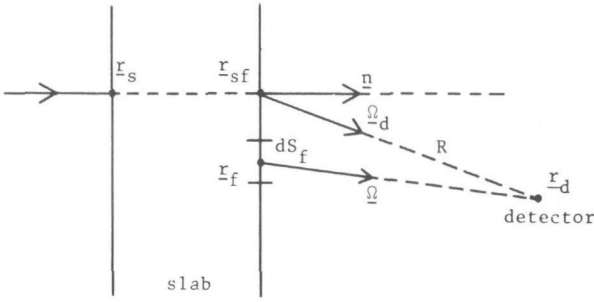


Fig. 21. Derivation of the detector response

crossing point of the line $\underline{r}_d - s\underline{\Omega}$ with the slab face, then the angular flux at the detector is equal to $\phi_b(\underline{r}_f, E, \underline{\Omega} | y_s, z_s)$. From Fig. 21 we see that

$$dS_f = \frac{|\underline{r}_f - \underline{r}_d|^2 d\Omega}{|\underline{n} \cdot \underline{\Omega}|} \quad (5.27)$$

and

$$F = \iint \eta(E) \phi_b(\underline{r}_f, E, \underline{\Omega} = \frac{\underline{r}_d - \underline{r}_f}{|\underline{r}_d - \underline{r}_f|} | y_s, z_s) \frac{|\underline{n} \cdot \frac{\underline{r}_d - \underline{r}_f}{|\underline{r}_d - \underline{r}_f|}|}{|\underline{r}_d - \underline{r}_f|^2} dE dS_f \quad (5.28)$$

The distance $R = |\underline{r}_d - \underline{r}_{sf}|$ was chosen as large as 100 m, so we may set $|\underline{r}_d - \underline{r}_f| \approx R$ and

$$\frac{\underline{r}_d - \underline{r}_f}{|\underline{r}_d - \underline{r}_f|} \approx \frac{\underline{r}_d - \underline{r}_{sf}}{|\underline{r}_d - \underline{r}_{sf}|} = \underline{\Omega}_d \quad (5.29)$$

Then F is closely approximated by

$$F = \iint \eta(E) \phi_b(\underline{r}_f, E, \underline{\Omega}_d | y_s, z_s) \frac{|\underline{n} \cdot \underline{\Omega}_d|}{R^2} dE dS_f \quad (5.30)$$

For this quantity, the flux averaging function is

$$f(\underline{r}, E, \underline{\Omega}) = \eta(E) \frac{|\underline{n} \cdot \underline{\Omega}_d|}{R^2} \delta(x - x_f) \delta(\underline{\Omega} - \underline{\Omega}_d) \quad (5.31)$$

Due to the δ -functions no collision estimator can be used in a forward calculation and we are forced to use an expected value estimator. From Eqs.(2.8) and (2.11) it follows that

$$F = \frac{|\underline{n} \cdot \underline{\Omega}_d|}{R^2} \iint \eta(E) \delta(x - x_f) \left[\frac{T(\underline{r}' \rightarrow \underline{r}, E, \underline{\Omega}_d)}{\Sigma_t(\underline{r}, E)} \chi(\underline{r}', E, \underline{\Omega}_d) dV' dV dE \right] \quad (5.32)$$

The integration over \underline{r} can be carried out as for Eq.(5.20)

$$F = \frac{1}{R^2} \iint \eta(E) \beta(\underline{r}', E, -\underline{\Omega}_d, |x_f - x'| / \Omega_{dx}) \chi(\underline{r}', E, \underline{\Omega}_d) dV' dE \quad (5.33)$$

Because χ is needed in a given direction we have to include just another step of the sampling procedure for a neutron history into the scoring function. With Eq.(2.10) we obtain

$$F = \frac{1}{R^2} \iint \eta(E) \beta(\underline{r}', E, -\underline{\Omega}_d, |x_f - x'| / \Omega_{dx}) \cdot \iint C(\underline{r}', E' \rightarrow E, \underline{\Omega}' \rightarrow \underline{\Omega}_d) \psi(\underline{r}', E', \underline{\Omega}') dV' dE' d\Omega' dE \quad (5.34)$$

Because $\underline{\Omega}_d \neq \underline{\Omega}_s$ there is no direct contribution of the neutron source. The averaging function for the collision density is given by

$$g(\underline{r}', E', \underline{\Omega}') = \frac{1}{R^2} \int \eta(E) \beta(\underline{r}', E, -\underline{\Omega}_d, |x_f - x'| / \Omega_{dx}) C(\underline{r}', E' \rightarrow E, \underline{\Omega}' \rightarrow \underline{\Omega}_d) dE \quad (5.35)$$

This scoring function for a neutron of weight w' at τ' can be obtained by selecting a nuclide A and reaction type j as usual and calculating the probability $p_{j,A}(\underline{\Omega}' \rightarrow \underline{\Omega}_d)$. If E is not uniquely determined by the scattering angle, E is selected from the appropriate pdf. Then the

score for the homogeneous slab is

$$w_s = w' p_{j,A}(\underline{\Omega}' \rightarrow \underline{\Omega}_d) \eta(E) \exp\{-\Sigma_t(E) |x_f - x'| / \Omega_{dx}\} / R^2 \quad (5.36)$$

With this estimator we calculated the energy integrated neutron flux for four detectors for both slab thicknesses by taking $\eta(E)=1$ for the entire energy range using the same neutron histories as for the flux calculation in the slab.

As for the calculation of the slab flux an alteration of the problem is necessary to calculate the detector response by adjoint Monte Carlo. To obtain the quantity of interest as given by Eq.(5.30), we assume again a neutron plane source emitting Q neutrons per unit time and per unit area impinging perpendicularly to the slab face, giving an angular flux $\phi_{p1}(\underline{r}, E, \underline{\Omega})$ in the slab. From Eq.(5.7) we have

$$\begin{aligned} \phi_{p1}(x_f, y_0, z_0, E, \underline{\Omega}) &= Q \iint \phi_b(x_f, y', z', E, \underline{\Omega}) dy' dz' \\ &= Q \iint \phi_b(x_f, y-y_1, z-z_1, E, \underline{\Omega}) dy dz = Q \int \phi_b(\underline{r}_f, E, \underline{\Omega} | y_1, z_1) dS_f \end{aligned} \quad (5.37)$$

with arbitrary y_0, y_1, z_0 and z_1 . Thus

$$F = \frac{|\underline{n} \cdot \underline{\Omega}_d|}{QR^2} \int \eta(E) \phi_{p1}(x_f, y_0, z_0, E, \underline{\Omega}_d) dE \quad (5.38)$$

and the averaging function f' for the neutron flux in the altered problem is

$$f'(\underline{r}, E, \underline{\Omega}) = \frac{|\underline{n} \cdot \underline{\Omega}_d|}{QR^2} \eta(E) \delta(x-x_f) \delta(y-y_0) \delta(z-z_0) \delta(\underline{\Omega}-\underline{\Omega}_d) \quad (5.39)$$

The source of adjoint particles is equal to f'/E and a normalized pdf for the source is

$$p(\underline{r}, E, \underline{\Omega}) = \delta(x-x_f) \delta(y-y_0) \delta(z-z_0) \delta(\underline{\Omega}-\underline{\Omega}_d) \frac{\eta(E)}{E} / \int \eta(E) \frac{dE}{E} \quad (5.40)$$

and the normalization factor is

$$w_n = \frac{|\underline{n} \cdot \underline{\Omega}_d|}{QR^2} \int \eta(E) \frac{dE}{E} \quad (5.41)$$

If $\eta(E)=1$ for the entire energy range, $\int \eta(E)dE/E$ diverges and we should use a different pdf for the source energy selection (at least for the thermal group), for instance a flat pdf, and correct with an appropriate weight factor. The scoring for the adjoint particles will be the same as for the calculation of the neutron flux in the slab. The results of the FOCUS calculations after processing 10000 adjoint particles for each detector and slab thickness are shown in table VIII. The calculation needed about 4.5 minutes computer time per detector for the 2.54 cm slab and about 8 minutes for the 15.24 cm slab. The results for the O6R code, which are obtained from the same neutron histories from which the slab flux was estimated, are also shown in table VIII.

Table VIII. Detector flux

detector number	15.24 cm slab				2.54 cm slab			
	FOCUS		O6R		FOCUS		O6R	
	ϕ n/cm ² /s	σ %						
1	3.70 10 ⁻¹⁰	3.2	3.83 10 ⁻¹⁰	2.2	1.58 10 ⁻⁹	2.5	1.58 10 ⁻⁹	1.1
2	2.80 10 ⁻¹⁰	3.0	2.91 10 ⁻¹⁰	2.6	1.31 10 ⁻⁹	2.0	1.37 10 ⁻⁹	1.2
3	1.62 10 ⁻¹⁰	3.4	1.74 10 ⁻¹⁰	3.4	9.50 10 ⁻¹⁰	1.9	9.79 10 ⁻¹⁰	1.4
4	1.16 10 ⁻¹¹	4.8	1.09 10 ⁻¹¹	12	7.98 10 ⁻¹¹	2.4	8.16 10 ⁻¹¹	3.9

V.3. Calculations on a critical assembly

To demonstrate the performance of the adjoint Monte Carlo technique for multiplying systems as developed in chapter IV, we chose from the reactor core physics benchmark problems collected by the Benchmark Problem Committee of the Mathematics and Computation Division of the American Nuclear Society [30] problem number 1, which is a simplified version of the fast critical assembly called Lady Godiva [31]. It consists of a bare sphere of highly enriched uranium with a radius of 8.71 cm. The atomic densities are given in table IX.

Table IX. Atomic densities for the GODIVA assembly

nuclide	atomic density in $10^{24}/\text{cm}^3$
^{235}U	0.045447
^{238}U	0.00256

The benchmark problem documentation reports results from several discrete ordinates codes and a Monte Carlo code for the calculation of the effective multiplication factor λ_0 and the surface leakage per energy group. All codes use the Hansen-Roach six group cross section set with isotropic scattering [32]. The energy group division is given in table X. To be able to compare several quantities, the benchmark calculations were repeated using the discrete ordinates code DTF-IV [33], with a Gaussian 16-point quadrature set for the discrete directions and 40 space intervals. For the FOCUS calculations we used the ENDF/B-IV data for uranium, which include besides elastic scattering, (n,2n) and (n,3n) reactions, inelastic continuum scattering and inelastic level scattering from 16 and 26 discrete levels for ^{235}U and ^{238}U respectively. With the NPTXS code [27] average point cross sections were generated for

Table X. Energy group division

energy group	energy range
1	3.0- ∞ MeV
2	1.4-3.0 MeV
3	0.9-1.4 MeV
4	0.4-0.9 MeV
5	0.1-0.4 MeV
6	0 -0.1 MeV

the unresolved resonance region. Because there will be a negligible number of neutrons at lower energies, only the energy range above 4 keV, being the lower energy limit of the unresolved resonance region for ^{238}U , is considered. The upper energy limit was taken 15 MeV. Because the neutron energy spectrum in this fast assembly will not differ very much from the fission spectrum, the energy biasing function $\phi_0(E)$ for the selection of source energies for adjoint particles of a new generation, was taken equal to the ^{235}U fission spectrum. From a simulation of 100 generations of adjoint particles with each generation containing about 1000 particles, the effective multiplication factor of the assembly was estimated to be 0.9987 from the last 95 generations with a standard deviation of 0.4%. This took about 25 minutes computer time on the IBM 370/158 computer. The DTF-IV calculation gave $\lambda_0=0.9967$.

To calculate the neutron flux at a point \underline{r}_0 of the assembly for an energy group with limits E_1 and E_2 , we have for the flux averaging function

$$f(\underline{r}, E, \underline{\Omega}) = \delta(\underline{r} - \underline{r}_0) \quad E_1 \leq E \leq E_2 \quad (5.42)$$

The source of adjoint particles is f/E and a normalized pdf is

$$p(\underline{r}, E, \underline{\Omega}) = \frac{1}{4\pi} \frac{1}{E \ln E_2/E_1} \delta(\underline{r} - \underline{r}_0) \quad (5.43)$$

Using this normalized pdf for the selection of source parameters for the adjoint particles of the first generation, all intermediate and final results must be multiplied by the factor

$$w = \frac{f(\underline{r}, E, \underline{\Omega})/E}{p(\underline{r}, E, \underline{\Omega})} = 4\pi \ln E_2/E_1 \quad (5.44)$$

Table XI shows the results for the calculation of the neutron flux at the centre of the assembly for each energy group, obtained after 6 generations of adjoint particles, using nominally 1000 particles per generation. To improve the statistics, the calculations were repeated 8 times for each energy group, which took about 13 minutes computer time per energy group. The results have been normalized to a unit

Table XI. Neutron flux at the centre of the GODIVA assembly

energy group	energy range	FOCUS		DTF-IV
		ϕ n/cm ² /s	σ^1 %	ϕ n/cm ² /s
1	>3.0 MeV	6.22 10 ⁻⁴	3.7	6.342 10 ⁻⁴
2	1.4-3.0 MeV	1.18 10 ⁻³	4.0	1.191 10 ⁻³
3	0.9-1.4 MeV	7.71 10 ⁻⁴	3.7	7.477 10 ⁻⁴
4	0.4-0.9 MeV	1.27 10 ⁻³	3.8	1.266 10 ⁻³
5	0.1-0.4 MeV	8.06 10 ⁻⁴	3.8	9.827 10 ⁻⁴
6	<0.1 MeV	1.30 10 ⁻⁴	4.5	1.517 10 ⁻⁴

¹Without statistical uncertainty due to normalization

neutron source strength, as in the DTF-IV calculations. The normalization factor was estimated to be $3.114 \cdot 10^4$ with a standard deviation of 2.1% from a normalization calculation of 25 runs with 5 generations of about 1000 particles per generation. The source pdf for the first generation of the normalization calculation is given by Eq.(4.119), which implies a spatial uniform source. Energy biasing with $E\phi_0(E)$ was also used for the first generation. For the first four energy groups the FOCUS and DTF-IV results are in good agreement. However, the last two energy groups show

significant differences. This may be due to possibly incorrect group cross section data for these energy groups in the DTF-IV calculation.

To show how the result for the neutron flux comes about after several generations of adjoint particles, table XII shows the intermediate results for a single run of the calculation of the flux at the centre of the assembly for the energy group 0.1-0.4 MeV. During the n -th generation $\rho_n^+(\tau)$ from Eq. (4.73) is simulated, using the scheme of Fig. 16 on page 101. The multiplication k_n of the n -th generation is equal to the total weight of adjoint particles generated in the n -th generation relative to the total source of this generation

$$k_n = \frac{\int \Gamma_{n+1}^+(\tau) d\tau}{\int \Gamma_n^+(\tau) d\tau} \quad (5.45)$$

For n sufficiently large, k_n approaches the effective multiplication factor λ_0 as can be derived from Eq. (4.88). For the calculation of k_n the source Γ_n^+ may be arbitrarily normalized. Because all particles of the first generation start at the centre of the assembly, the spatial distribution of the adjoint particles in the first few generations will

Table XII. Intermediate results for the 0.1-0.4 MeV flux calculation

generation	number of particles	k_n	σ %	F_n	σ %	N_{contr}
1	1000	1.232	3.4	$2.15 \cdot 10^1$	3.4	983
2	954	1.152	4.2	$2.47 \cdot 10^1$	5.9	472
3	1139	1.048	3.0	$2.59 \cdot 10^1$	7.4	363
4	1085	1.097	4.0	$2.84 \cdot 10^1$	8.8	284
5	1072	0.999	5.1	$2.84 \cdot 10^1$	11	231
6	1030	1.012	3.5	$2.87 \cdot 10^1$	11	189
7	1022	0.956	2.9	$2.75 \cdot 10^1$	11	160
8	914	1.034	3.8	$2.84 \cdot 10^1$	12	139
9	1036	1.019	3.4	$2.90 \cdot 10^1$	13	122
10	957	1.019	4.3	$2.95 \cdot 10^1$	14	111

be concentrated more near the centre of the assembly as compared to the fundamental mode distribution, which reduces leakage and results in a multiplication greater than λ_0 . For the very first generation the energy distribution of the source also deviates from the fundamental mode source distribution, which may lead to a multiplication for the first generation completely different from λ_0 . To set the Russian roulette that controls the number of particles generated for the next generation, the multiplication for the first generation must be estimated in a separate calculation. To obtain the standard deviation in k_n the total weight of progeny generated by each particle in the n -th generation has to be summed per source particle of that generation. From these sums and their squares the standard deviation is obtained in the usual way. With the scoring function $\eta(\tau)$ from Eq.(4.140), the estimate for k_n may also be used to estimate the neutron flux, according to Eq.(4.139). However, the important difference with the estimation of k_n is that for the estimation of the neutron flux (or any other average over the fundamental mode neutron distribution) the source Γ_n^+ may not be arbitrarily normalized, but the absolute value must be taken into account. If we call the estimate of the flux after the n -th generation F_n , we obtain F_1 by multiplying k_1 by the factor w from Eq.(5.44), because this is the ratio of the true source f/E for the first generation and the normalized one, actually used. For the next generations F_n is obtained from

$$F_n = k_n F_{n-1} \quad (5.46)$$

For n sufficiently large, the bias on F_n as an estimate for the neutron flux due to the presence of higher modes in the distribution of the adjoint particles, will vanish. The statistical uncertainty in F_n is not only caused by the uncertainty in k_n but also by the multiplication of the previous generations. To obtain the standard deviation in F_n we therefore have to sum all the scores from particles in the n -th generation that are descendants of the same parent particle of the first generation. From these sums and their squares the standard deviation can

be estimated. It will be clear that the number of particles N_{contr} from the first generation still having progeny in the n -th generation that contributes to F_n , will decrease with increasing n , which increases the standard deviation in F_n . N_{contr} is also shown in table XII.

For a further comparison with results from DTF-IV, we also calculated the volume integrated flux per energy group, the volume integrated absorption per group and the surface integrated leakage per group. To obtain the volume integrated neutron flux, the spatial distribution of the source for the first generation was taken uniform in the assembly instead of the δ -function as in Eq.(5.43). To obtain the absorption the source for the first generation becomes

$$f(\underline{r}, E, \underline{\Omega})/E = \Sigma_a(E)/E \quad E_1 \leq E \leq E_2 \quad (5.47)$$

and a probability table for the selection of the energy from the function $\Sigma_a(E)/E$ was first prepared. Because $\underline{\Omega}\phi(\underline{r}, E, \underline{\Omega})$ is the neutron current per unit area perpendicular to the direction $\underline{\Omega}$, the surface leakage is given by

$$F = \iiint_{\underline{n} \cdot \underline{\Omega} > 0} \underline{n} \cdot \underline{\Omega} \phi(\underline{r}_S, E, \underline{\Omega}) dS dE d\Omega \quad (5.48)$$

Table XIII. Comparison of FOCUS and DTF-IV

energy group	flux(n.cm/s)		absorption(n/s)		leakage(n/s)	
	FOCUS	DTF-IV	FOCUS	DTF-IV	FOCUS	DTF-IV
1	0.927(4.4) ¹	0.8516	0.0730(5.6)	0.05000	0.0884(4.3)	0.07998
2	1.706(4.1)	1.5943	0.1312(4.0)	0.09637	0.1570(4.1)	0.14686
3	1.075(4.3)	1.0003	0.0638(3.9)	0.06083	0.0986(4.2)	0.09123
4	1.778(4.2)	1.6816	0.1038(4.0)	0.10377	0.1451(4.3)	0.14726
5	1.093(4.3)	1.2561	0.0788(4.3)	0.09528	0.0828(5.4)	0.09179
6	0.161(5.6)	0.1886	0.0211(7.3)	0.02540	0.0106(6.8)	0.01124

¹ Percentage standard deviation without statistical uncertainty due to normalization

with \underline{r}_s on the surface and \underline{n} the normal vector on the surface at \underline{r}_s . The source for the first generation becomes

$$f(\underline{r}, E, \underline{\Omega})/E = \underline{n} \cdot \underline{\Omega} \delta(|\underline{r}| - R)/E \quad \underline{n} \cdot \underline{\Omega} > 0 \text{ and } E_1 \leq E \leq E_2 \quad (5.49)$$

with R the radius of the assembly. A normalized pdf for the source is

$$p(\underline{r}, E, \underline{\Omega}) = \frac{\underline{n} \cdot \underline{\Omega}}{\pi} \frac{\delta(|\underline{r}| - R)}{4\pi R^2} \frac{1}{E \ln E_1/E_2} \quad (5.50)$$

To sample this pdf \underline{r} is chosen uniform on the surface. Then $\mu = \underline{n} \cdot \underline{\Omega}$ is selected from the pdf $p(\mu) = 2\mu$ ($0 \leq \mu \leq 1$) and a random azimuthal angle ϕ is selected. The direction components are then calculated from μ and ϕ . The results are shown in table XIII together with the DTF-IV results. For the FOCUS calculations 8 runs of 6 generations of nominally 1000 particles were simulated for each quantity and each energy group, which took about 12 minutes computer time per item. As for the flux at the centre of the assembly, the volume integrated flux for the last two energy groups calculated by FOCUS and DTF-IV differ significantly. The volume integrated absorption also shows significant differences for the first two energy groups, which is possibly due to a too low absorption group cross section in the DTF-IV calculation for these energy groups.

As an illustration of the capabilities of adjoint Monte Carlo the neutron energy spectrum at the centre of the assembly has been calculated for a number of energies. The results are shown in Fig. 22. For each energy 3 runs have been made with 6 generations of nominally 1000 particles, which took about 4 minutes computer time. Because the type of quantity to be calculated mainly effects the standard deviation in the multiplication of the first generation and the computing time for the first generation only, the standard deviation and computing time per run is roughly equal for all quantities calculated.

For the calculation of the effective multiplication factor λ_0 , the same restrictions apply to the phase space for a non-zero score in a forward and an adjoint calculation. Besides, an estimate of λ_0 can be

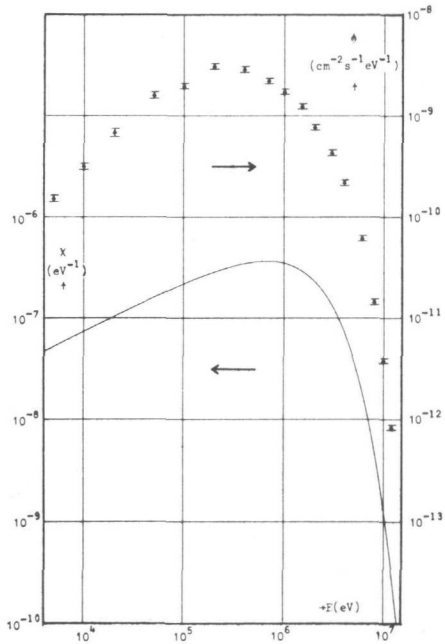


Fig. 22. Neutron flux spectrum at the centre of the GODIVA assembly and neutron source spectrum

obtained from one generation, irrespective of the multiplication of previous generations. Therefore, a comparison of the efficiency of FOCUS and a forward Monte Carlo code may be meaningful. From a simulation of 50 generations with nominally 300 neutrons per generation by the 06R code [20], λ_0 was estimated to be 0.9981 with a standard deviation of 0.7% from the last 45 generations. This calculation took about 6.5 minutes computer time. If the standard deviation times the square root of the computing time is taken as a measure of the efficiency, FOCUS turns out to be almost as efficient as 06R. However, it should be emphasized that the choice of the source energy biasing function strongly influences the efficiency of the adjoint calculation.

V.4. Discussion and conclusions

Comparison of the results of the adjoint Monte Carlo code FOCUS with results from other codes for several quantities of interest for the

benchmark problems discussed in the previous sections, shows a fair agreement. This establishes the validity of the theory developed in the chapters III and IV and the proper operation of the FOCUS code. The divergent quantities calculated and the different materials dealt with demonstrate the capabilities of FOCUS. The light nuclides appearing in the shielding benchmark problem do not present any difficulties as might be expected when using definition I from Eq.(3.15) for the adjoint cross sections. By the inclusion of a thermal group and of multiplying (critical) systems and allowance for all scattering reaction types and any degree of anisotropy, a complete and versatile adjoint Monte Carlo computer code has been realized.

Although it may be obvious to compare the efficiency of FOCUS with that of a forward Monte Carlo code from the results for the shielding benchmark problem presented in section V.2, one should realize that the statistical uncertainty strongly depends on the quantity calculated. For the volume integrated group fluxes shown in table VI the standard deviations from the O6R calculation will increase if the widths of the chosen energy groups decrease, but the standard deviations from the FOCUS calculations will hardly be affected or possibly decrease somewhat. Because forward Monte Carlo calculations are more suited for integral quantities and adjoint calculations for differential quantities, it has to be decided for each case again which method will be most efficient. Forward and adjoint Monte Carlo should not be regarded as competitive rather than supplementary. Furthermore, only the basic technique for the adjoint Monte Carlo solution of neutron transport problems is given. All variance reducing techniques in use in forward Monte Carlo calculations may still be applied to the adjoint calculation.

Some remarks should be made about eigenvalue problems for multiplying systems. In contrast with a forward solution of these problems, the adjoint solution has the disadvantage that the statistical uncertainty in the multiplication of all generations of adjoint particles previous to the one from which the desired quantity is estimated, determines the statistical uncertainty in the final estimate too. However, the

estimation of the effective multiplication factor, for which this disadvantage does not apply, can be made as efficient as from a forward Monte Carlo calculation, depending on the proper choice of a source energy biasing function for newly generated adjoint particles.

As a general conclusion we may state that the developed adjoint Monte Carlo theory and its practical realization in the computer code FOCUS is a useful tool to calculate those quantities, for which a Monte Carlo calculation is desired and a forward solution is not efficient. Therefore, a significant expansion is obtained of the applicability range of the Monte Carlo method for neutron transport problems.

APPENDIX A

MECHANICS OF INELASTIC NEUTRON SCATTERING

In this appendix we shall derive the relation between scattering angle and neutron energy before and after an inelastic collision with a nucleus. We shall denote all quantities after collision with a prime and all quantities before collision without one. Further, v denotes the neutron speed in the laboratory system, $\underline{\Omega}$ its flight direction in the laboratory system and m its mass. The speed in the centre of mass system is denoted by u . With an index A these quantities refer to the target nucleus.

If a neutron excites a nuclear level of energy Q of a target nucleus at rest in an inelastic collision (see Fig. A1), the law of conservation of momentum reads

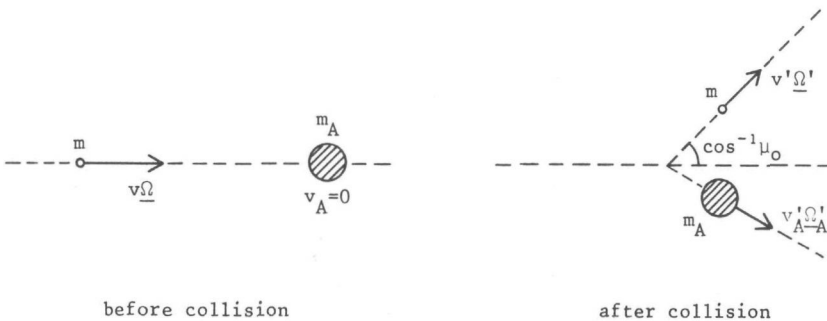


Fig. A1. Collision in the laboratory system

$$m\mathbf{v}\underline{\Omega} = m\mathbf{v}'\underline{\Omega}' + m_A\mathbf{v}'_{A-\underline{A}} \quad (\text{A.1})$$

From this we can express \mathbf{v}'_A as follows

$$A^2\mathbf{v}'_A{}^2 = v^2 + v'^2 - 2vv'\mu_0 \quad (\text{A.2})$$

with $\mu_0 = \underline{\Omega} \cdot \underline{\Omega}'$ the cosine of the scattering angle in the laboratory system and $A = m_A/m$ the mass of the target nucleus relative to the neutron mass. The law of conservation of energy reads

$$\frac{1}{2}mv^2 = \frac{1}{2}mv'^2 + \frac{1}{2}m_A\mathbf{v}'_A{}^2 + Q \quad (\text{A.3})$$

Elimination of \mathbf{v}'_A from Eqs.(A.2) and (A.3) gives

$$\mu_0 = \frac{1}{2} \left\{ (A+1) \frac{v'}{v} - (A-1) \frac{v}{v'} + A \frac{Q}{E} \frac{v}{v'} \right\} \quad (\text{A.4})$$

with $E = \frac{1}{2}mv^2$ the neutron energy in the laboratory system before collision.

If we look at the collision in the centre of mass system (see Fig. A2), the speed of the centre of mass \mathbf{v}_c is given by

$$\mathbf{v}_{c-\underline{\Omega}} = \frac{1}{A+1} \mathbf{v}\underline{\Omega} \quad (\text{A.5})$$

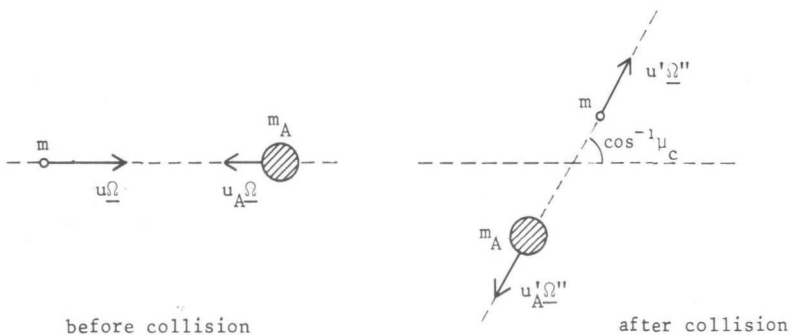


Fig. A2. Collision in the centre of mass system

The neutron speed in the centre of mass system is

$$\underline{u}_{\Omega} = \underline{v}_{\Omega} - v_{c_{\Omega}} \underline{\Omega} = \frac{A}{A+1} v_{\Omega} \underline{\Omega} \quad (\text{A.6})$$

and the speed of the target nucleus is

$$u_{A_{\Omega}} = -\frac{1}{A+1} v_{\Omega} \underline{\Omega} \quad (\text{A.7})$$

In the centre of mass system the total momentum is zero and energy is conserved, thus

$$m u'_{\Omega} + m_A u'_{A_{\Omega}} = 0 \quad (\text{A.8})$$

$$\frac{1}{2} m u'^2 + \frac{1}{2} m_A u_{A_{\Omega}}'^2 = \frac{1}{2} m u'^2 + \frac{1}{2} m_A u_{A_{\Omega}}'^2 + Q \quad (\text{A.9})$$

From Eqs.(A.6) to (A.9) we have

$$\frac{A^2}{(A+1)^2} v^2 + \frac{A}{(A+1)^2} v^2 = u'^2 + \frac{1}{A} u'^2 + 2 \frac{Q}{m} \quad (\text{A.10})$$

or

$$u' = \frac{A}{A+1} v \sqrt{1 - \frac{A+1}{A} \frac{Q}{E}} \quad (\text{A.11})$$

From this result we can see that the neutron must have at least an energy

$$\epsilon = \frac{A+1}{A} Q \quad (\text{A.12})$$

to excite the nuclear level. Knowing the neutron speed u' after collision in the centre of mass system, we have for the laboratory system

$$v'_{\Omega} = u'_{\Omega} + v_{c_{\Omega}} \underline{\Omega} \quad (\text{A.13})$$

The speed of the centre of mass after collision is equal to its speed before collision

$$v'_c \underline{\Omega} = v_c \underline{\Omega} \quad (\text{A.14})$$

The inner product of Eq.(A.13) with $\underline{\Omega}$ gives

$$v' \mu_o = u' \mu_c + v_c \quad (\text{A.15})$$

or

$$\mu \frac{v'}{ov} = \frac{A}{A+1} \mu_c \sqrt{1-\epsilon/E} + \frac{1}{A+1} \quad (\text{A.16})$$

with $\mu_c = \underline{\Omega} \cdot \underline{\Omega}'$ the cosine of the scattering angle in the centre of mass system. Substitution of μ_o from Eq.(A.4) leads to the relation between the energy after and before collision

$$\frac{E'}{E} = \frac{v'^2}{v^2} = \frac{A^2(1-\epsilon/E) + 2A\mu_c \sqrt{1-\epsilon/E} + 1}{(A+1)^2} \quad (\text{A.17})$$

Substitution of v'/v from Eq.(A.17) into Eq.(A.16) gives the relation between μ_o and μ_c

$$\mu_o = \frac{A\mu_c \sqrt{1-\epsilon/E} + 1}{\sqrt{A^2(1-\epsilon/E) + 2A\mu_c \sqrt{1-\epsilon/E} + 1}} \quad (\text{A.18})$$

In contrast to the case of elastic collisions ($\epsilon=0$) this relation also depends on the neutron energy E before collision. For the derivative of μ_o with respect to μ_c we have

$$\frac{\partial \mu_o(\mu_c, E)}{\partial \mu_c} = \frac{A^2(1-\epsilon/E) (A\sqrt{1-\epsilon/E} + \mu_c)}{\{A^2(1-\epsilon/E) + 2A\mu_c \sqrt{1-\epsilon/E} + 1\}^{3/2}} \quad (\text{A.19})$$

The derivative is everywhere positive if $A\sqrt{1-\epsilon/E} > 1$ or $E > \epsilon A^2 / (A^2 - 1)$.
 If $\epsilon < E < \epsilon A^2 / (A^2 - 1)$ then the derivative is zero for $\mu_c = -A\sqrt{1-\epsilon/E}$ and μ_o lies in the range $\sqrt{1-A^2(1-\epsilon/E)} \leq \mu_o \leq 1$. This is illustrated in Fig. A3. The inverse formula for Eq.(A.18) is

$$\mu_c = \frac{\mu_o}{A\sqrt{1-\epsilon/E}} \sqrt{A^2(1-\epsilon/E) + \mu_o^2 - 1} - \frac{1 - \mu_o^2}{A^2(1-\epsilon/E)} \quad E > \epsilon A^2 / (A^2 - 1) \quad (A.20)$$

For $\epsilon < E < \epsilon A^2 / (A^2 - 1)$ μ_c is double valued:

$$\mu_c = \pm \frac{\mu_o}{A\sqrt{1-\epsilon/E}} \sqrt{A^2(1-\epsilon/E) + \mu_o^2 - 1} - \frac{1 - \mu_o^2}{A^2(1-\epsilon/E)} \quad (A.21)$$

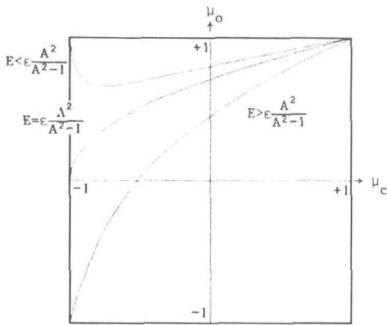


Fig. A3. Relation between μ_o and μ_c for inelastic scattering

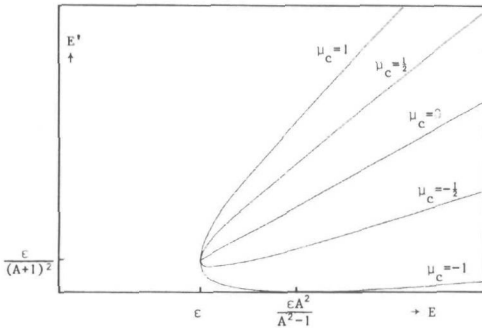


Fig. A4. Relation between E' and E with μ_c as a parameter

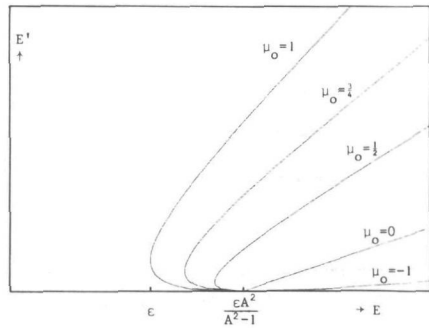


Fig. A5. Relation between E' and E with μ_o as a parameter

Fig. A4 shows graphically the relation between E' and E with μ_c as parameter. For all energies $E > \epsilon$ the maximum and minimum value for the energy E' after collision is obtained for $\mu_c = +1$ and -1 respectively and from Eq.(A.17) we have

$$\left(\frac{A\sqrt{1-\epsilon/E}-1}{A+1} \right)^2 E \leq E' \leq \left(\frac{A\sqrt{1-\epsilon/E}+1}{A+1} \right)^2 E \quad (\text{A.22})$$

For $E = \epsilon A^2 / (A^2 - 1)$ the minimum value of E' becomes zero. For $E = \epsilon$ the range of E' degenerates into one single point $E' = \epsilon / (A+1)^2$. The relation between E' and E with μ_o as parameter in stead of μ_c is shown in Fig. A5. For $\epsilon < E < \epsilon A^2 / (A^2 - 1)$ only a limited range of μ_o is possible and the maximum and minimum value of E' are both obtained for $\mu_o = +1$.

APPENDIX B

A PROPERTY OF THE DEFINITION I ADJOINT INELASTIC CROSS SECTION

In this appendix it will be shown that the adjoint inelastic cross section according to definition I of Eq.(3.15) for the case of a constant inelastic scattering cross section from the threshold energy and for isotropic scattering in the centre of mass system is also constant from a certain energy.

If ϵ is the threshold energy the adjoint inelastic cross section according to definition I is given by

$$\sigma_{si}^+(E') = \int_{E_{\min}}^{E_{\max}} \frac{\sigma_{si}}{E(1-\alpha)\sqrt{1-\epsilon/E}} dE \quad (\text{B.1})$$

where E_{\min} and E_{\max} are the minimum and maximum values of E for which the scattering function is non-zero, given E' .

With the substitution

$$z = \sqrt{1-\epsilon/E} \quad (\text{B.2})$$

we have for the adjoint cross section

$$\sigma_{si}^{\dagger}(E') = \frac{2\sigma_{si}}{1-\alpha} \int_{z_{\min}}^{z_{\max}} \frac{dz}{1-z^2} = \frac{\sigma_{si}}{1-\alpha} \ln \frac{(1+z_{\max})(1-z_{\min})}{(1-z_{\max})(1+z_{\min})} \quad (\text{B.3})$$

where z_{\min} corresponds to E_{\min} and z_{\max} to E_{\max} . To obtain z_{\min} and z_{\max} as a function of E' we use Eq.(A.17) from appendix A in the form

$$\frac{E'}{\epsilon} (1-z^2) = \frac{A^2 z^2 + 2A\mu_c z + 1}{(A+1)^2} \quad (\text{B.4})$$

From this quadratic equation we obtain for z

$$z = \frac{-A\mu_c \pm \sqrt{A^2\mu_c^2 + \{A^2 + (A+1)^2 E'/\epsilon\} \{(A+1)^2 E'/\epsilon - 1\}}}{A^2 + (A+1)^2 E'/\epsilon} \quad (\text{B.5})$$

From Fig. A4 in appendix A we see that E and thus z is a single-valued function of μ_c if $E' \geq \epsilon/(A+1)^2$ and that z_{\min} and z_{\max} are obtained for $\mu_c = +1$ and -1 respectively. Then Eq.(B.5) holds with only the $+$ sign in front of the square root term. For $E' < \epsilon/(A+1)^2$ z_{\min} and z_{\max} are both obtained for $\mu_c = -1$ using the $-$ and $+$ sign in Eq.(B.5) respectively. For $E' \geq \epsilon/(A+1)^2$ we have

$$z_{\min} = \frac{-A + (A+1) \sqrt{(A+1)^2 (E'/\epsilon)^2 + (A^2 - 1) E'/\epsilon}}{A^2 + (A+1)^2 E'/\epsilon} \quad (\text{B.6})$$

and

$$z_{\max} = \frac{A + (A+1) \sqrt{(A+1)^2 (E'/\epsilon)^2 + (A^2 - 1) E'/\epsilon}}{A^2 + (A+1)^2 E'/\epsilon} \quad (\text{B.7})$$

If we set for abbreviation

$$p = A^2 + (A+1)^2 E'/\epsilon \quad (\text{B.8})$$

and

$$q = (A+1) \sqrt{(A+1)^2 (E'/\epsilon)^2 + (A^2-1)E'/\epsilon} \quad (\text{B.9})$$

we have

$$\frac{(1+z_{\max})(1-z_{\min})}{(1-z_{\max})(1+z_{\min})} = \frac{(p+A+q)(p+A-q)}{(p-A-q)(p-A+q)} = \frac{(p+A)^2 - q^2}{(p-A)^2 - q^2} \quad (\text{B.10})$$

Because

$$q^2 = (A+1)^4 (E'/\epsilon)^2 + (A+1)^2 (A^2-1)E'/\epsilon \quad (\text{B.11})$$

and

$$\begin{aligned} (p \pm A)^2 &= \{A(A \pm 1) + (A+1)^2 E'/\epsilon\}^2 \\ &= A^2 (A \pm 1)^2 + 2A(A \pm 1)(A+1)^2 E'/\epsilon + (A+1)^4 (E'/\epsilon)^2 \end{aligned} \quad (\text{B.12})$$

we have

$$\begin{aligned} (p \pm A)^2 - q^2 &= A^2 (A \pm 1)^2 + (A+1)^2 \frac{E'}{\epsilon} \{2A(A \pm 1) - A^2 + 1\} \\ &= A^2 (A \pm 1)^2 + (A+1)^2 (A \pm 1)^2 \frac{E'}{\epsilon} = (A \pm 1)^2 p^2 \end{aligned} \quad (\text{B.13})$$

and

$$\frac{1+z_{\max}}{1-z_{\max}} \frac{1-z_{\min}}{1+z_{\min}} = \frac{(A+1)^2}{(A-1)^2} = \frac{1}{\alpha} \quad (\text{B.14})$$

independent of E' for $E' \geq \epsilon/(A+1)^2$

From Eq.(B.3) we have for the adjoint inelastic cross section

$$\sigma_{si}^\dagger(E') = \sigma_{si} \frac{\ln 1/\alpha}{1-\alpha} \quad E' > \epsilon/(A+1)^2 \quad (\text{B.15})$$

which proves the fact that the definition I adjoint inelastic cross section is constant for energies above $\epsilon/(A+1)^2$ if the inelastic scattering cross section is constant from the threshold energy and the scattering is isotropic in the centre of mass system.

REFERENCES

- [1] R.D.Richtmyer and J.von Neumann, "Statistical Methods in Neutron Diffusion", in: *John von Neumann Collected Works*, volume V, Pergamon Press, Oxford (1963), p. 751.
- [2] F.A.R.Schmidt, "Status of the Monte-Carlo Development", in: *Proc. Seminar on Numerical Reactor Calculations*, International Atomic Energy Agency, Vienna (1972), p. 699.
- [3] C.W.Maynard, "An Application of the Reciprocity Theorem to the Acceleration of Monte Carlo Calculations", *Trans. Am. Nucl. Soc.*, 3, 340 (1960).
- [4] G.I.Bell and S.Glasstone, *Nuclear Reactor Theory*, Van Nostrand Reinhold, New York (1970).
- [5] J.Spanier and E.M.Gelbard, *Monte Carlo Principles and Neutron Transport Problems*, Addison-Wesley, Reading, Massachusetts (1969).
- [6] G.Goertzel and M.H.Kalos, "Monte Carlo Methods in Transport Problems", in: *Progress in Nuclear Energy*, Series I, Volume 2, Pergamon Press, London (1958), p. 315.
- [7] M.H.Kalos, "On the Estimation of Flux at a Point by Monte Carlo", *Nucl. Sci. Eng.*, 16, 111 (1963).
- [8] P.M.Morse and H.Feshbach, *Methods of Theoretical Physics*, McGraw-Hill, London (1953).
- [9] J.E.Hoogenboom, "FOCUS - A non-multigroup adjoint Monte Carlo code with improved variance reduction", in *Proc. of the NEACRP meeting of a Monte Carlo Study Group*, ANL-75-2/NEA-CRP-L-118, Argonne National Laboratory (1975), p. 244.

- [10] E.A.Straker et al, "The MORSE code - A multigroup Neutron and Gamma-ray Monte Carlo Transport Code", ORNL-4585, Oak Ridge National Laboratory (1970).
- [11] B.Eriksson et al, "Monte Carlo Integration of the Adjoint Neutron Transport Equation", *Nucl. Sci. Eng.*, 37, 410 (1969).
- [12] L.Dresner, *Resonance absorption in Nuclear Reactors*, Pergamon Press, Oxford (1960).
- [13] R.R.Coveyou, V.R.Cain and K.J.Yost, "Adjoint and Importance in Monte Carlo Application", *Nucl. Sci. Eng.*, 27, 219 (1967).
- [14] J.E.Hoogenboom, "A generalized adjoint Monte Carlo technique", *Atomkernenergie*, 25, 232 (1975).
- [15] B.E.Watt, "A study of the spectrum of the neutrons of low energy from the fission of U^{235} ", *Phys. Rev.*, 87, 1037 (1952).
- [16] A.Ralston, *A first Course in Numerical Analysis*, McGraw-Hill, New York (1965).
- [17] R.C.Gast, "Monte Carlo Eigenfunction Iteration Strategies that are and are not Fair Games", WAPD-TM-878, Bettis Atomic Power Laboratory (1969).
- [18] M.H.Kalos, private communication.
- [19] J.E.Hoogenboom, "FOCUS - A versatile non-multigroup adjoint Monte Carlo neutron transport code", IRI-131-77-06/THD-H-RF-144, Interuniversity Reactor Institute, Delft, to be published.
- [20] C.L.Thompson and E.A.Straker, "O6R-ACTIFK, Monte Carlo Neutron Transport Code", ORNL-TM-3050, Oak Ridge National Laboratory (1969).
- [21] D.J.Lehmer, "Mathematical Methods in Large-Scale Computing Units", in: *Proc. 2nd Symposium on Large-Scale Digital calculating machinery*, Ann. Comp. Lab. Harvard Univ., 26, 141 (1951).
- [22] N.Metropolis, "Phase Shifts - Middle Squares - Wave Equation", in: *Symposium on Monte Carlo Methods*, John Wiley & Sons, New York (1956), p. 29.

- [23] J.E.Hoogenboom and P.F.A.de Leege, "ADX - A code to calculate adjoint neutron cross sections from the ENDF/B file", IRI-131-77-04/THD-H-RF-145, Interuniversity Reactor Institute, Delft, to be published.
- [24] D.Garber, C.Dunford and S.Pearlstein, "Data Formats and Procedures for the Evaluated Nuclear Data File, ENDF", BNL-NCS-50496/ENDF-102, Brookhaven National Laboratories (1975).
- [25] D.E.Cullen, "Program RIGEL", BNL-50300/ENDF-110, revised edition, Brookhaven National Laboratory (1971).
- [26] H.C.Honeck, "Retrieval Subroutines for the ENDF/B System", part of the report BNL-13582/ENDF-110, revised edition, Brookhaven National Laboratory (1969).
- [27] N.M.Greene et al, "AMPX: A modular code system for generating coupled multigroup neutron-gamma libraries from ENDF/B", ORNL-TM-3706, Oak Ridge National Laboratory (1974).
- [28] J.E.Hoogenboom, "ETOF - A program to prepare a cross section data tape from the ENDF/B file for the adjoint Monte Carlo code FOCUS", IRI-131-77-05/THD-H-RF-146, Interuniversity Reactor Institute, Delft, to be published.
- [29] G.L.Simmons (ed.), "Shielding Benchmark Problems", ORNL-RSIC-25 (suppl. 2), Oak Ridge National Laboratory (1974).
- [30] "Argonne Code Center: Benchmark problem book", ANL-7416, Argonne National Laboratory (1968).
- [31] R.E.Peterson and G.A.Newby, "An Unreflected U-235 Critical Assembly", *Nucl. Sci. Eng.*, 1, 112 (1956).
- [32] G.E.Hansen and W.H.Roach, "Six and Sixteen Group Cross sections for Fast and Intermediate Critical Assemblies", LAMS-2543, Los Alamos Scientific Laboratory (1961).
- [33] K.D.Lathrop, "DTF-IV, A FORTRAN-IV Program for Solving the Multigroup Transport Equation with Anisotropic Scattering", LA-3373, Los Alamos Scientific Laboratory (1965).

LIST OF IMPORTANT SYMBOLS

A	atomic mass
c	mean number of neutrons released in a collision
C	neutron collision kernel
D^\dagger	transformed adjoint collision kernel
E	energy
f	averaging function with respect to the flux, neutron scattering function
F	quantity to be calculated
g	averaging function with respect to the collision density
h	averaging function with respect to the emission density
H	neutron transition kernel after a scattering event
K	neutron transition kernel after an emission event
K^\dagger	adjoint transition kernel
M^\dagger	transformed adjoint transition kernel
N	atomic density
p	probability density function
p^\dagger	adjoint scattering probability
P^\dagger	adjoint weight factor
Q	inelastic level energy
\underline{r}	space coordinate
S	neutron source
T	neutron transport kernel
T^\dagger	adjoint transport kernel

v	neutron speed
w	weight, weight factor
α	defined by Eq.(3.33)
Γ^\dagger	transformed adjoint source density
ϵ	inelastic threshold
ζ^\dagger	transformed adjoint collision density
Λ^\dagger	transformed adjoint emission density
μ	cosine of scattering angle
$\bar{\nu}$	mean number of neutrons released in a fission
Π	fission spectrum
ρ^\dagger	transformed adjoint collision density
σ	microscopic neutron cross section
σ^\dagger	microscopic adjoint cross section
Σ	macroscopic neutron cross section
Σ^\dagger	macroscopic adjoint cross section
τ	general coordinate of the phase space
ϕ	neutron flux
χ	neutron emission density
χ^\dagger	adjoint particle density
ψ	neutron collision density
$\underline{\Omega}$	direction

subscripts

a	absorption
A	nuclide A
c	centre of mass system
f	fission
j	reaction type j
s	scattering
t	total
o	fundamental mode distribution, laboratory system, zero-th generation

ACKNOWLEDGEMENTS

I like to thank the board of directors of the Interuniversity Reactor Institute for making available the institute's facilities. I am indebted to P.F.A. de Leege for his programming assistance, especially in developing the ADX code and to J.G.F. Schut for drawing the figures. Last but not least, I like to thank Linda Dornseiffer and Elly Muns for typing the draft of this thesis and Hanneke Hoogenboom for typing the final version.

STELLINGEN

I

Bij de vermelding van resultaten van monte-carloberekeningen dient altijd de statistische onzekerheid in de berekende grootheid te worden opgegeven, alsmede het gebruikte aantal geschiedenissen. De vermelding van de benodigde computerrekentijd is vaak zinvol, mits tevens merk en type van de voor de berekening gebruikte computer worden genoemd.

II

De voortdurende uitbreiding van bestanden van geëvalueerde nucleaire gegevens, illustreert niet alleen een verfijning van de meettechnieken, maar verraadt tevens een gebrek aan geschikte modellen om de betreffende gegevens te beschrijven.

III

In tegenstelling tot wat diverse boeken over het ontstaan van de moderne monte-carlomethode beweren, is deze methode niet ontwikkeld tijdens en ten behoeve van het Amerikaanse atoombomproject in de 2^e wereldoorlog, maar eerst in 1947 door S.Ulam en J.von Neumann.

R.D.Richtmyer and J.von Neumann, *John von Neumann collected Works*, volume V, Pergamon Press, Oxford (1963)

IV

Het gebruik van dopplerverbrede resonantie werkzame doorsneden kan in monte-carloberekeningen op eenvoudige wijze vermeden worden.

V

De methode, die Case aangeeft voor het bepalen van legendrecomponenten, die de hoekafhankelijkheid van de werkzame doorsnede voor neutronenverstrooiing weergeven, is ten hoogste geschikt voor het bepalen van de eerste anisotrope component. De afleiding die Case geeft, kan sterk vereenvoudigd worden door het gebruik van momenten van de plaatsafhankelijke neutronenfluxverdeling.

K.M. Case, *Phys. Fluids*, 16 (1973)

VI

Computerprogramma's voor reactorfysische berekeningen zijn vaak niet op alle gepretendeerde mogelijkheden getoetst, voordat zij voor algemeen gebruik beschikbaar werden gesteld.

VII

De criteria, die de kerken vanuit hun specifieke ervaringen, opgedaan op het gebied van de ontwikkelingssamenwerking, hebben opgesteld voor ontwikkelingsprojecten, namelijk kleinschaligheid, actieve deelname van de allerarmste bevolkingsgroepen, vergroting van hun zelfstandigheid en bevordering van sociale gerechtigheid, zijn eveneens van belang voor de ontwikkelingssamenwerking, die op regeringsniveau wordt geboden.

VIII

Het tegenwoordig ook van overheidswege gepropageerde welzijnsbeleid, waarbij de levensbeschouwing niet meer als organisatieprincipe wordt gezien, gaat voorbij aan de bijdrage, die diverse groeperingen (met name via het vrijwilligerswerk) kunnen leveren en zal in de praktijk de levensbeschouwelijke dimensie aan het welzijnswerk ontnemen.

IX

Het is beter verbreiding van wijsheid te bevorderen dan spreiding van kennis.

X

Het bouwen van eensgezindwoningen dient krachtig ter hand te worden genomen.